

A NOVEL TIP30 COMPLEX REGULATES ENDOCYTIC TRAFFICKING OF SIGNALING  
RECEPTORS BY FACILITATING THE TRANSPORT OF VACUOLAR (H<sup>+</sup>)-ATPASES TO  
EARLY ENDOSOMES

By

Chengliang Zhang

A DISSERTATION

Submitted to  
Michigan State University  
in partial fulfillment of the requirements  
for the degree of

DOCTOR OF PHILOSOPHY

Genetics

2010

## ABSTRACT

### A NOVEL TIP30 COMPLEX REGULATES ENDOCYTIC TRAFFICKING OF SIGNALING RECEPTORS BY FACILITATING THE TRANSPORT OF VACUOLAR (H<sup>+</sup>)-ATPASES TO EARLY ENDOSOMES

By

Chengliang Zhang

TIP30, a 30-kDa HIV-1 Tat-interacting protein, is a tumor suppressor whose expression is altered in a variety of human cancers. Tip30-deficient mice spontaneously develop hepatocellular carcinomas and other tumors as well as mammary preneoplastic lesions. However, the molecular mechanism of TIP30 function remains largely unraveled.

In this study, we show that a novel protein complex consisting of TIP30, Endophilin B1 (Endo B1), acyl-CoA synthetase long-chain family member 4 (ACSL4) interacts with Rab5a, and facilitates Rab5a recruitment to early endosomes by promoting efficient fusion between Rab5a vesicles and endocytic vesicles. Rab5a vesicles are EEA1-negative vesicles carrying vacuolar (H<sup>+</sup>)-ATPases (V-ATPases), an endosome acidification enzyme that causes ligand-receptor dissociation. Inhibition of TIP30, ACSL4 or Endo B1 impairs Rab5a vesicles loading on early endosomes and causes the mislocalization of V-ATPases, leading to delayed EGF-EGFR dissociation and prolonged EGFR signaling. Furthermore, we show that both arachidonic acid and coenzyme A are essential for the fusion of Rab5a vesicles with endocytic vesicles *in vitro*. TIP30, ACSL4 and Endo B1 can promote vesicle fusion in the presence of arachidonic acid and coenzyme A and can transfer the arachidonyl group to endosomal phosphatidic acid to produce triacylglycerol, which induces membrane tethering and stacking. Together, these results identify a novel function for Rab5a in endocytic trafficking and suggest a mechanism, in which addition

of the hydrophobic arachidonyl group to phosphatidic acid by the TIP30 protein complex may bring membranes into close contact to allow for membrane fusion.

Supporting the above findings is the observation that *Tip30* deletion dramatically accelerated the onset of mammary tumors in the MMTV-Neu transgenic mouse model of breast cancer, which overexpresses another EGFR family member, HER2/Neu. Similar to liver cells, deletion of Tip30 in mouse mammary cells also caused the trapping of EGF-EGFR complexes in early endosomes, thereby leading to delayed EGFR destruction and sustained EGFR signaling in response to EGF treatment.

We further found that unlike tumors developing in MMTV-Neu mice, almost all of which are estrogen receptor-negative and progesterone receptor-negative (ER-/PR-), tumors arising in *Tip30*<sup>-/-</sup>/MMTV-Neu mice are almost exclusively ER+/PR- mammary tumors. Immunofluorescence studies showed that Tip30 is predominantly expressed in ER+ mammary epithelial cells (MECs) and its deletion leads to an increase in the number of phospho-ER positive cells in mammary glands and accelerated activation of Akt in MMTV-Neu mice.

## ACKNOWLEDGMENTS

I would like to express my sincere gratitude to my mentor, Dr. Hua Xiao, for the continuous support of my Ph.D. study and research. He has been motivating, encouraging, and enlightening. I have been amazingly fortunate to have an advisor who gave me the freedom to explore on my own and at the same time the guidance necessary for me to proceed through the doctoral program and complete my dissertation.

I am very grateful to my guidance committee, Dr. Karen Friderici, Dr. Hans Cheng, Dr. Jerry Dodgson and Dr. Richard Schwartz for their encouragement, insightful comments and helpful suggestions concerning my research as well as my future career.

I am also thankful to all former and current members of the Xiao lab for their help and support: George Chen, Dr. Isum Hoshino, Dr. Mikito Mori, Dr. David Ankrapp, Aimin Li, and Shenglan Gao.

I want to thank Dr. Melinda Frame for her help with confocal microscopy, Dr. Alicia Pastor for her help with Electron Microscopy, and Douglas Whitten in the Proteomics core facility for his excellent work in protein identification.

I would like to acknowledge members in the Histopathology Lab: Amy S. Porter, Kathy A. Joseph and Rick A. Rosebury.

Special thanks to my friends, Dr. Jianjun Luo, Dr. Bill Underwood, Dr. Yanfeng Zhang, Dr. Xiaoli Gao, Dr. Young Nam Lee, for helping me get through the difficult times, and for their help with my experiments.

Thanks to Genetics Program and Plant Research Laboratory for offering me the opportunity to study at Michigan State University and for the initial financial support. I thank all people who work in Genetics Program and Department of Biomedical and Integrative Physiology for their help and support throughout my study at MSU. I am especially grateful to Dr. Barbara Sears for her various forms of support.

This thesis is dedicated to my parents and my wife for their never-ending love, concern, support and strength all these years, which motivates me to work hard and do my best.

## TABLE OF CONTENTS

LIST OF TABLES .....	ix
LIST OF FIGURES .....	x
LIST OF ABBREVIATIONS.....	xii
Chapter 1 Introduction .....	1
1.1 Receptor-mediated endocytosis .....	2
1.1.1 Endosomes as a platform for receptor signaling.....	2
1.1.2 Dissociation of receptor-ligand complexes.....	4
1.1.3 Vacuolar (H <sup>+</sup> )-ATPases (V-ATPases) and the termination of receptor endosomal signaling.....	5
1.2 Vesicle membrane fusion.....	6
1.2.1 Fatty acids and vesicle membrane fusion .....	6
1.2.2 Role of SNARE and SM (Sec1/Munc18-like) proteins in membrane fusion.....	9
1.2.3 Endophilins and membrane fusion.....	11
1.3 Rab GTPases in vesicle transport .....	11
1.3.1 Rabs proteins are critical for vesicle transport.....	12
1.3.2 Rab5 is required for endocytic trafficking.....	14
1.4 TIP30 is a tumor suppressor .....	14
1.5 Objectives .....	17
REFERENCES .....	18
Chapter 2 Rab5a vesicles transport vacuolar (H <sup>+</sup> )-ATPases to early endosomes via membrane fusion.....	31
Abstract.....	32
Introduction.....	33
Results.....	35
TIP30 interacts with Rab5a, Endo B1 and ACSL4.....	35
Inhibition of TIP30, ACSL4 or Endo B1 leads to delayed EGFR degradation and sustained EGFR signaling.....	46
TIP30, ACSL4 and Endo B1 are involved in endocytic trafficking of EGF-EGFR.....	47
TIP30, ACSL4, and Endo B1 promote the recruitment of Rab5a to early endosomes .....	53
Rab5a vesicles transport V-ATPases to early endosomes .....	54
TIP30 complex and arachidonic acid promote fusion between endocytic and Rab5a vesicles <i>in vitro</i> .....	58
Vesicle tethering and stacking induced by acylation of phosphatidic acid .....	63
Discussion.....	68
Function of TIP30, ACSL4 and Endo B1 in endocytic trafficking .....	68
A role for Rab5a in transport of endosomal targeting proteins .....	69
Lipids and membrane fusion.....	70
Materials and methods .....	72

EGFR internalization and immunofluorescence .....	72
Purification of endocytic and Rab5a vesicles .....	73
<i>In vitro</i> vesicle fusion assay .....	73
Lipid acylation .....	74
Statistical analysis .....	74
Acknowledgments .....	74
Supplemental materials and methods .....	89
Cell culture, DNA constructs and shRNAs .....	89
Immunoprecipitation .....	89
Purification of recombinant proteins .....	90
Mouse hepatocyte isolation .....	90
MS/MS spectrometry analysis .....	91
REFERENCES .....	92
Chapter 3 <i>Tip30</i> Deletion in MMTV-Neu Mice Leads to the Development of Estrogen Receptor-Positive and Progesterone Receptor-Negative Mammary Tumors via Enhancing EGFR Signaling .....	99
Abstract .....	100
Introduction .....	101
Results .....	103
<i>Tip30</i> deletion significantly accelerates mammary tumorigenesis in MMTV-Neu mice .....	103
Deletion of <i>Tip30</i> results in a shift from development of ER-/PR- tumors to ER+/PR- tumors in the MMTV-Neu mouse model .....	108
Estrogen and progesterone promote growth of <i>Neu+ /Tip30<sup>-/-</sup></i> mammary tumors. ....	112
Deletion of <i>Tip30</i> leads to a progressively increased numbers of p-ER $\alpha$ and p-Akt positive cells in the mammary gland from MMTV-Neu mice. ....	113
Tip30 deletion leads to delayed EGFR degradation and sustained EGFR signaling. ....	122
Discussion .....	123
Materials and Methods .....	126
Mice, primary MECs and tumor cells .....	126
Immunofluorescence and immunohistochemistry .....	127
EGFR internalization assay .....	128
Statistical Analysis .....	128
Disclosure of Potential Conflicts of Interest .....	128
Acknowledgments .....	128
REFERENCES .....	130
Chapter 4 Conclusions, Discussions and Future Directions .....	135
4.1 EGF dissociates from EGFR and exits the early endosomes in membrane-bound vesicles .....	136
4.2 Rab5a vesicles deliver endosomal targeting proteins via membrane fusion .....	138
4.3 TIP30, ACSL4 and Endo B1 form a protein complex that interacts with Rab5a and mediates the fusion of Rab5a vesicles with endocytic vesicles .....	140
4.4 Arachidonic acid and the synthesis of arachidonyl-coA by ACSL4 is essential for membrane fusion .....	141

4.5 Tip30 deletion in MMTV-Neu transgenic mice leads to the development of ER+/PR- tumors .....	142
REFERENCES .....	144

## LIST OF TABLES

Table 1.1 A summary of known functions of Rab proteins .....	13
Table 3.1 ER $\alpha$ and PR staining in mammary tumors .....	106

## LIST OF FIGURES

Figure 1.1 The classic view of the endocytic pathway. ....	3
Figure 1.2 Proposed mechanism of SNARE protein function in membrane fusion. ....	9
Figure 1.3 TIP30 localizes in the cytosol and inhibits the AKT signaling pathway. ....	16
Figure 2.1 TIP30 interacts with Rab5a, ACSL4, and Endo B1. ....	36
Figure 2.2 TIP30, Rab5a, ACSL4, and Endo B1 promote the endocytic downregulation of EGFR. ....	40
Figure 2.3 TIP30 and Rab5a depletion delays the exit of EGF from early endosomes. ....	48
Figure 2.4 TIP30, ACSL4, and Endo B1 are required for the localization of Rab5a to early endosomes. ....	51
Figure 2.5 Rab5a vesicles transport V-ATPase to early endosomes. ....	55
Figure 2.6 The TIP30 protein complex, arachidonic acid and coenzyme A promote the fusion between endocytic and Rab5a vesicles. ....	59
Figure 2.7 Acylation of phosphatidic acid promotes vesicle tethering and stacking. ....	65
Supplemental Figure 2.8 Related to Figure 2.1, TIP30, ACSL4 and Endo B1 forms a protein complex that may function on the EGFR endocytic pathway. ....	76
Supplemental Figure 2.9 Related to Figure 2.2, Knockdown of TIP30, Rab5a, ACSL4, and Endo B1 in PLC/PRF/5 cells. ....	78
Supplemental Figure 2.10 Related to Figure 2.3 and 2.4, Deletion of TIP30, ACSL4, or Endo B1 Delays EGF-EGFR dissociation and inhibits the recruitment of Rab5a to endocytic vesicles. ....	79
Supplemental Figure 2.11 Related to Figure 2.5, Rab5a vesicles carry V-ATPases. ....	81
Supplemental Figure 2.12 Related to Figure 2.6, Examination of vesicle fusion using TEM and the purification of recombinant proteins. ....	83
Supplemental Figure 2.13 Related to Figure 2.6, Spectrometric analysis of PA derivatives. ....	85

Figure 3.1 <i>Tip30</i> deletion significantly accelerates the onset of mammary tumors in MMTV- Neu mice. ....	104
Figure 3.2 Mammary tumors arising in <i>Neu+ /Tip30<sup>-/-</sup></i> mice are exclusively ER+/PR-.....	106
Figure 3.3 Growth of ER+/PR- tumors arising in <i>Neu+ /Tip30<sup>-/-</sup></i> mice depends upon estrogen and progesterone. ....	109
Figure 3.4 Representative immunohistochemical staining of p-ER $\alpha$ in mammary glands and mammary tumors from <i>Neu+ /Tip30<sup>-/-</sup></i> and <i>Neu+ /Tip30<sup>+/+</sup></i> mice. ....	114
Figure 3.5 Representative immunohistochemical staining for p-Akt in mammary tumors and mammary glands from <i>Neu+ /Tip30<sup>-/-</sup></i> and <i>Neu+ /Tip30<sup>+/+</sup></i> mice. ....	116
Figure 3.6 Deletion of <i>Tip30</i> in MECs leads to delayed EGFR degradation. ....	119
Figure 4.1 Function of the TIP30 complex.....	137
Figure 4.2 Phase separation of Rab5a in Triton X-114 .....	139

## LIST OF ABBREVIATIONS

**Abbreviation** Description

**ACSL4** Acyl-CoA synthetase long-chain family member 4

**APPL** Amyloid precursor protein-like

**BSA** Bovine serum albumin

**C-terminus** Carboxyl terminus

**EDTA** Ethylenediaminetetraacetic acid

**EEA1** Early endosomal antigen 1

**EGF** Epidermal growth factor

**EGFR** EGF receptor

**Endo B1** Endophilin B1

**ER** Endoplasmic reticulum

**ER** Estrogen receptor

**EYFP** Enhance yellow fluorescent protein

**g** gram

**GDI** GDP dissociation inhibitor

**GTP** Guanosine 5' triphosphate

**HA** Hemagglutinin

**HCC** Hepatocellular carcinomas

**HIV** Human immunodeficiency virus

**kDa** Kilo Dalton

**kDa** Kilodalton

**Lamp** Lysosomal-associated membrane protein

**LDL** Low-density lipoprotein

**LDLR** Low-density lipoprotein receptor

**ml** milli-liter

**M** Mol

**MAPK** Mitogen-activated protein kinase

**MVB** Multivesicular bodies

**NSF** NEM sensitive factor

**N-terminus** Amino-terminus

**PA** Phosphatidic acid

**PBS** Phosphate based buffer solution

**pH** potential Hydroxyl

**PI** Phosphoinositide

**PI(4)P** Phosphatidylinositide-4-phosphate

**PLD** Phospholipase D

**Rab** Ras like from brain

**SCLC** Small cell lung carcinoma

**SDS** Sodium dodecyl sulfate

**shRNA** Shot hairpin RNA

**siRNA** small interference RNA

**SM** Sec1/Munc18-like

**SNAP** Soluble NSF acceptor protein

**SNAP-25** Synaptosome associated protein-25

**SNARE** SNAP receptor

**TfR** Transferrin receptor

**TGF- $\alpha$**  Transforming growth factor-  $\alpha$

**TIP30** 30-kDa HIV-1 Tat-interacting protein

**VAMP** Vesicle-associated membrane protein

**V-ATPases** Vacuolar ( $H^+$ )-ATPases

**Ypt** Yeast protein transport

$\alpha$  alpha

$\alpha$ - anti

$\beta$  beta

$\mu$  micro

## **Chapter 1 Introduction**

## **1.1 Receptor-mediated endocytosis**

Receptor-mediated endocytosis is utilized by eukaryotic cells to rapidly internalize nutrients and other macromolecules and to reduce receptor number and signaling at the plasma membrane (Figure 1.1). Upon binding ligands, internalized receptors are initially delivered to the sorting station early endosomes, where they are either recycled back to the plasma membrane or transported to late endosomes and lysosomes for degradation (Maxfield and McGraw, 2004; Seto et al., 2002; Wiley, 2003).

### **1.1.1 Endosomes as a platform for receptor signaling**

Although early endosomes have been long considered as a conduit for the degradation or recycling of cell surface receptors, accumulating evidences shows that they are also an essential site for signal transduction. Activated receptors in early endosomes can transmit signals that are different from those that arise from the plasma membrane (Murphy et al., 2009b; von Zastrow and Sorkin, 2007; Wang et al., 2002). For instance, phospholipase C $\gamma$ -1 (PLC- $\gamma$ ) is activated by the epidermal growth factor receptor (EGFR) at the plasma membrane, whereas the activation of the extracellular signal-regulated kinases 1 and 2 (ERK1/2) and the phosphoinositide 3-kinase (PI3K) requires the normal endocytic trafficking of EGFR (Vieira et al., 1996). Other receptors, such as the insulin receptor, the high-affinity nerve growth factor (NGF) receptor TrkA, platelet-derived growth factor receptor (PDGFR), and the vascular endothelial growth factor receptor-2 (VEGFR2), also transmit signals to ERK1/2 and the PI3K/AKT pathway from endosomes (Delcroix et al., 2003; Grimes et al., 1996; Kelly and Ruderman, 1993; Lampugnani et al., 2006; Wang et al., 2004; Watson et al., 2001; Wu et al., 2001).

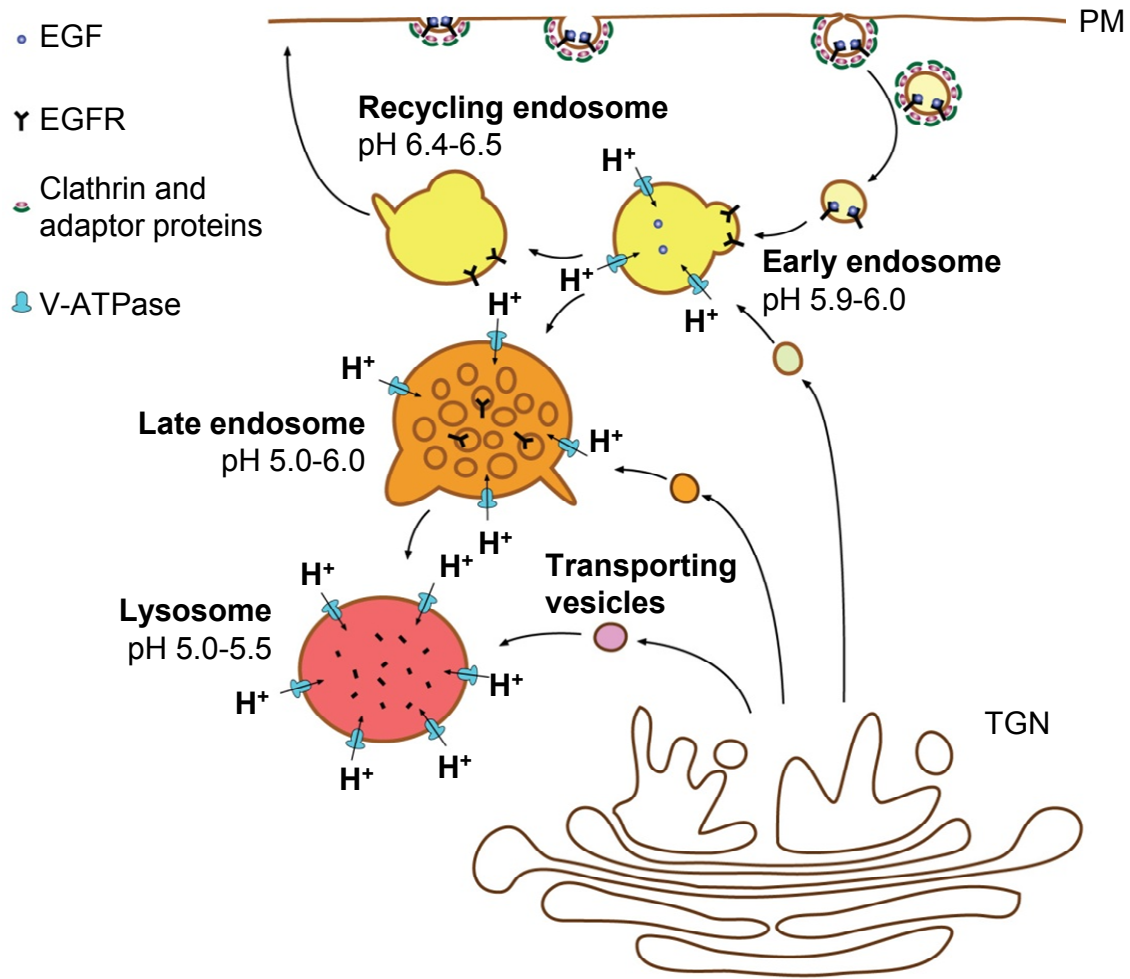


Figure 1.1 The classic view of the endocytic pathway.

Upon ligand binding, receptors are rapidly internalized and enclosed in clathrin coated endocytic vesicles, which fuse with early endosomes. Receptors dissociate from their ligands due to lower pH in the early endosome and are further sorted into recycling endosomes for reuse or sent to late endosomes and lysosomes for destruction. Drawing not to scale.

For interpretation of the references to color in this and all other figures, the reader is referred to the electronic version of this dissertation.

The specific physiological significance of signaling from the endosome membrane remains a challenging question. Given that endosome-based signals functionally distinct from those emanating from the plasma membrane (Murphy et al., 2009b; Vieira et al., 1996; Watson et al., 2001; Wu et al., 2001), endosomes may serve as a platform to assemble and activate certain downstream signal transducers and to provide another layer of receptor signaling control.

### **1.1.2 Dissociation of receptor-ligand complexes**

Both the recycling of unliganded receptors to the cell surface and the delivery of receptors to lysosomes for degradation via multivesicular bodies (MVB) require the dissociation of receptor-ligand complexes. It is becoming increasingly clear that early endosomes host the dissociation of many receptor-ligand complexes (Forgac, 2007; Maxfield and McGraw, 2004; Mellman, 1996a). Dissociation of internalized insulin was shown to occur in the endosomes of rat hepatoma cells (Backer et al., 1990; Murphy et al., 1984). Insulin receptors and other digestible molecules are then transported to lysosome for degradation. Transporting receptors, such as the transferrin receptor (TfR) and the low density lipoprotein receptor (LDLR), release their cargoes in early endosomes, allowing for the recycling of receptors to the plasma membrane (Brown and Goldstein, 1986; Yamashiro et al., 1984).

The endocytic trafficking of EGF-EGFR complexes was considered different from other receptor-ligand complexes because earlier studies suggested that they traveled to lysosomes for demolition as a unit in human foreskin fibroblasts (Carpenter and Cohen, 1976, 1979). However, recent studies argue against this view by demonstrating that EGFR is inactivated before being degraded and that EGF dissociates from EGFR prior to lysosomal transfer (Authier and Chauvet, 1999; Burke et al., 2001; Murphy et al., 2009b; Umebayashi et al., 2008). That signaling

receptors must be deactivated before being recycled or degraded is emerging as a common theme during receptor-mediated endocytosis.

### **1.1.3 Vacuolar (H<sup>+</sup>)-ATPases (V-ATPases) and the termination of receptor endosomal signaling**

The V-ATPases are proton pumps that are central to pH homeostasis. They reside on the membrane of many intracellular organelles, including endosomes, lysosomes and exocytotic vesicles, and at the plasma membrane of some cells. Therefore, the V-ATPases play crucial roles in various cellular processes, such as membrane trafficking, protein degradation, bone resorption and sperm maturation, by regulating luminal acidification of diverse organelles and the acidity of extracellular environment (Forgac, 2007; Marshansky and Futai, 2008).

Due to the action of V-ATPases, the lumen of endocytic vesicles becomes increasingly acidic when going from early endosome (pH 5.9-6.0) to late endosome (pH = 5.0-6.0) and lysosomes (pH 5.0-5.5) (Mellman et al., 1986). Acidic luminal pH created by V-ATPases contributes to the dissociation of receptor-ligand complexes and the termination of receptor endosomal signaling in early endosomes.

Despite the important roles played by V-ATPases on the endocytic pathway, little is known about how these multi-subunit transmembrane complexes are transported to the early endosomes. Proteins destined for residence at the membrane of endosomes are transported in membrane-enclosed vesicles (Bonifacino and Glick, 2004; Palade, 1975). Therefore, it is reasonable to assume that V-ATPases is transported by vesicles and that the loading of V-ATPases on the early endosomes is mediated by vesicle membrane fusion.

## **1.2 Vesicle membrane fusion**

Vesicles are constantly forming at the plasma membrane during endocytosis, and at the endoplasmic reticulum (ER) and the Golgi during exocytosis (Griffiths and Simons, 1986; Mellman, 1996a). They selectively fuse with recipient vesicles or the plasma membrane, thus play a central role in the transport of molecules between a variety of specific membrane-enclosed compartments.

Vesicle membrane fusion is the crucial step in all vesicular trafficking events and a fundamental cellular activity for the transfer of proteins and lipids between different compartments. Two types of events are considered essential for the fusion of a transport vesicle with its target membrane. First, transport vesicles must recognize its specific target membranes. Second, fusion must occur between transport vesicles and target membranes to accomplish the transactions. It is believed that proteins are in charge of the mutual recognition between the fusion partners and the initiation of membrane fusion. However, the merger of the two lipid bilayers is the central event during membrane fusion. Two membranes must overcome two dominant forces, a repulsive hydration force arising from water tightly bound to the hydrophilic lipid headgroups and an attractive hydrophobic force between the hydrocarbon interiors of the bilayers, to get closer enough to make fusion happen (Bonifacino and Glick, 2004; Burger, 2000; McMahon et al., 2010).

### **1.2.1 Fatty acids and vesicle membrane fusion**

The last two decades witnessed an explosion of knowledge on a number of factors involved in vesicle membrane fusion, including proteins, fatty acids, acyl-CoA esters and membrane lipids.

Arachidonic acid, a long-chain polyunsaturated fatty acid (PUFA), has been demonstrated to be a very effective fusogen. It can significantly promote  $\text{Ca}^{2+}$ -triggered fusion of isolated chromaffin granules (Creutz, 1981), endosome-endosome fusion (Mayorga et al., 1993) and GTP-dependent fusion of microsomes (Paiement et al., 1994). Moreover, membrane-bound arachidonic acid can drive annexin II-mediated membrane fusion of the lamellar body with the plasma membrane during the exocytosis (Chattopadhyay et al., 2003).

How arachidonic acid promotes membrane fusion remains unclear. In neuronal cells, arachidonic acids were found capable of removing the inhibitory Munc18 protein from syntaxin *in vitro*, thus allowing for the formation of the soluble N-ethylmaleimide-sensitive factor attachment protein receptor (SNARE) complexes, which are composed of vesicle-associated membrane protein 2 (VAMP2), SNAP-25, and syntaxin1 (Rickman and Davletov, 2005). However, a later *in vitro* study show that Munc18 remained attaching to syntaxin1 after arachidonic acid stimulated formation of the SNARE complexes. The function of arachidonic acids in SNARE complex formation need to be further investigated.

Fatty acyl-coenzyme A (CoA) esters are substrates for  $\beta$ -oxidation, for the synthesis and remodeling of lipids, and for protein acylation reactions. One acyl-CoA, palmitoyl-CoA, was shown indispensable for the budding of transport vesicles from Golgi cisternae and fusion of transport vesicles with Golgi cisternae (Glick and Rothman, 1987; Pfanner et al., 1990b; Pfanner et al., 1989). Vesicle transport was blocked by inhibitor of long-chain acyl-CoA synthetase and a nonhydrolyzable analogue of palmitoyl-CoA, suggesting that fatty acid has to be activated by CoA to stimulate transport and that the acyl group has to be transferred on other molecules.

Many of the proteins that mediate synaptic vesicle fusion and trafficking were indicated as the recipients of the acyl groups (Huang and El-Husseini, 2005; Linder and Deschenes, 2007). Palmitoyl groups covalently link to cysteine residues of synaptotagmin,  $\alpha$ -SNAP (soluble N-ethylmaleimide-sensitive-factor-attachment protein- $\alpha$ ) and SNARE proteins Ykt6, VAMP and SNAP-25 (synaptosome associated protein-25). Palmitoylation of these proteins was thought to function in anchoring them to membranes or in their sorting to particular membrane microdomains such as lipid rafts. Palmitoylation of Ykt6 has been suggested to provide a method of regulating the rate of intracellular membrane flow and vesicle fusion in the secretory pathway (Fukasawa et al., 2004). However, the significance of palmitoylation of these proteins in vesicle membrane fusion is unclear.

Phosphatidic acid (PA) is another fusogenic lipid that plays important roles in vesicle transport. It is proposed that PA, with a very small negatively charged headgroup, induces negative membrane curvature at the inward membrane curve (Kooijman et al., 2003). Phospholipase D (PLD) hydrolyzes membrane phosphatidylcholine to produce PA. The two isoforms of PLDs, PLD1 and PLD2, are involved in vesicle trafficking during endocytosis and exocytosis (Cazzolli et al., 2006; Donaldson, 2009). Depletion of PLD2 inhibited recycling of transferrin receptors in HeLa cells (Padron et al., 2006). Endocytic trafficking and endosomal signaling of EGFR are also regulated by PLD1 and its regulators, protein kinase C $\alpha$  and RalA (Shen et al., 2001). The role of PLD derived PA has been shown to be required for key exocytotic processes in a variety of cells, including adipocytes (Huang et al., 2005a), neuroendocrine cells (Humeau et al., 2001), mast cells (Peng and Beaven, 2005) and pancreatic beta-cells (Hughes et al., 2004). These observations strongly suggest that lipid modifications are essential for various vesicle membrane fusion events.

### 1.2.2 Role of SNARE and SM (Sec1/Munc18-like) proteins in membrane fusion

SNARE proteins are receptors for SNAP (soluble NSF attachment protein) and NSF (N-ethylmaleimide-sensitive factor). They belong to a family of membrane-tethered coiled-coil proteins that are required for vesicle membrane fusion. SNARE proteins have been shown to mediate fusion of lipid bilayers in assays using reconstituted liposomes; therefore they are considered the best candidates for the cellular fusogens. It was proposed that vesicle-associated v-SNARE proteins syntaxin and SNAP-25 pair with cognate t-SNARE protein VAMP on the target membrane to form four-helix bundle (SNAREpin) that brings lipid bilayers into close proximity. The pairing starts at the N termini of the SNARE proteins and then proceeds in a zipper-like manner towards the C-terminal trans-membrane regions (Figure 1.2). The resulting mechanical force might overcome the energy barrier and bring the lipid bilayers close enough for fusion to occur (Jahn and Scheller, 2006; Weber et al., 1998).

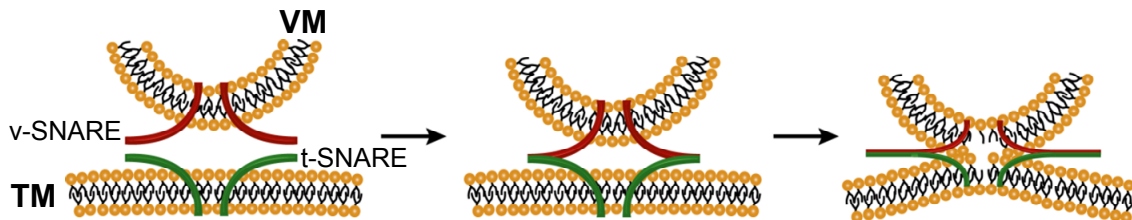


Figure 1.2 Proposed mechanism of SNARE protein function in membrane fusion. VM, vesicle membrane; TM, target membrane. Drawing not to scale.

Fusion assays using *in vitro* reconstituted lipid bilayers have played a key role in supporting the hypothesis that SNARE proteins are the minimal fusion machinery. It has been shown that when synaptic vesicle membrane protein VAMP2, a v-SNARE protein, and two plasma membrane t-SNARE proteins syntaxin1A and SNAP25 were reconstituted into phospholipids to

form donor and acceptor vesicles, respectively, they were sufficient to promote specific fusion between the two types of vesicles (Weber et al., 1998). However, it is clear that *in vivo* many proteins also play key roles in vesicle fusion apart from the SNARE proteins (McMahon et al., 2010; Weber et al., 1998). In neuroendocrine cells, for instance, Munc-18 (mammalian uncoordinated-18) protein, a member of the SM protein family, was shown to facilitate syntaxin trafficking to the cell surface by interacting with syntaxin and preventing premature SNARE complex formation between syntaxin and SNAP-25 (Medine et al., 2007).

Although plenty of information has been obtained using artificial membranes, studies also indicate that artificial membrane fusion is far from being able to represent fusion between biological membranes. Recently, endosome-endosome fusion was successfully mimicked using reconstituted proteoliposomes with up to 17 recombinant proteins purified from bacteria (Ohya et al., 2009). These proteins include Rab5, Rab5 effectors, SNARE proteins and SNARE accessory factors, and other proteins that are currently known to be important for vesicle fusion. They can promote fusion of proteoliposomes to physiologically meaningful rate; however, they are not capable of promoting efficient fusion between biological intact endosomes, suggesting that the SNARE proteins are not the fusogenic factors that are minimally required for membrane fusion. In addition, high fusion rate was reached with reconstituted proteoliposomes utilizing bacterially expressed proteins that essentially lack posttranslational modifications, whereas many proteins that are involved in membrane fusion are posttranslationally modified *in vivo*, such as the palmitoylation of synaptotagmin,  $\alpha$ -SNAP and SNARE proteins Ykt6, VAMP and SNAP-25 (Fukasawa et al., 2004; Huang and El-Husseini, 2005; Linder and Deschenes, 2007), as well as the isoprenylation of Rab5 (Kinsella and Maltese, 1991). This further indicates that fusion of biological membrane has very different requirements than artificial lipid bilayers.

The data presented by Ohya et al also imply that some components critical to vesicle fusion are missing in the *in vitro* assay system and that these components most likely function prior to SNARE proteins (McMahon et al., 2010; Ohya et al., 2009). One important molecule that is obviously not needed for artificial membrane fusion is arachidonic acid, which has been proven to be essential for fusions between many kinds of vesicles, including endosome-endosome fusion (Chattopadhyay et al., 2003; Creutz, 1981; Mayorga et al., 1993; Paiement et al., 1994).

### **1.2.3 Endophilins and membrane fusion**

Endophilins are a group of proteins that contain an N-terminal amphipathic helix, a BAR (Bin/Amphiphysin/Rvs) domain and a C-terminal SH3 domain. They play important roles in endocytotic membrane trafficking. Endophilin is required for synaptic vesicle recycling in *Drosophila* and in *Caenorhabditis elegans* (Guichet et al., 2002; Ringstad et al., 1999; Schuske et al., 2003; Verstreken et al., 2002). In mammalian cells, endophilin is localized to synaptic vesicles and is required for neurotransmitter release from endocytic vesicles (Gad et al., 2000; Ringstad et al., 1999; Simpson et al., 1999).

Important mechanistic insights into endophilin functions have been gained from the studies on the BAR domains, which are highly conserved in many proteins that involve in membrane dynamics. The dimeric BAR domains of endophilins are banana shaped and can sense and bind membrane curvature via its concave face to remodel liposomes structure (Powell, 2009). The structural features of BAR domains and their ability to turn liposome into the “spaghetti-like” tubular structures *in vitro* are well documented (Gallop et al., 2006; Masuda et al., 2006a; Wang et al., 2008; Weissenhorn, 2005).

### **1.3 Rab GTPases in vesicle transport**

Rab GTPases were originally identified as Ras-like from brain (Salminen and Novick, 1987). They constitute the largest family of the Ras GTPase superfamily. The yeast *S. cerevisiae* genome sequence encodes 11 Rab proteins, including Sec4p and the Ypt (Yeast protein transport) proteins. Human cells contain approximately 70 Rab proteins that are localized to distinct subcellular compartments and are key to membrane-trafficking events (Schwartz et al., 2007).

### **1.3.1 Rabs proteins are critical for vesicle transport**

Transmembrane proteins that reside in the endoplasmic reticulum (ER), Golgi, endosomes, lysosomes, and plasma membrane are synthesized on the rough ER and remain embedded in the membrane as they move to their final destinations. These proteins are transported from one membrane compartment to another by vesicles. It is well documented that Rab proteins regulate discrete transport steps along the biosynthetic/secretory pathways, as well as the endocytic pathways (Table 1).

Although many Rab proteins have been subjected to extensive studies, the precise function of these proteins remained elusive. Rab proteins are anchored to the cytoplasmic face of all vesicles involved in intracellular transport via prenyl groups covalently linked to two cysteines in the C-terminus. This special way of membrane anchorage makes Rab proteins the best candidates that determine the identity of transporting vesicles and the specificity for their fusion with distinct recipient membrane. Therefore, it was proposed that Rab proteins may act as identity tags for distinct transporting vesicles and that they bring transporting vesicles to their specific recipient membranes and tether those membranes by recruiting multitude of effectors (Grosshans et al., 2006; Pfeffer, 2001; Takai et al., 2001; Zerial and McBride, 2001).

Table 1.1 A summary of known functions of Rab proteins

Name	Implicated function
Rab1, Rab2	Transport of cargo between the ER and the Golgi apparatus (Griffiths et al., 1994; Sannerud et al., 2006; Saraste et al., 1995; Tisdale et al., 1992).
Rab3	Synaptic vesicle exocytosis (Ng and Tang, 2008).
Rab3, Rab26, Rab27, Rab37	Various types of regulated exocytic events (Handley et al., 2007; Masuda et al., 2000; Tsuboi and Fukuda, 2006; Yoshie et al., 2000).
Rab4, Rab35	Endosomal recycling back to the plasma membrane (Kouranti et al., 2006; Sonnichsen et al., 2000).
Rab5	Endosome fusion (Gorvel et al., 1991).
Rab5, Rab14, Rab22	Maturation of early phagosomes (Duclos et al., 2000; Kyei et al., 2006; Perskvist et al., 2002; Roberts et al., 2006).
Rab6	Endosomes to the Golgi transport; Transport of secretory vesicles to the plasma membrane (Grigoriev et al., 2007; White et al., 1999; Young et al., 2005).
Rab6, Rab33,	Intra-Golgi trafficking (Smith et al., 2007; Starr et al., 2010).
Rab7	Endosomes and phagosomes maturation ; autophagy; melanosome trafficking (Ceresa and Bahr, 2006; Feng et al., 1995; Gomez et al., 2001; Gutierrez et al., 2004; Kinchen et al., 2008; Roberts et al., 2006; Vitelli et al., 1997).
Rab8, Rab10, Rab14	Constitutive biosynthetic trafficking from the trans-Golgi network (TGN) to the plasma membrane (Huber et al., 1993; Junutula et al., 2004; Schuck et al., 2007).
Rab8, Rab11, Rab17, Rab23	Ciliogenesis (Knodler et al., 2010; Yoshimura et al., 2007).
Rab9	Trafficking from late endosomes to the TGN (Barbero et al., 2002).
Rab11, Rab15, Rab17, Rab25	Recycling from the TGN to the plasma membrane (Casanova et al., 1999; Sonnichsen et al., 2000; Zacchi et al., 1998; Zuk and Elferink, 2000).
Rab13	Endosomal recycling; junctional complex dynamics in epithelial cells (Kohler et al., 2004; Marzesco et al., 2002).
Rab18	Formation of lipid droplets (Martin et al., 2005).
Rab22, Rab31	Trafficking between the TGN and early endosomes (Kauppi et al., 2002; Rodriguez-Gabin et al., 2001).
Rab23	Ciliary trafficking (Boehlke et al., 2010).
Rab24, Rab33	Macroautophagy (Itoh et al., 2008; Munafo and Colombo, 2002).
Rab32	Mitochondrial fission (Alto et al., 2002).
Rab32, Rab38	Biogenesis of melanosomes (Wasmeier et al., 2006).

### **1.3.2 Rab5 is required for endocytic trafficking**

Rab5 is one of the best studied members of the Rab GTPases family. Functional studies indicate that Rab5 is a key regulator of receptor-mediated endocytosis. Downregulation mediated by siRNA against Rab5 inhibits the transition from early endosome to late endosome, leading to delayed endocytic degradation of EGFR (Chen et al., 2009b). Rab5 is required for a form of receptor tyrosine kinase induced actin remodeling and sub-compartmental organization and sorting of early endosomes (de Renzis et al., 2002; Lanzetti et al., 2004). It is demonstrated that Rab5 controls the endosomal release of amyloid precursor protein-like 1 (APPL1) and APPL2, which then translocate to the nucleus where they activate a histone deacetylase (Miaczynska et al., 2004a). More recently, Rab5 was identified as an essential regulator for phagosome maturation (Kitano et al., 2008).

Earlier studies suggested that Rab5 is required for efficient fusion between biological endosomes *in vitro* (Gorvel et al., 1991). A later study identified a Rab5 effector EEA1, whose association with the endosomal membrane depends on Rab5 and phosphoinositide 3-kinase (PI(3)K) activity (Simonsen et al., 1998). It was soon found that EEA1 can bypass Rab5 and PI(3)K to promote endosomal tethering (Christoforidis et al., 1999). However, a recent study showed that Rab5 and EEA can only increase endosomal fusion 3% and 10%, respectively (Ohya et al., 2009), suggesting that both Rab5 and EEA are not capable of promoting significant fusion between biological intact endosomes. This observation also leaves an important question open again: what is the function of Rab5 on the endocytic pathways?

### **1.4 TIP30 is a tumor suppressor**

TIP30, also called CC3 or HTATIP2, was initially identified as a metastasis suppressor by a differential display analysis of mRNA from the highly metastatic human variant small cell lung carcinoma (v-SCLC) versus less metastatic classic SCLC cell lines (Shtivelman, 1997). It was independently isolated as an HIV-1 Tat-interacting protein that may enhance Tat-activated transcription (Xiao et al., 1998). Tip30-deficient mice with C57BL6/J and 129SvJ mixed genetic background spontaneously developed a spectrum of tumors, suggesting TIP30 as a novel tumor suppressor (Ito et al., 2003). In the past several years, aberrant expression of TIP30 has been associated with a variety of human cancers, including human liver (Ito et al., 2003; Lu et al., 2008), lung (Tong et al., 2009), breast (Zhao et al., 2007), prostate (Singh et al., 2008; Zhang et al., 2008), and gastric cancers (Li et al., 2009), as well as colorectal carcinoma (Chen et al., 2010).

In mammary epithelial cells, TIP30 may function as a transcription repressor to inhibit ER $\alpha$ -mediated c-myc transcription by interacting with ER $\alpha$ -interacting coactivator CIA (Jiang et al., 2004a). Deletion of Tip30 in primary mammary epithelial cells leads to increased proliferation and rapid immortalization relative to wild-type cells. Extensive ductal hyperplasia was observed in Tip30-deficient mouse mammary glands with age (Pecha et al., 2007).

Approximately 30% of the tumors developed in Tip30-deficient mice are hepatocellular carcinomas (HCC) (Ito et al., 2003). However, the mechanism of how TIP30 functions in liver cells is largely unknown. It has been shown that TIP30 may upregulate other tumor

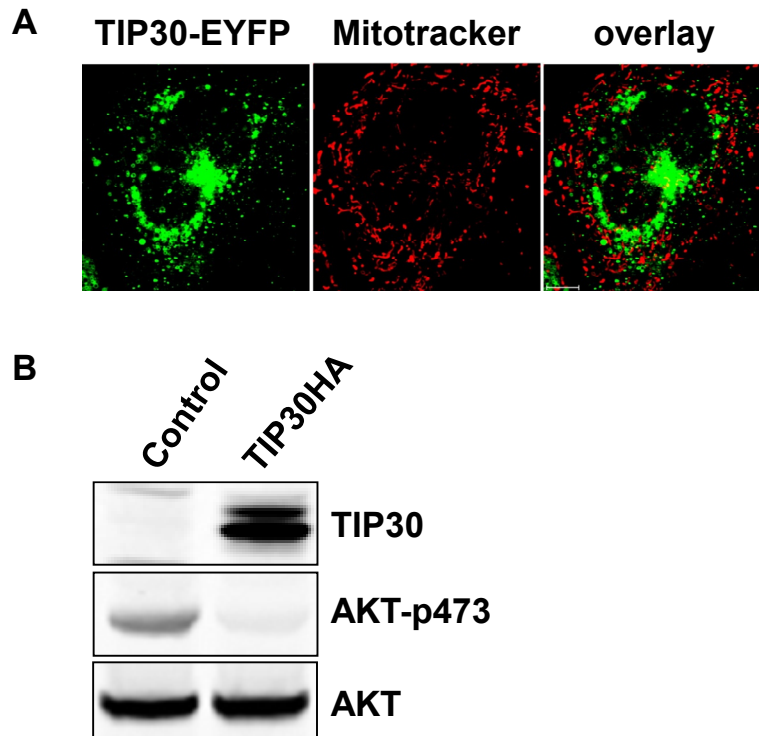


Figure 1.3 TIP30 localizes in the cytosol and inhibits the AKT signaling pathway.

(A) The majority of TIP30 appear in the cytosol. Live human hepatocellular carcinoma Hep3B cells expressing TIP30-EYFP (green) were imaged using LSM510 meta confocal microscope after incubating with mitotracker (red).

(B) Ectopic expression of TIP30 inhibits the phosphorylation of AKT. Whole cell extracts were prepared from human hepatocellular carcinoma HepG2 cells expressing TIP30HA or empty vectors and were subjected to immunoblot analysis using the indicated antibodies.

suppressors such as p53 and E-cadherin and downregulate some oncoproteins such as N-cadherin and c-MYC in HCC cells (Jiang et al., 2007; Zhao et al., 2006). Our preliminary results showed that the majority of TIP30 was found in the cytoplasm (Figure1.3A) and that ectopic expression of TIP30 inhibits the activation of the AKT signaling pathway in human HCC cells (Figure1.3B).

These observations link the TIP30 function directly with receptor signaling that originates from the plasma membrane.

## 1.5 Objectives

The major objective of this study was to determine the molecular mechanism by which TIP30 inhibits the AKT signaling pathway and to gain more insight into how TIP30 functions in liver cells.

We performed co-immunoprecipitation to identify cellular proteins that interact with TIP30. Three proteins, Rab5a, Endophilin B1 (Endo B1), acyl-CoA synthetase long-chain family member 4 (ACSL4) have been found tightly associating with TIP30 to form a protein complex. Since both Rab5a and Endo B1 are involved in receptor-mediated endocytosis, we examined how these proteins regulate the endocytic trafficking of EGFR. Human liver cancer PLC/PRF/5 cells were subjected to EGFR internalization assay after knocking down the expression of each of these genes with specific shRNAs. Compare to control cells, all cells with depleted TIP30, Rab5a, Endo B1, or ACSL4 have much delayed EGFR degradation and sustained EGFR signaling, suggesting that these proteins are required for EGFR endocytic trafficking. Further studies revealed that these proteins facilitate the fusion of endocytic vesicles with Rab5a vesicles, which is responsible for transporting vacuolar (H<sup>+</sup>)-ATPases (V-ATPases); thus are required for the dissociation of EGF-EGFR complex in endosomes. Furthermore, *in vitro* membrane fusion assay showed that in addition to the protein complex other molecules, such as arachidonic acid, co-enzymeA and ATP are also required for the fusion of biological membranes. Our membrane fusion assay using *in vitro* modified lipids suggest that the TIP30 complex may promote membrane fusion through fatty acylating phosphatidic acid.

## **REFERENCES**

## REFERENCES

- Alto, N.M., Soderling, J., and Scott, J.D. (2002). Rab32 is an A-kinase anchoring protein and participates in mitochondrial dynamics. *J Cell Biol* 158, 659-668.
- Authier, F., and Chauvet, G. (1999). *In vitro* endosome-lysosome transfer of dephosphorylated EGF receptor and Shc in rat liver. *FEBS Letters* 461, 25-31.
- Backer, J.M., Kahn, C.R., and White, M.F. (1990). The dissociation and degradation of internalized insulin occur in the endosomes of rat hepatoma cells. *Journal of Biological Chemistry* 265, 14828-14835.
- Barbero, P., Bittova, L., and Pfeffer, S.R. (2002). Visualization of Rab9-mediated vesicle transport from endosomes to the trans-Golgi in living cells. *J Cell Biol* 156, 511-518.
- Boehlke, C., Bashkurov, M., Buescher, A., Krick, T., John, A.K., Nitschke, R., Walz, G., and Kuehn, E.W. (2010). Differential role of Rab proteins in ciliary trafficking: Rab23 regulates smoothed levels. *J Cell Sci* 123, 1460-1467.
- Bonifacino, J.S., and Glick, B.S. (2004). The Mechanisms of Vesicle Budding and Fusion. *Cell* 116, 153-166.
- Brown, M.S., and Goldstein, J.L. (1986). A receptor-mediated pathway for cholesterol homeostasis. *Science* 232, 34-47.
- Burger, K.N.J. (2000). Greasing Membrane Fusion and Fission Machineries. *Traffic* 1, 605-613.
- Burke, P., Schooler, K., and Wiley, H.S. (2001). Regulation of Epidermal Growth Factor Receptor Signaling by Endocytosis and Intracellular Trafficking. *Mol Biol Cell* 12, 1897-1910.
- Carpenter, G., and Cohen, S. (1976). 125I-labeled human epidermal growth factor. Binding, internalization, and degradation in human fibroblasts. *J Cell Biol* 71, 159-171.
- Carpenter, G., and Cohen, S. (1979). Epidermal growth factor. *Annu Rev Biochem* 48, 193-216.
- Casanova, J.E., Wang, X., Kumar, R., Bhartur, S.G., Navarre, J., Woodrum, J.E., Altschuler, Y., Ray, G.S., and Goldenring, J.R. (1999). Association of Rab25 and Rab11a with the apical recycling system of polarized Madin-Darby canine kidney cells. *Mol Biol Cell* 10, 47-61.
- Cazzolli, R., Shemon, A.N., Fang, M.Q., and Hughes, W.E. (2006). Phospholipid signalling through phospholipase D and phosphatidic acid. *IUBMB Life* 58, 457-461.

- Ceresa, B.P., and Bahr, S.J. (2006). rab7 activity affects epidermal growth factor:epidermal growth factor receptor degradation by regulating endocytic trafficking from the late endosome. *J Biol Chem* 281, 1099-1106.
- Chattopadhyay, S., Sun, P., Wang, P., Abonyo, B., Cross, N.L., and Liu, L. (2003). Fusion of Lamellar Body with Plasma Membrane Is Driven by the Dual Action of Annexin II Tetramer and Arachidonic Acid. *Journal of Biological Chemistry* 278, 39675-39683.
- Chen, P.I., Kong, C., Su, X., and Stahl, P.D. (2009). Rab5 isoforms differentially regulate the trafficking and degradation of epidermal growth factor receptors. *J Biol Chem* 284, 30328-30338.
- Chen, X., Cao, X., Dong, W., Luo, S., Suo, Z., and Jin, Y. (2010). Expression of TIP30 tumor suppressor gene is down-regulated in human colorectal carcinoma. *Dig Dis Sci* 55, 2219-2226.
- Christoforidis, S., McBride, H.M., Burgoyne, R.D., and Zerial, M. (1999). The Rab5 effector EEA1 is a core component of endosome docking. *Nature* 397, 621-625.
- Creutz, C.E. (1981). cis-Unsaturated Fatty Acids Induce the Fusion of Chromaffin Granules Aggregated by Synexin. *The Journal of Cell Biology* 91, 247-256.
- de Renzis, S., Sonnichsen, B., and Zerial, M. (2002). Divalent Rab effectors regulate the sub-compartmental organization and sorting of early endosomes. *Nat Cell Biol* 4, 124-133.
- Delcroix, J.-D., Valletta, J.S., Wu, C., Hunt, S.J., Kowal, A.S., and Mobley, W.C. (2003). NGF Signaling in Sensory Neurons: Evidence that Early Endosomes Carry NGF Retrograde Signals. *Neuron* 39, 69-84.
- Donaldson, J.G. (2009). Phospholipase D in endocytosis and endosomal recycling pathways. *Biochimica et Biophysica Acta (BBA) - Molecular and Cell Biology of Lipids* 1791, 845-849.
- Duclos, S., Diez, R., Garin, J., Papadopoulou, B., Descoteaux, A., Stenmark, H., and Desjardins, M. (2000). Rab5 regulates the kiss and run fusion between phagosomes and endosomes and the acquisition of phagosome leishmanicidal properties in RAW 264.7 macrophages. *J Cell Sci* 113 Pt 19, 3531-3541.
- Feng, Y., Press, B., and Wandinger-Ness, A. (1995). Rab 7: an important regulator of late endocytic membrane traffic. *J Cell Biol* 131, 1435-1452.
- Forgac, M. (2007). Vacuolar ATPases: rotary proton pumps in physiology and pathophysiology. *Nat Rev Mol Cell Biol* 8, 917-929.
- Fukasawa, M., Varlamov, O., Eng, W.S., Söllner, T.H., and Rothman, J.E. (2004). Localization and activity of the SNARE Ykt6 determined by its regulatory domain and palmitoylation.

Proceedings of the National Academy of Sciences of the United States of America *101*, 4815-4820.

Gad, H., Ringstad, N., Low, P., Kjaerulff, O., Gustafsson, J., Wenk, M., Di Paolo, G., Nemoto, Y., Crun, J., Ellisman, M.H., *et al.* (2000). Fission and uncoating of synaptic clathrin-coated vesicles are perturbed by disruption of interactions with the SH3 domain of endophilin. *Neuron* *27*, 301-312.

Gallop, J.L., Jao, C.C., Kent, H.M., Butler, P.J., Evans, P.R., Langen, R., and McMahon, H.T. (2006). Mechanism of endophilin N-BAR domain-mediated membrane curvature. *EMBO J* *25*, 2898-2910.

Glick, B.S., and Rothman, J.E. (1987). Possible role for fatty acyl-coenzyme A in intracellular protein transport. *Nature* *326*, 309-312.

Gomez, P.F., Luo, D., Hirosaki, K., Shinoda, K., Yamashita, T., Suzuki, J., Otsu, K., Ishikawa, K., and Jimbow, K. (2001). Identification of rab7 as a melanosome-associated protein involved in the intracellular transport of tyrosinase-related protein 1. *J Invest Dermatol* *117*, 81-90.

Gorvel, J.P., Chavrier, P., Zerial, M., and Gruenberg, J. (1991). rab5 controls early endosome fusion *in vitro*. *Cell* *64*, 915-925.

Griffiths, G., Ericsson, M., Krijnse-Locker, J., Nilsson, T., Goud, B., Soling, H.D., Tang, B.L., Wong, S.H., and Hong, W. (1994). Localization of the Lys, Asp, Glu, Leu tetrapeptide receptor to the Golgi complex and the intermediate compartment in mammalian cells. *J Cell Biol* *127*, 1557-1574.

Griffiths, G., and Simons, K. (1986). The trans Golgi network: sorting at the exit site of the Golgi complex. *Science* *234*, 438-443.

Grigoriev, I., Splinter, D., Keijzer, N., Wulf, P.S., Demmers, J., Ohtsuka, T., Modesti, M., Maly, I.V., Grosveld, F., Hoogenraad, C.C., *et al.* (2007). Rab6 regulates transport and targeting of exocytotic carriers. *Dev Cell* *13*, 305-314.

Grimes, M.L., Zhou, J., Beattie, E.C., Yuen, E.C., Hall, D.E., Valletta, J.S., Topp, K.S., LaVail, J.H., Bunnnett, N.W., and Mobley, W.C. (1996). Endocytosis of Activated TrkA: Evidence that Nerve Growth Factor Induces Formation of Signaling Endosomes. *J Neurosci* *16*, 7950-7964.

Grosshans, B.L., Ortiz, D., and Novick, P. (2006). Rabs and their effectors: Achieving specificity in membrane traffic. *Proceedings of the National Academy of Sciences* *103*, 11821-11827.

Guichet, A., Wucherpfennig, T., Dudu, V., Etter, S., Wilsch-Brauniger, M., Hellwig, A., Gonzalez-Gaitan, M., Huttner, W.B., and Schmidt, A.A. (2002). Essential role of endophilin A in synaptic vesicle budding at the *Drosophila* neuromuscular junction. *EMBO J* *21*, 1661-1672.

- Gutierrez, M.G., Munafo, D.B., Beron, W., and Colombo, M.I. (2004). Rab7 is required for the normal progression of the autophagic pathway in mammalian cells. *J Cell Sci* *117*, 2687-2697.
- Handley, M.T., Haynes, L.P., and Burgoyne, R.D. (2007). Differential dynamics of Rab3A and Rab27A on secretory granules. *J Cell Sci* *120*, 973-984.
- Huang, K., and El-Husseini, A. (2005). Modulation of neuronal protein trafficking and function by palmitoylation. *Current Opinion in Neurobiology* *15*, 527-535.
- Huang, P., Altshuler, Y.M., Hou, J.C., Pessin, J.E., and Frohman, M.A. (2005). Insulin-stimulated plasma membrane fusion of Glut4 glucose transporter-containing vesicles is regulated by phospholipase D1. *Mol Biol Cell* *16*, 2614-2623.
- Huber, L.A., Pimplikar, S., Parton, R.G., Virta, H., Zerial, M., and Simons, K. (1993). Rab8, a small GTPase involved in vesicular traffic between the TGN and the basolateral plasma membrane. *J Cell Biol* *123*, 35-45.
- Hughes, W.E., Elgundi, Z., Huang, P., Frohman, M.A., and Biden, T.J. (2004). Phospholipase D1 regulates secretagogue-stimulated insulin release in pancreatic beta-cells. *J Biol Chem* *279*, 27534-27541.
- Humeau, Y., Vitale, N., Chasserot-Golaz, S., Dupont, J.L., Du, G., Frohman, M.A., Bader, M.F., and Poulain, B. (2001). A role for phospholipase D1 in neurotransmitter release. *Proc Natl Acad Sci U S A* *98*, 15300-15305.
- Ito, M., Jiang, C., Krumm, K., Zhang, X., Pecha, J., Zhao, J., Guo, Y., Roeder, R.G., and Xiao, H. (2003). TIP30 deficiency increases susceptibility to tumorigenesis. *Cancer Res* *63*, 8763-8767.
- Itoh, T., Fujita, N., Kanno, E., Yamamoto, A., Yoshimori, T., and Fukuda, M. (2008). Golgi-resident small GTPase Rab33B interacts with Atg16L and modulates autophagosome formation. *Mol Biol Cell* *19*, 2916-2925.
- Jahn, R., and Scheller, R.H. (2006). SNAREs [mdash] engines for membrane fusion. *Nat Rev Mol Cell Biol* *7*, 631-643.
- Jiang, C., Ito, M., Piening, V., Bruck, K., Roeder, R.G., and Xiao, H. (2004). TIP30 interacts with an estrogen receptor alpha-interacting coactivator CIA and regulates c-myc transcription. *J Biol Chem* *279*, 27781-27789.
- Jiang, C., Pecha, J., Hoshino, I., Ankrapp, D., and Xiao, H. (2007). TIP30 mutant derived from hepatocellular carcinoma specimens promotes growth of HepG2 cells through up-regulation of N-cadherin. *Cancer Res* *67*, 3574-3582.

- Junutula, J.R., De Maziere, A.M., Peden, A.A., Ervin, K.E., Advani, R.J., van Dijk, S.M., Klumperman, J., and Scheller, R.H. (2004). Rab14 is involved in membrane trafficking between the Golgi complex and endosomes. *Mol Biol Cell* *15*, 2218-2229.
- Kauppi, M., Simonsen, A., Bremnes, B., Vieira, A., Callaghan, J., Stenmark, H., and Olkkonen, V.M. (2002). The small GTPase Rab22 interacts with EEA1 and controls endosomal membrane trafficking. *J Cell Sci* *115*, 899-911.
- Kelly, K.L., and Ruderman, N.B. (1993). Insulin-stimulated phosphatidylinositol 3-kinase. Association with a 185-kDa tyrosine-phosphorylated protein (IRS-1) and localization in a low density membrane vesicle. *Journal of Biological Chemistry* *268*, 4391-4398.
- Kinchen, J.M., Doukoumetzidis, K., Almendinger, J., Stergiou, L., Tosello-Trampont, A., Sifri, C.D., Hengartner, M.O., and Ravichandran, K.S. (2008). A pathway for phagosome maturation during engulfment of apoptotic cells. *Nat Cell Biol* *10*, 556-566.
- Kinsella, B.T., and Maltese, W.A. (1991). rab GTP-binding proteins implicated in vesicular transport are isoprenylated *in vitro* at cysteines within a novel carboxyl-terminal motif. *J Biol Chem* *266*, 8540-8544.
- Kitano, M., Nakaya, M., Nakamura, T., Nagata, S., and Matsuda, M. (2008). Imaging of Rab5 activity identifies essential regulators for phagosome maturation. *Nature* *453*, 241-245.
- Knodler, A., Feng, S., Zhang, J., Zhang, X., Das, A., Peranen, J., and Guo, W. (2010). Coordination of Rab8 and Rab11 in primary ciliogenesis. *Proc Natl Acad Sci U S A* *107*, 6346-6351.
- Kohler, K., Louvard, D., and Zahraoui, A. (2004). Rab13 regulates PKA signaling during tight junction assembly. *J Cell Biol* *165*, 175-180.
- Kooijman, E.E., Chupin, V., Kruijff, B.d., and Burger, K.N.J. (2003). Modulation of Membrane Curvature by Phosphatidic Acid and Lysophosphatidic Acid. *Traffic* *4*, 162-174.
- Kouranti, I., Sachse, M., Arouche, N., Goud, B., and Echard, A. (2006). Rab35 regulates an endocytic recycling pathway essential for the terminal steps of cytokinesis. *Curr Biol* *16*, 1719-1725.
- Kyei, G.B., Vergne, I., Chua, J., Roberts, E., Harris, J., Junutula, J.R., and Deretic, V. (2006). Rab14 is critical for maintenance of Mycobacterium tuberculosis phagosome maturation arrest. *EMBO J* *25*, 5250-5259.
- Lampugnani, M.G., Orsenigo, F., Gagliani, M.C., Tacchetti, C., and Dejana, E. (2006). Vascular endothelial cadherin controls VEGFR-2 internalization and signaling from intracellular compartments. *J Cell Biol* *174*, 593-604.

- Lanzetti, L., Palamidessi, A., Areces, L., Scita, G., and Di Fiore, P.P. (2004). Rab5 is a signalling GTPase involved in actin remodelling by receptor tyrosine kinases. *Nature* *429*, 309-314.
- Li, X., Zhang, Y., Cao, S., Chen, X., Lu, Y., Jin, H., Sun, S., Chen, B., Liu, J., Ding, J., *et al.* (2009). Reduction of TIP30 correlates with poor prognosis of gastric cancer patients and its restoration drastically inhibits tumor growth and metastasis. *Int J Cancer* *124*, 713-721.
- Linder, M.E., and Deschenes, R.J. (2007). Palmitoylation: policing protein stability and traffic. *Nat Rev Mol Cell Biol* *8*, 74-84.
- Lu, B., Ma, Y., Wu, G., Tong, X., Guo, H., Liang, A., Cong, W., Liu, C., Wang, H., Wu, M., *et al.* (2008). Methylation of Tip30 promoter is associated with poor prognosis in human hepatocellular carcinoma. *Clin Cancer Res* *14*, 7405-7412.
- Marshansky, V., and Futai, M. (2008). The V-type H<sup>+</sup>-ATPase in vesicular trafficking: targeting, regulation and function. *Current Opinion in Cell Biology* *20*, 415-426.
- Martin, S., Driessen, K., Nixon, S.J., Zerial, M., and Parton, R.G. (2005). Regulated localization of Rab18 to lipid droplets: effects of lipolytic stimulation and inhibition of lipid droplet catabolism. *J Biol Chem* *280*, 42325-42335.
- Marzesco, A.M., Dunia, I., Pandjaitan, R., Recouvreur, M., Dauzonne, D., Benedetti, E.L., Louvard, D., and Zahraoui, A. (2002). The small GTPase Rab13 regulates assembly of functional tight junctions in epithelial cells. *Mol Biol Cell* *13*, 1819-1831.
- Masuda, E.S., Luo, Y., Young, C., Shen, M., Rossi, A.B., Huang, B.C., Yu, S., Bennett, M.K., Payan, D.G., and Scheller, R.H. (2000). Rab37 is a novel mast cell specific GTPase localized to secretory granules. *FEBS Lett* *470*, 61-64.
- Masuda, M., Takeda, S., Sone, M., Ohki, T., Mori, H., Kamioka, Y., and Mochizuki, N. (2006). Endophilin BAR domain drives membrane curvature by two newly identified structure-based mechanisms. *EMBO J* *25*, 2889-2897.
- Maxfield, F.R., and McGraw, T.E. (2004). Endocytic recycling. *Nat Rev Mol Cell Biol* *5*, 121-132.
- Mayorga, L.S., Colombo, M.I., Lennartz, M., Brown, E.J., Rahman, K.H., Weiss, R., Lennon, P.J., and Stahl, P.D. (1993). Inhibition of endosome fusion by phospholipase A2 (PLA2) inhibitors points to a role for PLA2 in endocytosis. *Proc Natl Acad Sci U S A* *90*, 10255-10259.
- McMahon, H.T., Kozlov, M.M., and Martens, S. (2010). Membrane Curvature in Synaptic Vesicle Fusion and Beyond. *Cell* *140*, 601-605.
- Medine, C.N., Rickman, C., Chamberlain, L.H., and Duncan, R.R. (2007). Munc18-1 prevents the formation of ectopic SNARE complexes in living cells. *J Cell Sci* *120*, 4407-4415.

- Mellman, I. (1996). ENDOCYTOSIS AND MOLECULAR SORTING. *Annual Review of Cell and Developmental Biology* 12, 575-625.
- Mellman, I., Fuchs, R., and Helenius, A. (1986). Acidification of the Endocytic and Exocytic Pathways. *Annual Review of Biochemistry* 55, 663-700.
- Miaczynska, M., Christoforidis, S., Giner, A., Shevchenko, A., Uttenweiler-Joseph, S., Habermann, B., Wilm, M., Parton, R.G., and Zerial, M. (2004). APPL proteins link Rab5 to nuclear signal transduction via an endosomal compartment. *Cell* 116, 445-456.
- Munafò, D.B., and Colombo, M.I. (2002). Induction of autophagy causes dramatic changes in the subcellular distribution of GFP-Rab24. *Traffic* 3, 472-482.
- Murphy, J.E., Padilla, B.E., Hasdemir, B., Cottrell, G.S., and Bunnett, N.W. (2009). Endosomes: A legitimate platform for the signaling train. *Proceedings of the National Academy of Sciences* 106, 17615-17622.
- Murphy, R.F., Powers, S., and Cantor, C.R. (1984). Endosome pH measured in single cells by dual fluorescence flow cytometry: rapid acidification of insulin to pH 6. *The Journal of Cell Biology* 98, 1757-1762.
- Ng, E.L., and Tang, B.L. (2008). Rab GTPases and their roles in brain neurons and glia. *Brain Res Rev* 58, 236-246.
- Ohya, T., Miaczynska, M., Coskun, U., Lommer, B., Runge, A., Drechsel, D., Kalaidzidis, Y., and Zerial, M. (2009). Reconstitution of Rab- and SNARE-dependent membrane fusion by synthetic endosomes. *Nature* 459, 1091-1097.
- Padron, D., Tall, R.D., and Roth, M.G. (2006). Phospholipase D2 Is Required for Efficient Endocytic Recycling of Transferrin Receptors. *Mol Biol Cell* 17, 598-606.
- Paiement, J., Lavoie, C., Gavino, G.R., and Gavino, V.C. (1994). Modulation of GTP-dependent fusion by linoleic and arachidonic acid in derivatives of rough endoplasmic reticulum from rat liver. *Biochimica et Biophysica Acta (BBA) - Biomembranes* 1190, 199-212.
- Palade, G. (1975). Intracellular aspects of the process of protein synthesis. *Science* 189, 347-358.
- Pecha, J., Ankrapp, D., Jiang, C., Tang, W., Hoshino, I., Bruck, K., Wagner, K.U., and Xiao, H. (2007). Deletion of Tip30 leads to rapid immortalization of murine mammary epithelial cells and ductal hyperplasia in the mammary gland. *Oncogene* 26, 7423-7431.
- Peng, Z., and Beaven, M.A. (2005). An essential role for phospholipase D in the activation of protein kinase C and degranulation in mast cells. *J Immunol* 174, 5201-5208.

- Perskvist, N., Roberg, K., Kulyte, A., and Stendahl, O. (2002). Rab5a GTPase regulates fusion between pathogen-containing phagosomes and cytoplasmic organelles in human neutrophils. *J Cell Sci* *115*, 1321-1330.
- Pfanner, N., Glick, B.S., Arden, S.R., and Rothman, J.E. (1990). Fatty acylation promotes fusion of transport vesicles with Golgi cisternae. *The Journal of Cell Biology* *110*, 955-961.
- Pfanner, N., Orci, L., Glick, B.S., Amherdt, M., Arden, S.R., Malhotra, V., and Rothman, J.E. (1989). Fatty acyl-coenzyme a is required for budding of transport vesicles from Golgi cisternae. *Cell* *59*, 95-102.
- Pfeffer, S.R. (2001). Rab GTPases: specifying and deciphering organelle identity and function. *Trends in Cell Biology* *11*, 487-491.
- Powell, K. (2009). Cell biology: ahead of the curve. *Nature* *460*, 318-320.
- Rickman, C., and Davletov, B. (2005). Arachidonic acid allows SNARE complex formation in the presence of Munc18. *Chem Biol* *12*, 545-553.
- Ringstad, N., Gad, H., Low, P., Di Paolo, G., Brodin, L., Shupliakov, O., and De Camilli, P. (1999). Endophilin/SH3p4 is required for the transition from early to late stages in clathrin-mediated synaptic vesicle endocytosis. *Neuron* *24*, 143-154.
- Roberts, E.A., Chua, J., Kyei, G.B., and Deretic, V. (2006). Higher order Rab programming in phagolysosome biogenesis. *J Cell Biol* *174*, 923-929.
- Rodriguez-Gabin, A.G., Cammer, M., Almazan, G., Charron, M., and Larocca, J.N. (2001). Role of rRAB22b, an oligodendrocyte protein, in regulation of transport of vesicles from trans Golgi to endocytic compartments. *J Neurosci Res* *66*, 1149-1160.
- Salminen, A., and Novick, P.J. (1987). A ras-like protein is required for a post-Golgi event in yeast secretion. *Cell* *49*, 527-538.
- Sannerud, R., Marie, M., Nizak, C., Dale, H.A., Pernet-Gallay, K., Perez, F., Goud, B., and Saraste, J. (2006). Rab1 defines a novel pathway connecting the pre-Golgi intermediate compartment with the cell periphery. *Mol Biol Cell* *17*, 1514-1526.
- Saraste, J., Lahtinen, U., and Goud, B. (1995). Localization of the small GTP-binding protein rab1p to early compartments of the secretory pathway. *J Cell Sci* *108 ( Pt 4)*, 1541-1552.
- Schuck, S., Gerl, M.J., Ang, A., Manninen, A., Keller, P., Mellman, I., and Simons, K. (2007). Rab10 is involved in basolateral transport in polarized Madin-Darby canine kidney cells. *Traffic* *8*, 47-60.

- Schuske, K.R., Richmond, J.E., Matthies, D.S., Davis, W.S., Runz, S., Rube, D.A., van der Blik, A.M., and Jorgensen, E.M. (2003). Endophilin Is Required for Synaptic Vesicle Endocytosis by Localizing Synaptojanin. *Neuron* *40*, 749-762.
- Schwartz, S.L., Cao, C., Pylypenko, O., Rak, A., and Wandinger-Ness, A. (2007). Rab GTPases at a glance. *J Cell Sci* *120*, 3905-3910.
- Seto, E.S., Bellen, H.J., and Lloyd, T.E. (2002). When cell biology meets development: endocytic regulation of signaling pathways. *Genes Dev* *16*, 1314-1336.
- Shen, Y., Xu, L., and Foster, D.A. (2001). Role for phospholipase D in receptor-mediated endocytosis. *Mol Cell Biol* *21*, 595-602.
- Shtivelman, E. (1997). A link between metastasis and resistance to apoptosis of variant small cell lung carcinoma. *Oncogene* *14*, 2167-2173.
- Simonsen, A., Lippe, R., Christoforidis, S., Gaullier, J.M., Brech, A., Callaghan, J., Toh, B.H., Murphy, C., Zerial, M., and Stenmark, H. (1998). EEA1 links PI(3)K function to Rab5 regulation of endosome fusion. *Nature* *394*, 494-498.
- Simpson, F., Hussain, N.K., Qualmann, B., Kelly, R.B., Kay, B.K., McPherson, P.S., and Schmid, S.L. (1999). SH3-domain-containing proteins function at distinct steps in clathrin-coated vesicle formation. *Nat Cell Biol* *1*, 119-124.
- Singh, A.P., Bafna, S., Chaudhary, K., Venkatraman, G., Smith, L., Eudy, J.D., Johansson, S.L., Lin, M.F., and Batra, S.K. (2008). Genome-wide expression profiling reveals transcriptomic variation and perturbed gene networks in androgen-dependent and androgen-independent prostate cancer cells. *Cancer Lett* *259*, 28-38.
- Smith, A.C., Heo, W.D., Braun, V., Jiang, X., Macrae, C., Casanova, J.E., Scidmore, M.A., Grinstein, S., Meyer, T., and Brumell, J.H. (2007). A network of Rab GTPases controls phagosome maturation and is modulated by *Salmonella enterica* serovar Typhimurium. *J Cell Biol* *176*, 263-268.
- Sonnichsen, B., De Renzis, S., Nielsen, E., Rietdorf, J., and Zerial, M. (2000). Distinct membrane domains on endosomes in the recycling pathway visualized by multicolor imaging of Rab4, Rab5, and Rab11. *J Cell Biol* *149*, 901-914.
- Starr, T., Sun, Y., Wilkins, N., and Storrie, B. (2010). Rab33b and Rab6 are functionally overlapping regulators of Golgi homeostasis and trafficking. *Traffic* *11*, 626-636.
- Takai, Y., Sasaki, T., and Matozaki, T. (2001). Small GTP-Binding Proteins. *Physiol Rev* *81*, 153-208.

- Tisdale, E.J., Bourne, J.R., Khosravi-Far, R., Der, C.J., and Balch, W.E. (1992). GTP-binding mutants of rab1 and rab2 are potent inhibitors of vesicular transport from the endoplasmic reticulum to the Golgi complex. *J Cell Biol* 119, 749-761.
- Tong, X., Li, K., Luo, Z., Lu, B., Liu, X., Wang, T., Pang, M., Liang, B., Tan, M., Wu, M., *et al.* (2009). Decreased TIP30 expression promotes tumor metastasis in lung cancer. *Am J Pathol* 174, 1931-1939.
- Tsuboi, T., and Fukuda, M. (2006). Rab3A and Rab27A cooperatively regulate the docking step of dense-core vesicle exocytosis in PC12 cells. *J Cell Sci* 119, 2196-2203.
- Umebayashi, K., Stenmark, H., and Yoshimori, T. (2008). Ubc4/5 and c-Cbl Continue to Ubiquitinate EGF Receptor after Internalization to Facilitate Polyubiquitination and Degradation. *Mol Biol Cell* 19, 3454-3462.
- Verstreken, P., Kjaerulff, O., Lloyd, T.E., Atkinson, R., Zhou, Y., Meinertzhagen, I.A., and Bellen, H.J. (2002). Endophilin Mutations Block Clathrin-Mediated Endocytosis but Not Neurotransmitter Release. *Cell* 109, 101-112.
- Vieira, A.V., Lamaze, C., and Schmid, S.L. (1996). Control of EGF Receptor Signaling by Clathrin-Mediated Endocytosis. *Science* 274, 2086-2089.
- Vitelli, R., Santillo, M., Lattero, D., Chiariello, M., Bifulco, M., Bruni, C.B., and Bucci, C. (1997). Role of the small GTPase Rab7 in the late endocytic pathway. *J Biol Chem* 272, 4391-4397.
- von Zastrow, M., and Sorkin, A. (2007). Signaling on the endocytic pathway. *Current Opinion in Cell Biology* 19, 436-445.
- Wang, Q., Kaan, H.Y., Hooda, R.N., Goh, S.L., and Sonderrmann, H. (2008). Structure and plasticity of Endophilin and Sorting Nexin 9. *Structure* 16, 1574-1587.
- Wang, Y., Pennock, S., Chen, X., and Wang, Z. (2002). Endosomal Signaling of Epidermal Growth Factor Receptor Stimulates Signal Transduction Pathways Leading to Cell Survival. *Mol Cell Biol* 22, 7279-7290.
- Wang, Y., Pennock, S.D., Chen, X., Kazlauskas, A., and Wang, Z. (2004). Platelet-derived Growth Factor Receptor-mediated Signal Transduction from Endosomes. *Journal of Biological Chemistry* 279, 8038-8046.
- Wasmeier, C., Romao, M., Plowright, L., Bennett, D.C., Raposo, G., and Seabra, M.C. (2006). Rab38 and Rab32 control post-Golgi trafficking of melanogenic enzymes. *J Cell Biol* 175, 271-281.

- Watson, F.L., Heerssen, H.M., Bhattacharyya, A., Klesse, L., Lin, M.Z., and Segal, R.A. (2001). Neurotrophins use the Erk5 pathway to mediate a retrograde survival response. *Nat Neurosci* 4, 981-988.
- Weber, T., Zemelman, B.V., McNew, J.A., Westermann, B., Gmachl, M., Parlati, F., Sollner, T.H., and Rothman, J.E. (1998). SNAREpins: minimal machinery for membrane fusion. *Cell* 92, 759-772.
- Weissenhorn, W. (2005). Crystal structure of the endophilin-A1 BAR domain. *J Mol Biol* 351, 653-661.
- White, J., Johannes, L., Mallard, F., Girod, A., Grill, S., Reinsch, S., Keller, P., Tzschaschel, B., Echard, A., Goud, B., *et al.* (1999). Rab6 coordinates a novel Golgi to ER retrograde transport pathway in live cells. *J Cell Biol* 147, 743-760.
- Wiley, H.S. (2003). Trafficking of the ErbB receptors and its influence on signaling. *Exp Cell Res* 284, 78-88.
- Wu, C., Lai, C.-F., and Mobley, W.C. (2001). Nerve Growth Factor Activates Persistent Rap1 Signaling in Endosomes. *J Neurosci* 21, 5406-5416.
- Xiao, H., Tao, Y., Greenblatt, J., and Roeder, R.G. (1998). A cofactor, TIP30, specifically enhances HIV-1 Tat-activated transcription. *Proc Natl Acad Sci U S A* 95, 2146-2151.
- Yamashiro, D.J., Tycko, B., Fluss, S.R., and Maxfield, F.R. (1984). Segregation of transferrin to a mildly acidic (pH 6.5) para-golgi compartment in the recycling pathway. *Cell* 37, 789-800.
- Yoshie, S., Imai, A., Nashida, T., and Shimomura, H. (2000). Expression, characterization, and localization of Rab26, a low molecular weight GTP-binding protein, in the rat parotid gland. *Histochem Cell Biol* 113, 259-263.
- Yoshimura, S., Egerer, J., Fuchs, E., Haas, A.K., and Barr, F.A. (2007). Functional dissection of Rab GTPases involved in primary cilium formation. *J Cell Biol* 178, 363-369.
- Young, J., Stauber, T., del Nery, E., Vernos, I., Pepperkok, R., and Nilsson, T. (2005). Regulation of microtubule-dependent recycling at the trans-Golgi network by Rab6A and Rab6A'. *Mol Biol Cell* 16, 162-177.
- Zacchi, P., Stenmark, H., Parton, R.G., Orioli, D., Lim, F., Giner, A., Mellman, I., Zerial, M., and Murphy, C. (1998). Rab17 regulates membrane trafficking through apical recycling endosomes in polarized epithelial cells. *J Cell Biol* 140, 1039-1053.
- Zerial, M., and McBride, H. (2001). Rab proteins as membrane organizers. *Nat Rev Mol Cell Biol* 2, 107-117.

Zhang, H., Zhang, Y., Duan, H.O., Kirley, S.D., Lin, S.X., McDougal, W.S., Xiao, H., and Wu, C.L. (2008). TIP30 is associated with progression and metastasis of prostate cancer. *Int J Cancer* 123, 810-816.

Zhao, J., Ni, H., Ma, Y., Dong, L., Dai, J., Zhao, F., Yan, X., Lu, B., Xu, H., and Guo, Y. (2007). TIP30/CC3 expression in breast carcinoma: relation to metastasis, clinicopathologic parameters, and P53 expression. *Hum Pathol* 38, 293-298.

Zhao, J., Zhang, X., Shi, M., Xu, H., Jin, J., Ni, H., Yang, S., Dai, J., Wu, M., and Guo, Y. (2006). TIP30 inhibits growth of HCC cell lines and inhibits HCC xenografts in mice in combination with 5-FU. *Hepatology* 44, 205-215.

Zuk, P.A., and Elferink, L.A. (2000). Rab15 differentially regulates early endocytic trafficking. *J Biol Chem* 275, 26754-26764.

**Chapter 2 Rab5a vesicles transport vacuolar (H<sup>+</sup>)-ATPases to early endosomes via  
membrane fusion**

Chengliang Zhang, Aimin Li, Xinchun Zhang, and Hua Xiao

Submitted for publication

## **Abstract**

Rab5a is a multifunctional GTPase crucial for endocytic trafficking. Here we show that a novel protein complex consisting of TIP30, Endophilin B1 (Endo B1) and acyl-CoA synthetase long-chain family member 4 (ACSL4) interacts with Rab5a and facilitates Rab5a localization to early endosomes by promoting efficient fusion between Rab5a vesicles and endocytic vesicles. Rab5a vesicles are EEA1-negative vesicles carrying vacuolar ( $H^+$ )-ATPases (V-ATPases), an endosome acidification enzyme that causes ligand-receptor dissociation. Inhibition of TIP30, ACSL4 or Endo B1 impairs the fusion of Rab5a vesicles with early endosomes in response to EGF, leading to delayed EGF-EGFR dissociation and prolonged EGFR signaling. Furthermore, we show that TIP30, ACSL4 and Endo B1 act in concert to promote the fusion of Rab5a vesicles with early endosomes via fatty acylating phosphatidic acid. Together, these results reveal a critical role of TIP30, Endo B1 and ACSL4 in receptor-mediated endocytosis and suggest a novel mechanism underlying membrane fusion.

## Introduction

Receptor mediated endocytosis is a mechanism utilized by eukaryotic cells to rapidly take up specific nutrients and reduce receptor signaling at the plasma membrane. Internalized ligand-receptor complexes are enclosed in early endosomes, also called sorting endosomes, where they are either recycled or delivered to lysosomes for destruction (Maxfield and McGraw, 2004; Mellman, 1996a). Signaling receptors continue to activate certain downstream pathways from early endosomes (Miaczynska et al., 2004b; Murphy et al., 2009b; Polo and Di Fiore, 2006; Sorkin and von Zastrow, 2009), until ligand-receptor complexes dissociate due to lower luminal pH created by vacuolar V-ATPases, the major proton pump responsible for endosomal and lysosomal acidification (Backer et al., 1990; Maxfield and McGraw, 2004; Nishi and Forgac, 2002; Yamashiro et al., 1984). Inactivation of V-ATPase blocks the transition from early to late endosomes (Clague et al., 1994). Therefore, the proper endosomal targeting and activity of V-ATPases contribute to the tight regulation of both endocytic trafficking and receptor endosomal signaling.

Membrane fusion is a cellular event at the center of intracellular organelle biogenesis and membrane protein traffic. It generally requires cellular factors to bring donor and recipient membranes into close proximity, to increase membrane curvature, and to disturb their lipid bilayers (Martens and McMahon, 2008; McMahon et al., 2010). In addition to fusogenic lipids such as acyl-CoA (Pfanner et al., 1990a; Pfanner et al., 1989), arachidonic acid (Chattopadhyay et al., 2003; Mayorga et al., 1993), as well as phosphoinositides, phosphatidic acid and diacylglycerol (Hauke and Di Paolo, 2007; Jun et al., 2004; Mima et al., 2008), many proteins including Rab5, Rab5 effectors, SNARE proteins and SNARE accessory factors are necessary for various membrane fusion events (Stenmark, 2009; Wickner and Schekman, 2008). Recently,

efficient endosome fusion was successfully mimicked using proteoliposomes reconstituted with 17 recombinant core fusion proteins in the absence of previously reported fusogenic lipids, raising a critical question of whether fusogenic lipids or additional cellular factors are required for efficient fusion between intact biological endosomes (McMahon et al., 2010; Ohya et al., 2009).

One of the core fusion proteins is the small GTPase Rab5a, a membrane protein that regulates early endosome fusion *in vitro* (Gorvel et al., 1991), motility of early endosomes on microtubules (Nielsen et al., 1999), and the traffic between endosomes and lysosomes (Rosenfeld et al., 2001). Deletion of Rab5a in cells inhibits the transport of EGFR from early endosomes to lysosomes and consequently causes sustained EGFR signaling and delayed degradation (Chen et al., 2009a). Despite its importance to endocytic transport, how Rab5a reaches early endosomes and downregulates receptor signaling remains only partially understood.

Here we show that Rab5a localizes to early endosomes through membrane fusion between endocytic vesicles and Rab5a vesicles. A protein complex composed of TIP30, ACSL4, and Endo B1 interacts with Rab5a and promotes efficient fusion of these two vesicles *in vivo* and *in vitro* probably by acting in concert to transfer arachidonyl group to PA. Furthermore, endosomal targeting enzymes V-ATPases are carried to early endosomes by Rab5a vesicles and their proper localization relies on Rab5a TIP30, ACSL4, and Endo B1. Thus, these studies identify a novel function for Rab5a in endocytic trafficking and suggest a mechanism, in which addition of the hydrophobic arachidonyl group to phosphatidic acid may bring membranes into close contact to allow for membrane fusion.

## Results

### TIP30 interacts with Rab5a, Endo B1 and ACSL4

TIP30, also known as HTATIP2 or CC3 (Shtivelman, 1997; Xiao et al., 1998), is a tumor suppressor that can act as a transcription cofactor to repress transcription in the nucleus (Jiang et al., 2004b; Zhao et al., 2008a). However, TIP30 also localizes in the cytoplasm in which its function is poorly understood (Ito et al., 2003; Lee et al., 2004; Tong et al., 2009; Zhao et al., 2007). To identify cytosolic proteins that interact with TIP30, we stably expressed TIP30 protein with an HA tag fused to its C-terminal end (TIP30-HA) in human hepatocellular carcinoma cells (PLC/PRF/5). Co-immunoprecipitation (co-IP) assays were performed using whole cell extracts generated from cells expressing TIP30-HA or control vector. Silver staining of the immunoprecipitates resolved on SDS-PAGE revealed multiple major bands (Figure 2.1A). Mass spectrometric analysis identified Rab5a, ACSL4, and EndoB1 (also known as Bif-1) in the immunoprecipitates. Association of these proteins with TIP30-HA was confirmed by immunoblot analysis using specific antibodies (Figure 2.1B). The interactions were further confirmed by reciprocal IP. When Rab5a, Endo B1 or ACSL4 were HA-tagged, each could be specifically coimmunoprecipitated with endogenous TIP30 and the other three endogenous proteins (Figure 2.1C). Although Endo B1 failed to be immunoprecipitated with ACSL4-HA possibly due to the interference of HA at its C-terminus, endogenous ACSL4 was detected in Endo B1-HA immunoprecipitates. Notably, Rab5a co-immunoprecipitated with the other proteins in the presence of 0.2 mM EDTA, indicating that the interaction is independent of its nucleotide binding status. Notably, Rab5a co-immunoprecipitated with the other proteins in the presence of 0.2 mM EDTA, indicating that the interaction is independent of its nucleotide binding status.

Figure 2.1 TIP30 interacts with Rab5a, ACSL4, and Endo B1.

**(A)** Silver stain of TIP30 and its interacting proteins after co-immunoprecipitation (co-IP). Whole cell extracts derived from cells expressing empty vector or TIP30-HA were immunoprecipitated with  $\alpha$ -HA agarose beads. The immunoprecipitates were eluted with HA peptides, resolved on SDS-PAGE, and subjected to silver stain.

**(B)** Immunoblot confirmed the association of Rab5a, ACSL4, and Endo B1 with TIP30. The immunoprecipitates were resolved on SDS-PAGE and analyzed by immunoblotting with the indicated antibodies. The two polypeptides that reacted with anti-HA antibodies might result from posttranslational modifications on TIP30. Input was 10% of the volume of lysates used in the IP assays. The EGFR blot serves as a negative control.

**(C)** Reciprocal co-IP. Whole cell extracts made from cells expressing HA-Rab5a, ACSL4-HA, Endo B1-HA, or empty vector were subjected to co-IP with  $\alpha$ -HA agarose beads. The immunoprecipitates were subjected to immunoblot analysis with the indicated antibodies. Input was 10% of the volume of lysates used in the IP assays.

**(D)** BiFC analysis was performed on 293T cells by co-expressing TIP30-VC155 with VN173, VN173-Rab5a, ACSL4-VN173, or Endo B1-VN173. Green indicates fluorescent signal from Venus, a GFP variant. Bottom panels show overlays of DIC and representative confocal microscope images. Scale bars, 10  $\mu$ m.

**(E)** TIP30 and EGF-EGFR are colocalized in endosomes in response to EGF treatment. HepG2 cells co-expressing TIP30-CFP (green) and EGFR-DsRed (red) were treated with 10 ng/ml Alexa<sup>647</sup>-EGF (blue) for 10 min and then analyzed by confocal microscopy. A typical image is shown. Boxed areas are magnified. Scale bar, 10  $\mu$ m.

Figure 2.1 Cont'd

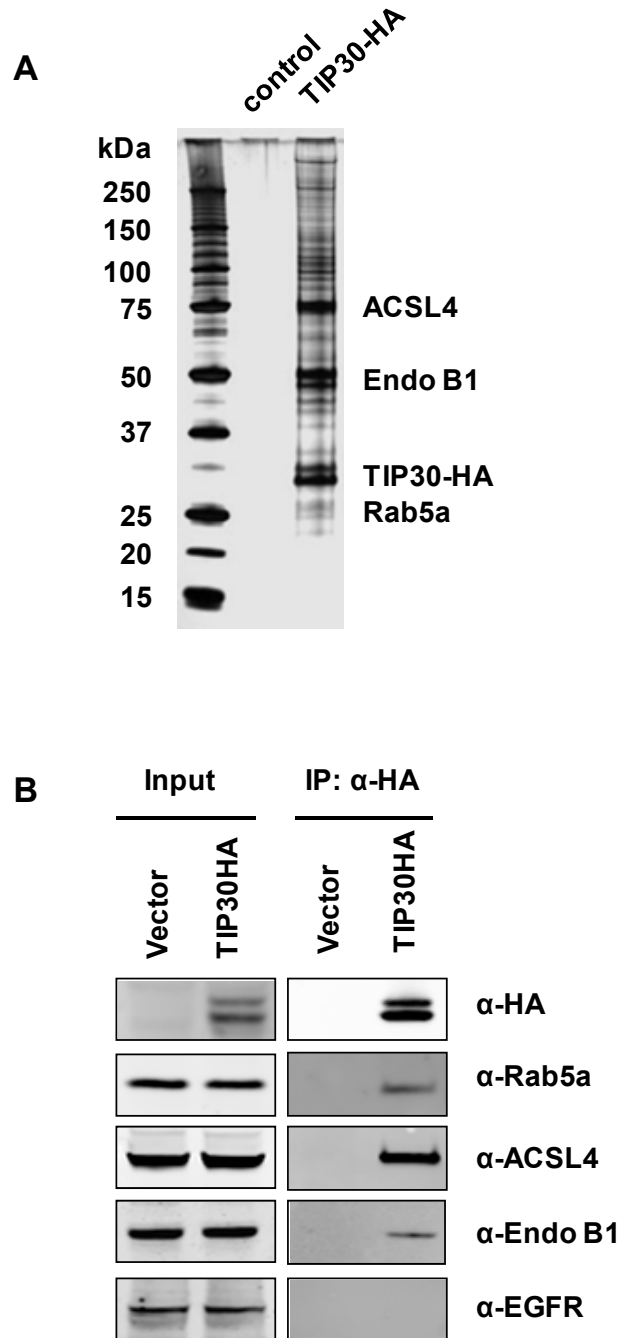
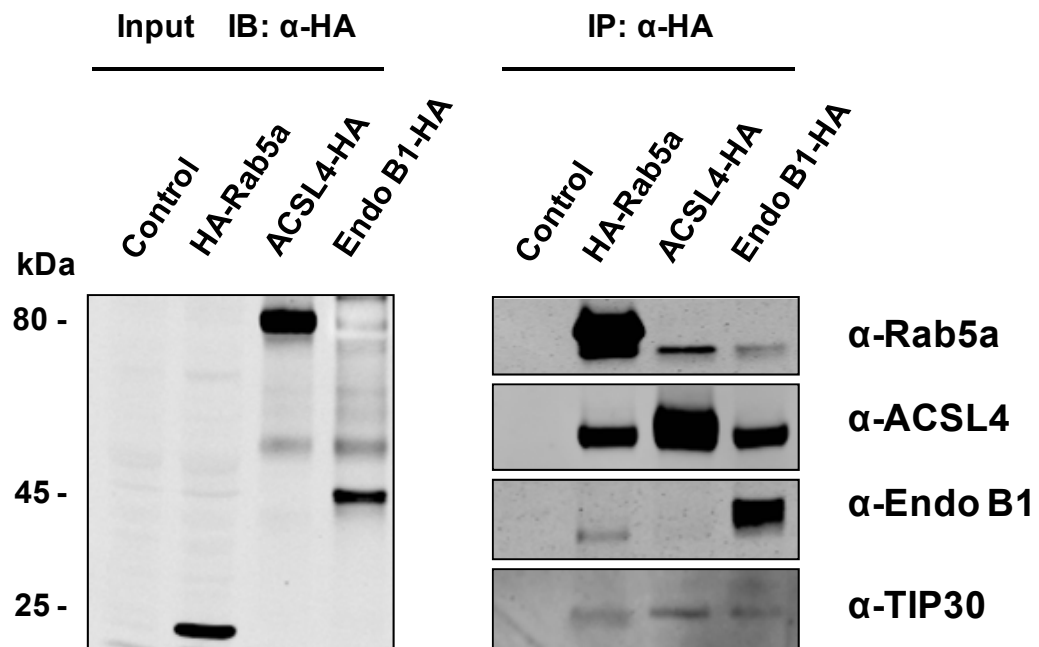


Figure 2.1 Cont'd

**C**



**D**

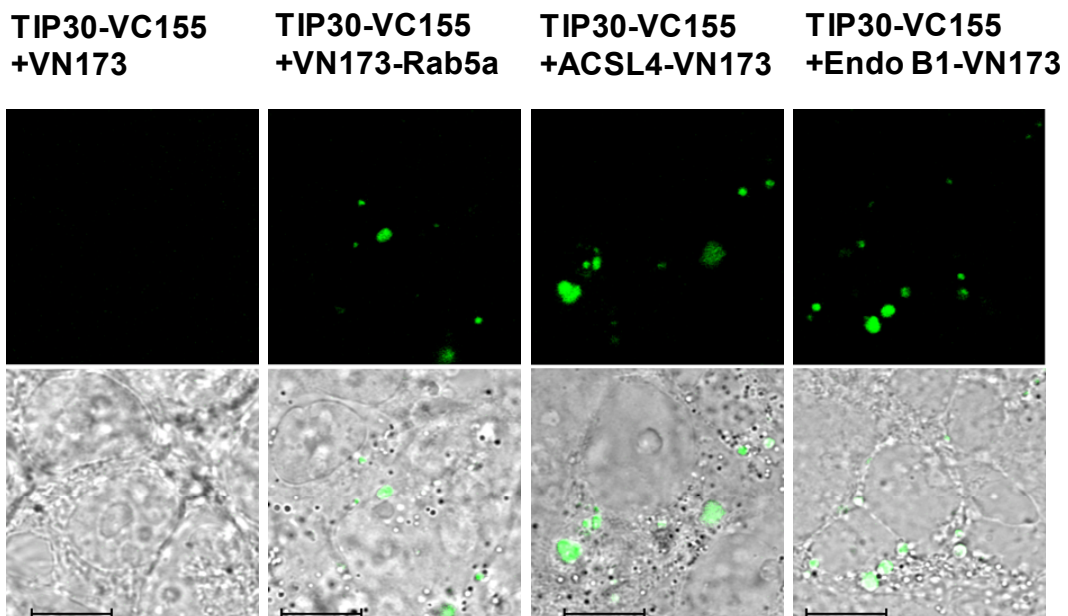


Figure 2.1 Cont'd

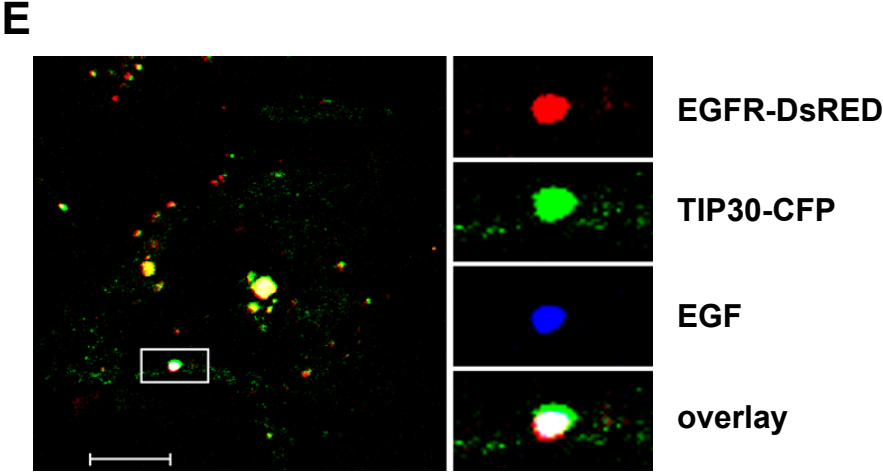


Figure 2.2 TIP30, Rab5a, ACSL4, and Endo B1 promote the endocytic downregulation of EGFR.

(A-E) Knockdown of TIP30, Rab5a, ACSL4, or Endo B1 results in delayed EGFR degradation and sustained EGFR signaling. Control PLC/PRF/5 cells (A), TIP30 (B), Rab5a (C), Endo B1 (D), and ACSL4 (E) knockdown cells were collected at various time points after EGF internalization and subjected to immunoblot analysis with the indicated antibodies. Results are typical and representative of experiments on cells from two different shRNAs.

(F) Quantification of EGFR protein levels in (A-E) using Odyssey 2.1 software.

(G) Deletion of *Tip30* in mouse primary hepatocytes leads to delayed EGFR degradation and sustained EGFR signaling. Primary hepatocytes were isolated from wild type and *Tip30*<sup>-/-</sup> mice. Endocytosis induced EGFR degradation was analyzed as described in (A-E).

(H) Quantification of EGFR protein levels in (G) using Odyssey 2.1 software.

Figure 2.2 Cont'd

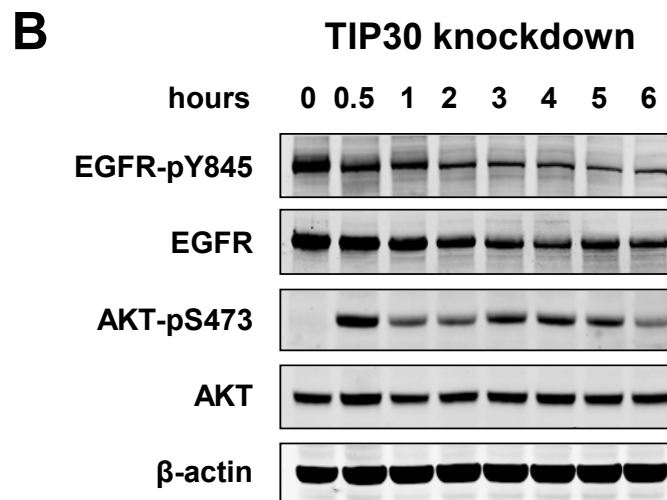
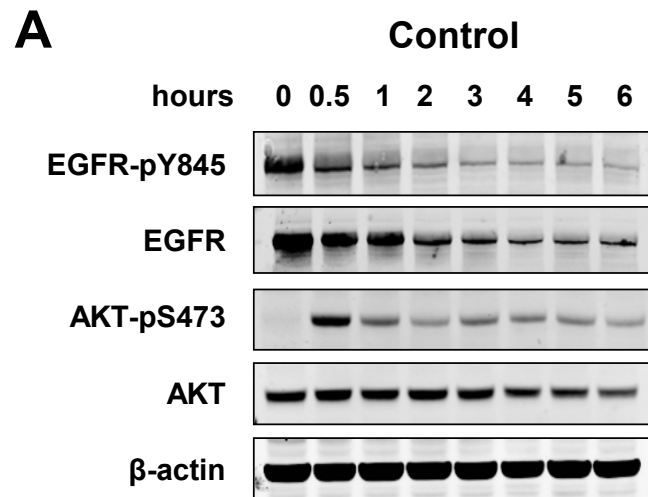


Figure 2.2 Cont'd

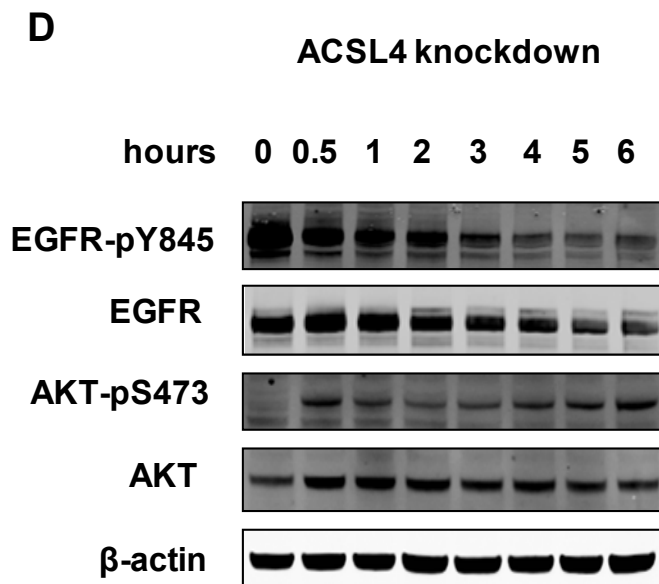
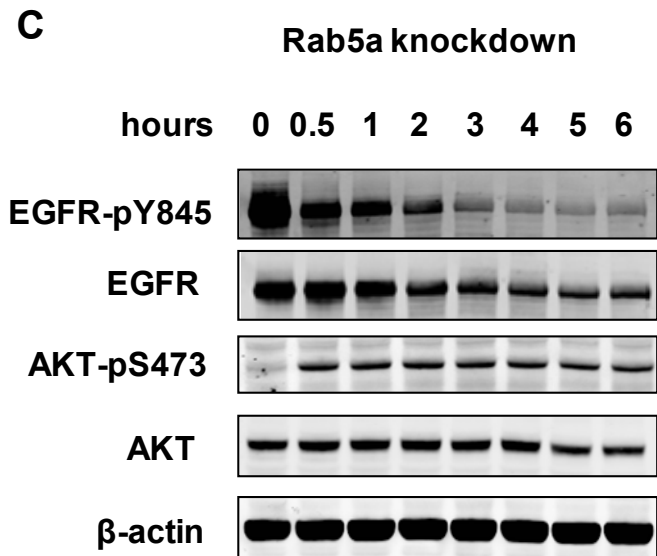


Figure 2.2 Cont'd

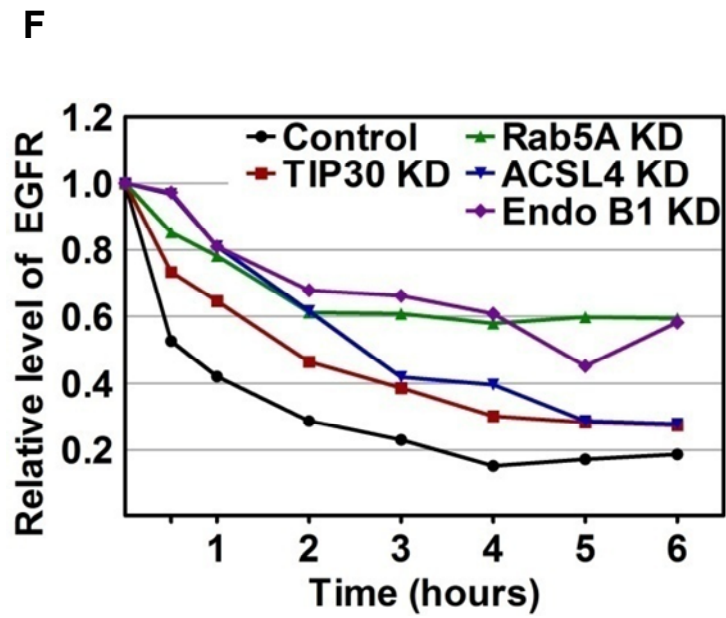
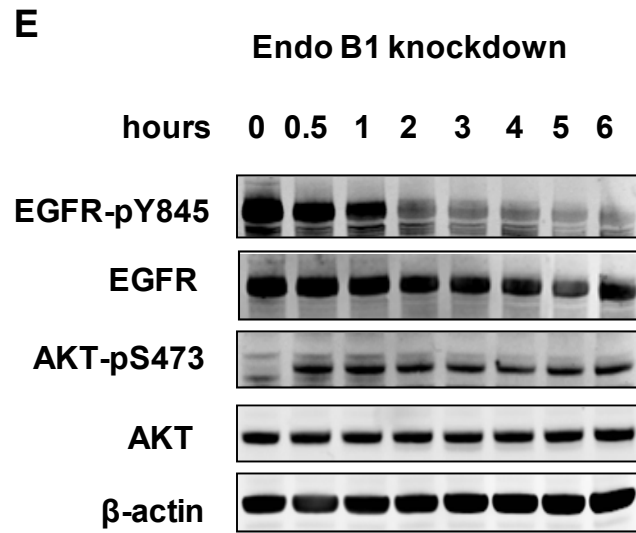
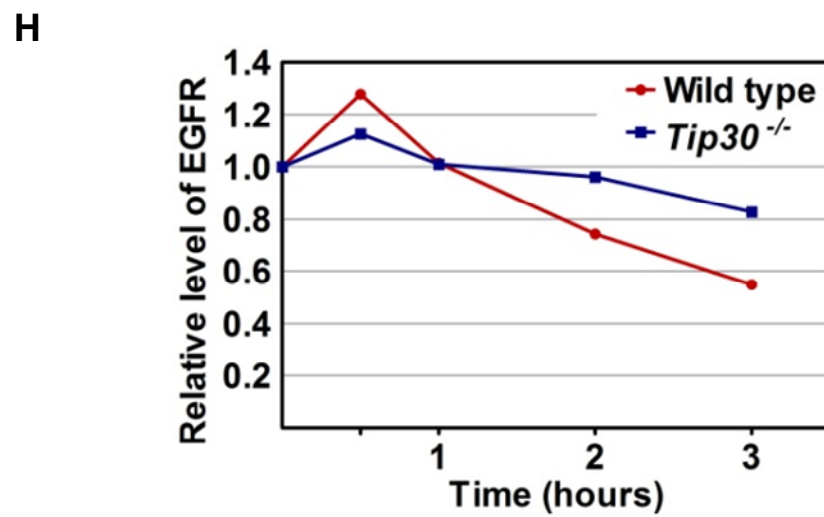
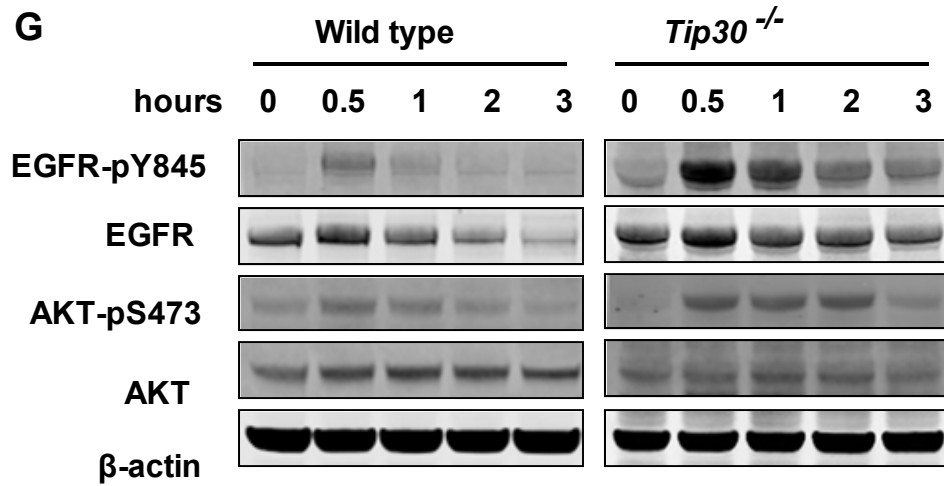


Figure 2.2 Cont'd



In addition, we observed that endogenous TIP30, ACSL4 and EndoB1 were co-sedimented at a position between the 150 and 443 kDa marker proteins in a 15-35% glycerol gradient (Figure S2.8A), and that bacterially expressed recombinant ACSL4 and Endo B1 were able to directly bind purified baculovirus-expressed recombinant TIP30 (Figure S2.8B). These results indicate that TIP30, ACSL4 and Endo B1 may form a protein complex to interact with Rab5a.

We next used bimolecular fluorescence complementation (BiFC) analysis (Hu et al., 2005) to visualize the association of TIP30 with these proteins in living cells. We observed that coexpressing TIP30-VC155 with VN173-Rab5a, ACSL4-VN173, or Endo B1-VN173 in cells reconstituted fluorescence, whereas coexpression of TIP30-VC155 and control VN173 did not (Figure 2.1D), indicating that TIP30 directly or indirectly interacts with these proteins in living cells.

Rab5a colocalizes with EGFR in endosomes in response to EGF (Lakadamyali et al., 2006; Leonard et al., 2008). To test if TIP30 is also targeted to endosomes, we coexpressed TIP30-CFP and EGFR-DsRed fusion proteins and examined their localization in HepG2 cells lacking detectable endogenous TIP30 and EGFR. Confocal microscopy analysis showed that TIP30-CFP partially colocalized with EGF and EGFR-DsRed in endosomes 10 min after cells were treated with Alexa-647 conjugated EGF (Figure 2.1E), suggesting that TIP30 was also targeted to endosomes. Consistently, immunostaining of endogenous TIP30 and EGFR revealed that TIP30 was partially localized to EGF-EGFR positive endosomes (Figure S2.8C). Taken together, our protein-protein interaction and colocalization studies suggest that TIP30, ACSL4 and Endo B1 form a protein complex that interacts with Rab5a.

## **Inhibition of TIP30, ACSL4 or Endo B1 leads to delayed EGFR degradation and sustained EGFR signaling**

Knockdown of Rab5a expression in HeLa cells retards EGFR transport from early endosomes to late endosomes and delays the degradation of EGFR (Chen et al., 2009a). The interaction of TIP30, ACSL4, and Endo B1 with Rab5a raises the possibility that these proteins may also function in endocytic pathways. We performed EGFR internalization analysis to investigate whether the inhibition of TIP30, ACSL4, or Endo B1 affects the endocytic downregulation of EGFR. Instead of continuous incubation with EGF, serum starved cells were first incubated with EGF on ice to allow for ligand binding to receptor, and then washed to remove unbound EGF before being moved to 37 °C for internalization. Nascent protein synthesis was blocked by cycloheximide in the culture medium. This approach eliminates the interference from continuous ligand entrance and new receptor synthesis, thus enabling us to monitor both the traffic and fate of EGF-EGFR complexes. We found that knockdown of TIP30, Rab5a, ACSL4, or Endo B1 in PLC/PRF/5 cells (Figure S2.9A-S2.9D) resulted in a slower reduction of total EGFR protein levels (Figure 2.2A-2.2F). To corroborate these findings, we further examined whether phosphorylation of EGFR at Y845 (EGFR-pY845) and AKT at S473 (AKT-pS473), a downstream target of EGFR signaling, were affected. Remarkably, the levels of EGFR-pY845 and AKT-pS473 sustained much longer in TIP30, ACSL4, Endo B1 or Rab5a knockdown cells than in control cells (Figure 2.2A-2.2F).

To assess the effect of TIP30 deletion on EGFR endocytosis in normal cells and to exclude off-target effects of shRNAs, we performed EGFR internalization analysis using primary hepatocytes isolated from wild type and TIP30 knockout mouse littermates. Deletion of *Tip30* in primary hepatocytes delayed EGF-induced EGFR degradation (Figure 2.2G and 2.2H); and the

phosphorylation of EGFR at Y845 and Akt at S473 was higher and sustained longer in *Tip30*<sup>-/-</sup> hepatocytes than in wild type hepatocytes. Together, these data provide strong evidence that TIP30, ACSL4, Endo B1 are involved in the efficient endocytic downregulation of EGFR protein level and signaling.

### **TIP30, ACSL4 and Endo B1 are involved in endocytic trafficking of EGF-EGFR**

Despite the earlier studies indicating that dissociation and degradation of endocytic EGF-EGFR complex occurred in lysosomes, cumulative evidence has clearly demonstrated that EGFR is inactivated before being degraded and that EGF dissociates from EGFR prior to lysosomal transfer (Authier and Chauvet, 1999; Burke et al., 2001; Murphy et al., 2009b; Umebayashi et al., 2008). To test whether depletion of TIP30, Rab5a, ACSL4, and Endo B1 affects EGF dissociation from EGFR, we tracked Alexa-488 conjugated EGF (Alexa<sup>488</sup>-EGF) and EGFR at different time points after internalization. As expected, fluorescent EGF partially colocalizes with EGFR and Rab5a in control cells after 15 and 30 min internalization (Figure S2.10A). Interestingly, EGF exited in membrane-bound vesicles from EGFR positive endosomes in control cells after 60 min internalization (Figure 2.3A). In contrast, the majority of EGF remained colocalized with EGFR in TIP30 or Rab5a knockdown cells (control cells: 7 ± 3%; TIP30 knockdown cells: 36 ± 4%; Rab5a knockdown cells: 46 ± 5%; n = 60, p < 0.01 versus control cells; Figure 2.3A and 2.3C). The EGF vesicles were devoid of early endosome markers EEA1 and Rab5a, as well as late endosomal and lysosomal marker LAMP1 (Figure 2.3D), indicating that they are neither early/late endosomes nor lysosomes.

Figure 2.3 TIP30 and Rab5a depletion delays the exit of EGF from early endosomes.

**(A)** Knockdown of TIP30 or Rab5a causes delayed exit of EGF from early endosomes. Cells expressing control shRNA or shRNA against TIP30 or Rab5a were subjected to EGFR internalization analysis. After internalization of Alexa<sup>488</sup>-EGF (blue) for 60 min, cells were fixed and double-immunostained for EGFR (red) and EEA1 (green). Nucleus was stained by DAPI (gray). Magenta results from overlap between red and blue. Results are representative of at least three independent experiments on cells expressing two different shRNAs. Boxed areas are magnified. Scale bars, 10  $\mu$ m.

**(B)** Deletion of *Tip30* in mouse primary hepatocytes leads to trapping of EGF in early endosomes. Wild type and *Tip30*<sup>-/-</sup> primary hepatocytes were subjected to same EGFR internalization analysis as described in (A). Boxed areas are magnified. Scale bars, 10  $\mu$ m.

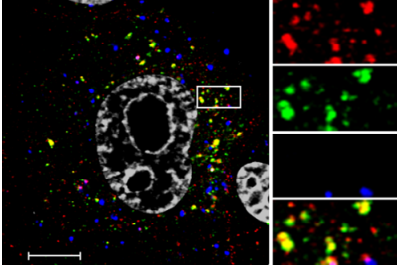
**(C)** Quantitative analysis of EGF-EGFR colocalization 60 min after EGF internalization. Sixty cells represented by Figure 2.2A, 2.2B and Figure 2.4A in each group were analyzed using MBF\_imageJ. Pearson's colocalization coefficients were calculated and converted to percentages. Data represent means  $\pm$  SEM. \* $P < 0.05$ , \*\* $P < 0.01$ , relative to control or wild type cells; t test.

**(D)** EGF exits endosomes in vesicles. Cells were stained for EGFR and LAMP1 60 min after EGF internalization. Scale bars, 10  $\mu$ m.

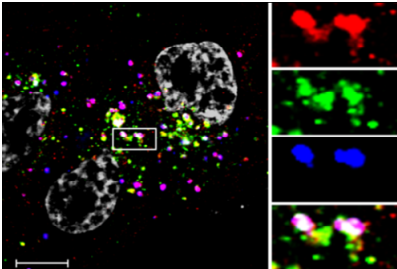
Figure 2.3 Cont'd

**A** EGFR EEA1 EGF

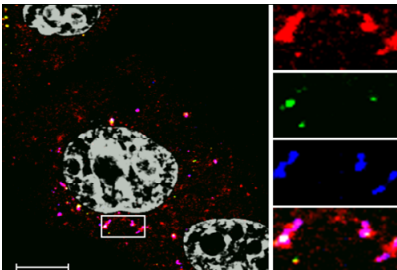
PLC/PRF/5 control, 60 min



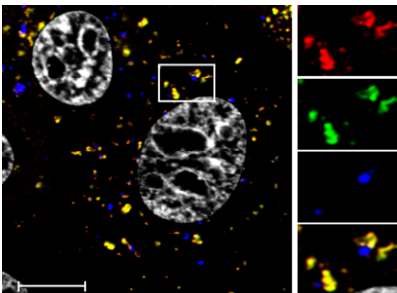
TIP30 KD, 60 min



Rab5a KD, 60 min

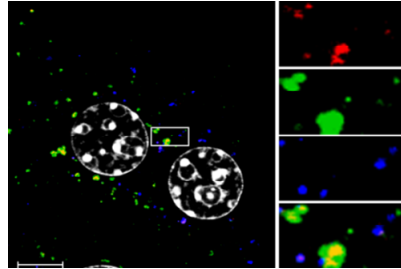


**D** EGFR LAMP1 EGF

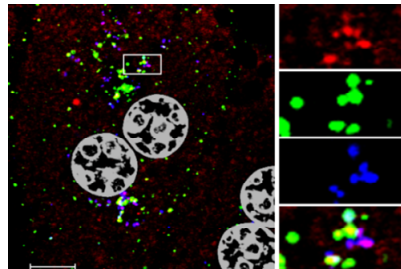


**B** EGFR EEA1 EGF

WT Hepatocytes, 60 min

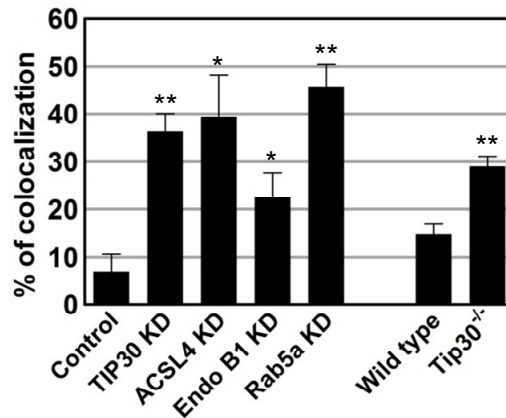


*Tip30*<sup>-/-</sup> Hepatocytes, 60 min



**C**

EGF-EGFR colocalization



We next performed EGFR internalization analysis using wild type and *Tip30*<sup>-/-</sup> primary hepatocytes. Consistent with the preceding results, *Tip30* deletion increased the colocalization of EGF and EGFR nearly 2 fold (wild type primary hepatocytes: 15 ± 2%; *Tip30*<sup>-/-</sup> primary hepatocytes: 29 ± 2%; n = 20, p < 0.01; Figure 2.3B and 2.3C).

Likewise, knockdown of ACSL4 or Endo B1 expression also increased the colocalization of EGF and EGFR (ACSL4 knockdown cells: 40 ± 8%; Endo B1 knockdown cells: 23 ± 5%; n = 60, p < 0.05 versus control cells; Figure 2.3A and 2.3C). The majority of EGF colocalized with EGFR even after 120 min internalization in knockdown and *Tip30*<sup>-/-</sup> cells (Figure S2.10A-S2.10C). Taken together, these results suggest that TIP30, ACSL4, Endo B1, and Rab5a not only physically interact but also function together in promoting EGF dissociation from EGFR during endocytic trafficking.

Figure 2.4 TIP30, ACSL4, and Endo B1 are required for the localization of Rab5a to early endosomes.

(A) Knockdown of TIP30, ACSL4, or Endo B1 inhibits the recruitment of Rab5a to early endosomes. Control and TIP30, ACSL4, or Endo B1 knockdown cells were subjected to EGFR internalization analysis. Sixty min after internalization of Alexa<sup>488</sup>-EGF (blue), cells were immunostained for EGFR (red) and Rab5a (green). Nucleus is stained by DAPI (gray). Results are typical and representative of three experiments on cells from two different shRNAs. The boxed areas are magnified. Scale bars, 10  $\mu$ m.

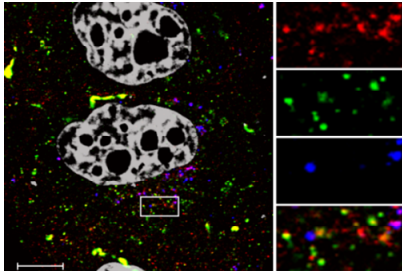
(B) *Tip30* deletion in primary hepatocytes inhibits the recruitment of Rab5a to early endosomes. Primary hepatocytes were stained for EGFR (red) and Rab5a (green) after 60 min EGF (blue) internalization. The boxed areas are magnified. Scale bars, 10  $\mu$ m.

(C) Quantitative analysis of Rab5a-EGFR colocalization after 60 min EGF internalization was performed as described in Figure 2.2C. Data represent means  $\pm$  SEM. \* $P < 0.05$ , \*\* $P < 0.01$ , relative to control or wild type cells; t test.

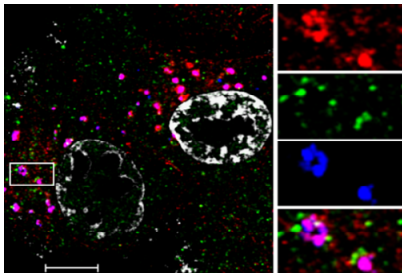
Figure 2.4 Cont'd

**A** EGFR Rab5a EGF

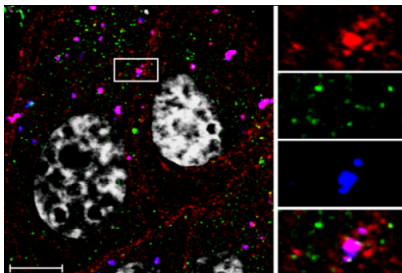
PLC/PRF/5 control, 60 min



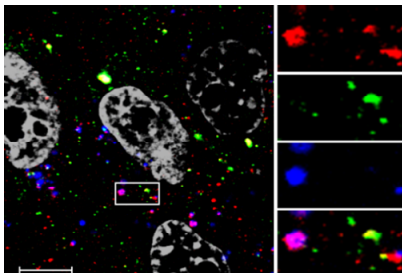
TIP30 KD, 60 min



ACSL4 KD, 60 min

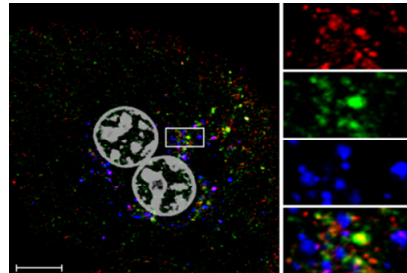


Endo B1 KD, 60 min

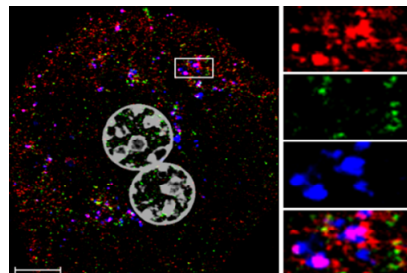


**B** EGFR Rab5a EGF

WT Hepatocytes, 60 min

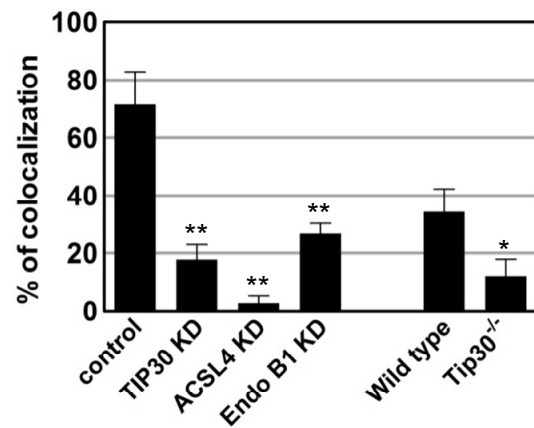


*Tip30*<sup>-/-</sup> Hepatocytes, 60 min



**C**

Rab5a-EGFR colocalization



## TIP30, ACSL4, and Endo B1 promote the recruitment of Rab5a to early endosomes

Endocytic vesicles gain Rab5a dynamically mostly by membrane fusion with Rab5-positive endosomes in the course of cargo transport (Rink et al., 2005). This is further supported by the observation that Rab5a is mainly localized on numerous membranous vesicles in the perinuclear region of cells under steady state condition and is rapidly recruited to early endocytic vesicles at the cell periphery in response to EGF (Lakadamyali et al., 2006; Leonard et al., 2008). The similar effects of TIP30 and Rab5a knockdown on EGFR endocytosis prompted us to test whether TIP30 is involved in the recruitment of Rab5a to early endosomes. In control cells, Rab5a appeared in EGFR positive endosomes, from which EGF had exited after 60 min EGF internalization (Figure 2.4A). By contrast, the colocalization of Rab5a and EGFR was significantly decreased in TIP30 knockdown cells (control cells:  $72 \pm 11\%$ ; TIP30 knockdown cells,  $18 \pm 5\%$ ;  $n = 60$ ,  $p < 0.01$ ; Figure 2.4A and 2.4C) and *Tip30*<sup>-/-</sup> primary hepatocytes (wild type hepatocytes:  $34 \pm 8\%$ ; *Tip30*<sup>-/-</sup> hepatocytes:  $12 \pm 5\%$ ;  $n = 20$ ,  $p < 0.05$ ; Figure 2.4B and 2.4C). Similar results were obtained with ACSL4 or Endo B1 knockdown cells (ACSL4 knockdown cells:  $3 \pm 2\%$ ; Endo B1 knockdown cells:  $27 \pm 4\%$ ;  $n = 60$ ,  $p < 0.01$  versus control cells; Figure 2.4A and 2.4C). Interestingly, there were a few Rab5a positive early endosomes in Endo B1 knockdown cells, which was probably the result of incomplete knockdown. However, these Rab5a positive endosomes appeared different from those in control cells. They did not release EGF even after 120 min of internalization (Figure S2.10B), indicating that Endo B1 has an additional function after Rab5a recruitment. This provides a possible explanation for the observation that Endo B1 knockdown cells have less EGF-EGFR colocalization and more Rab5a-EGFR overlap, but have longer lasting EGFR stability compared to TIP30 and ACSL4

knockdown cells (Figure 2.3C, 2.4C and 2.2A-2.2F). Together, these results indicate that TIP30, ACSL4, and Endo B1 promote efficient Rab5a recruitment to early endosomes.

### **Rab5a vesicles transport V-ATPases to early endosomes**

Curiously, we noted that Rab5a appeared in vesicles when it was not localized to EGFR-positive endosomes (Figure 2.4A and 2.4B). To further characterize those EGFR-negative Rab5a vesicles, we co-stained EEA1 and Rab5a in wild type mouse primary hepatocytes 30 min after EGF internalization. The EGFR-negative Rab5a vesicles were also negative for EEA1 and transferrin receptor (Figure S2.11A and S2.11B), suggesting that they are neither plasma membrane-derived endocytic vesicles nor recycling endosomes, but likely transporting vesicles that originate from the trans-Golgi network.

Dissociation of ligand-receptor complexes inside endosomes is caused by the low luminal pH created by V-ATPases. The previous observations that lack of Rab5a in early endosomes was concomitant with delayed EGF-EGFR dissociation induced by loss of TIP30 or its interacting proteins suggested the possibility that Rab5a vesicles deliver V-ATPases to early endosomes. To address this issue, we examined the intracellular localization of V-ATPases for the regulatory subunit H (ATP6V1H). A significant reduction of ATP6V1H localization to EGFR positive endosomes was observed in TIP30, Rab5a, ACSL4, or Endo B1 knockdown cells (control cells:  $46 \pm 7\%$ ; TIP30 knockdown cells:  $25 \pm 4\%$ ; Rab5a knockdown cells:  $19 \pm 1\%$ ; ACSL4 knockdown cells:  $19 \pm 2\%$ ; Endo B1 knockdown cells:  $21 \pm 1\%$ ;  $n = 60$ ,  $p < 0.05$  versus control cells; Figure 2.5A and 2.5C) and in *Tip30*<sup>-/-</sup> primary hepatocytes (wild type hepatocytes:  $61 \pm 4\%$ ; *Tip30*<sup>-/-</sup> hepatocytes:  $23 \pm 6\%$ ;  $n = 20$ ,  $p < 0.01$ ; Figure 2.5B and 2.5C). ATP6V1H positive

staining was observed in Rab5a vesicles lacking EGF in TIP30 knockdown cells (Figure S2.11C).

Figure 2.5 Rab5a vesicles transport V-ATPase to early endosomes.

(A) Depletion of TIP30, ACSL4, or Endo B1 inhibits the loading of V-ATPase on endocytic vesicles. Cells were immunostained for EGFR (red) and a V-ATPase subunit ATP6V1H (green) after 60 min EGF (blue) internalization. Results are typical and representative of three experiments on cells from two different shRNAs. The boxed areas are magnified. Scale bars, 10  $\mu\text{m}$ .

(B) Deletion of *Tip30* in mouse primary hepatocytes results in V-ATPase mislocalization. Immunostaining was performed as described in (B). Scale bars, 10  $\mu\text{m}$ .

(C) Colocalization of V-ATPase and EGFR was analysed using MBF\_ImageJ. Pearson's colocalization coefficients were calculated and converted to percentages.  $*P < 0.05$ ,  $**P < 0.01$ , relative to control or wild type cells; t test.

(D) EGF is released after EGF endocytic vesicles merge with Rab5a vesicles. Live cells expressing ATP6V1H-DsRed (red) and EYFP-Rab5a (green) were imaged by confocal microscopy at the indicated times after Alexa<sup>647</sup>-EGF internalization and images of a single focal plane were acquired. A typical EGF endocytic vesicle movement was shown. Arrows points toward the two vesicles undergoing merger and EGF release.

Figure 2.5 Cont'd

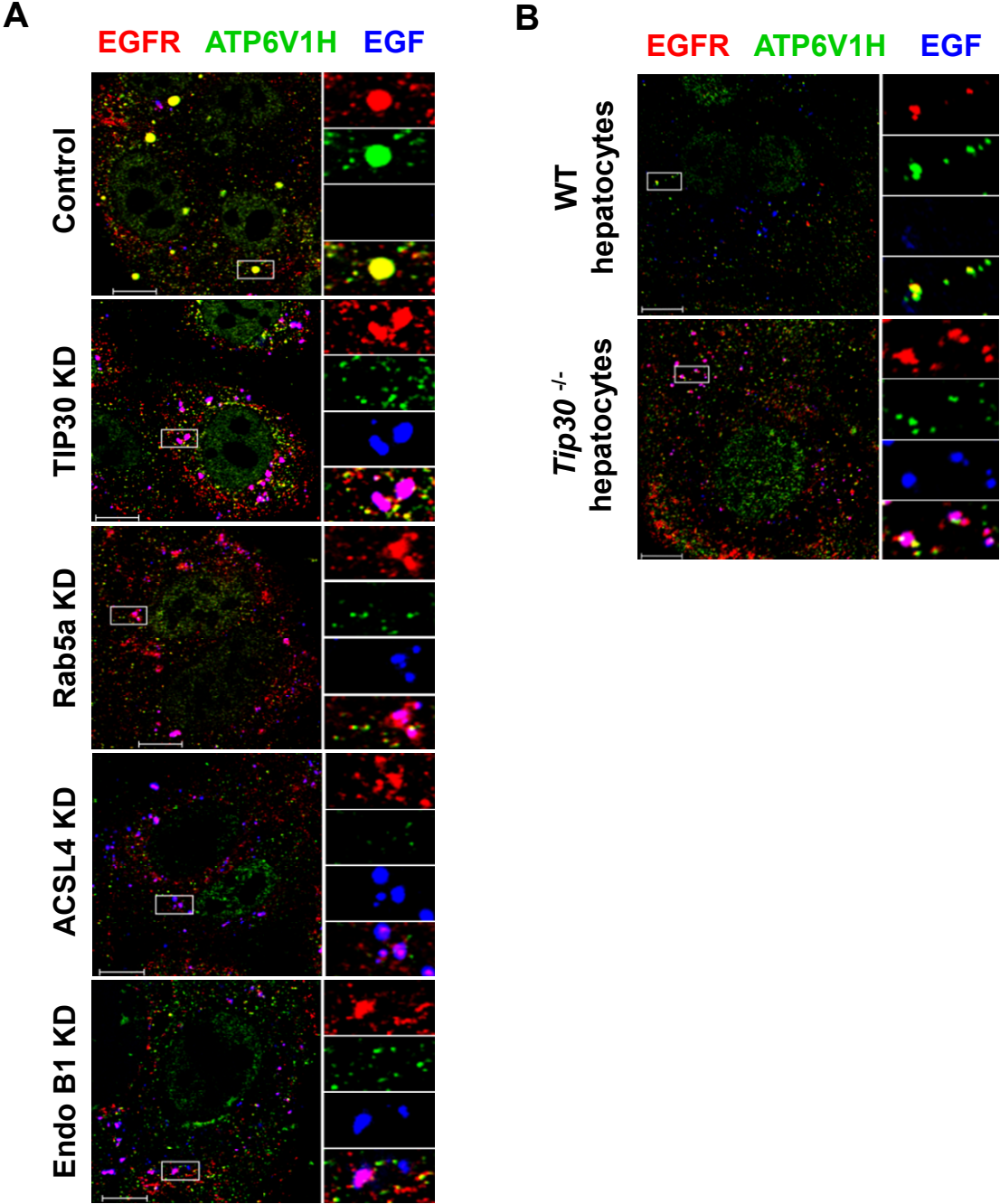
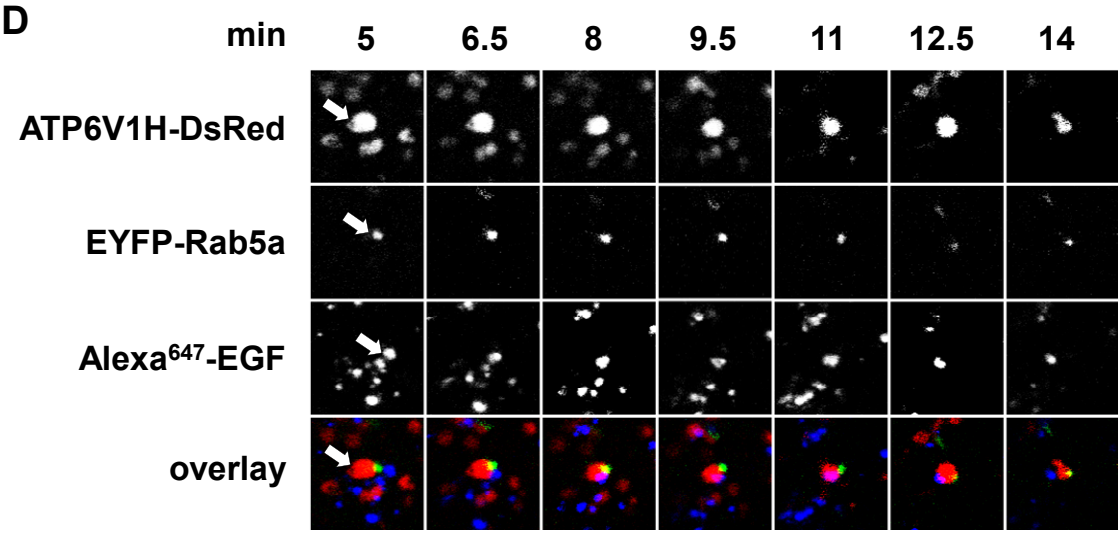
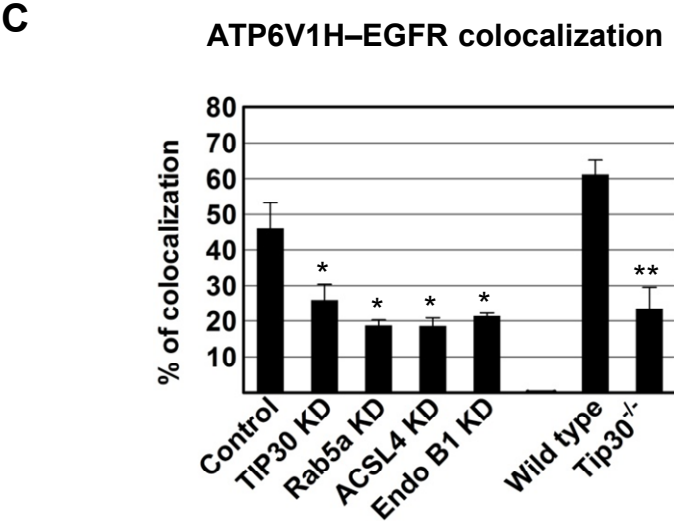


Figure 2.5 Cont'd



Moreover, in live PLC/PRF/5 cells co-expressing EYFP-Rab5a and ATP6V1H-DsRed, EGF-positive endosomes fused with Rab5a-ATP6V1H vesicles at 11 min after EGF internalization and released EGF 3 min after the merge (Figure 2.5D). Taken together, these data indicate that Rab5a may contribute to ligand-receptor dissociation by transporting V-ATPases to endocytic vesicles and that TIP30, ACSL4 and Endo B1 are required for efficient transport.

### **TIP30 complex and arachidonic acid promote fusion between endocytic and Rab5a vesicles *in vitro***

Since Rab5a on vesicles is transported to early endosomes by membrane fusion events (Leonard et al., 2008; Rink et al., 2005), we sought to investigate whether the TIP30 complex facilitates membrane fusion between Rab5a vesicles and early endosomes. First, we adopted a previously validated *in vitro* cell free fusion assay (Bethani et al., 2009; Brandhorst et al., 2006) with modifications. Instead of using two groups of early endosomes, we prepared Rab5a vesicles from starved HepG2 cells expressing EYFP-Rab5a fusion proteins and endocytic vesicles from EGF treated HepG2 cells expressing EGFR-DsRed fusion proteins (Fuchs and Ellinger, 2002; Gorvel et al., 1995). The two types of vesicles that contain equal amount of proteins were incubated in the fusion buffer at 37 °C followed by examination with confocal microscope. Putative vesicle fusion was represented by the fluorescence overlap between EGFR-DsRed and EYFP- Rab5a. Since ACSL4 is an acyl-CoA ligase with high substrate preference for arachidonic acid (C20:4) (Cao et al., 1998), we also tested if arachidonic acid and coenzyme A are needed. Vesicles resulting from reactions that were kept on ice evenly distributed on the slides, appearing as small vesicles with low fluorescence intensity and virtually no overlap between the two types of vesicles (Figure 2.6A, lane 1).

Figure 2.6 The TIP30 protein complex, arachidonic acid and coenzyme A promote the fusion between endocytic and Rab5a vesicles.

(A) Aliquots of isolated EGFR-DsRed and EYFP-Rab5a vesicles (both contain 20  $\mu\text{g}$  proteins) were mixed and incubated in the reactions with the indicated components. Reaction mixtures were spotted on glass slides and images were taken using confocal microscope. Panels 1, 4 and 6 were scanned with 3 $\times$  amplification gain setting due to lower fluorescence intensity of individual vesicles. Images are single plane and are representative for at least three independent experiments. Scale bars, 5  $\mu\text{m}$ .

(B) Signal overlap was quantified using MBF\_ImageJ. Pearson's colocalization coefficients were calculated from three independent experiments and converted to percentages. Data represent means  $\pm$  SEM.  $**P < 0.01$ ,  $***P < 0.001$ ; t test.

(C) Analysis of vesicle fusion with electron microscope. Vesicles incubated in the complete reaction with or without arachidonic acid were stained with uranyl acetate and examined using TEM. Scale bars, 500 nm.

(D) The graphs show the percentages of vesicles with different diameters. At least 6 images from two independent experiments were counted. Data represent means  $\pm$  SEM.  $n = 150$ ;  $**P < 0.01$ , t test.

(E) Bacterially expressed recombinant TIP30, ACSL4 and Endo B1 promote fusion between endocytic and Rab5a vesicles. Vesicles (20  $\mu\text{g}$  proteins) incubated with the indicated proteins (20 ng each) were examined using confocal microscope. Scale bars, 5  $\mu\text{m}$

(F) Quantification of images represented in (D) was performed similarly as in (B)

Figure 2.6 Cont'd

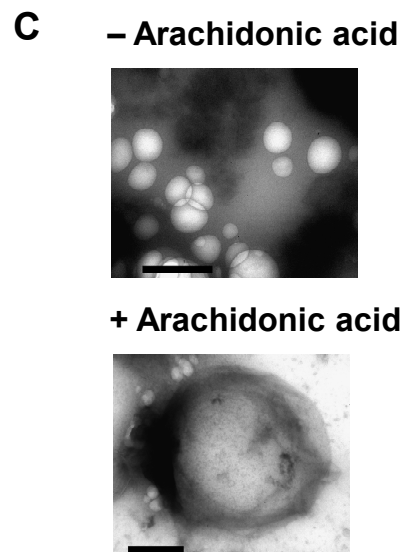
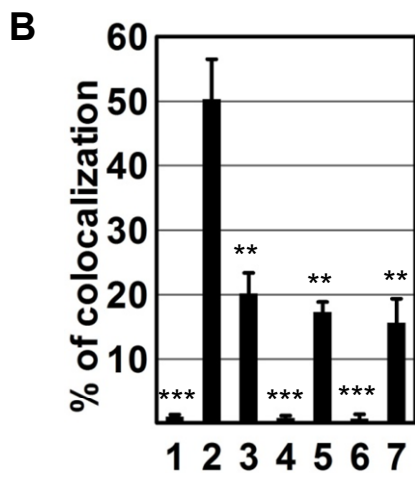
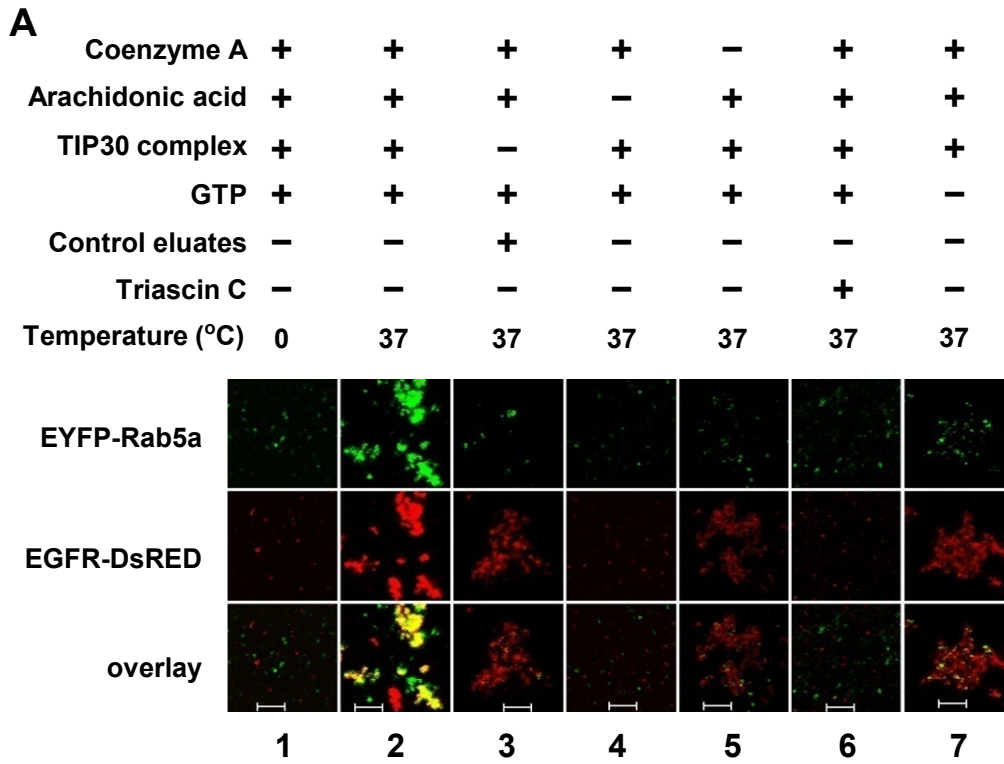
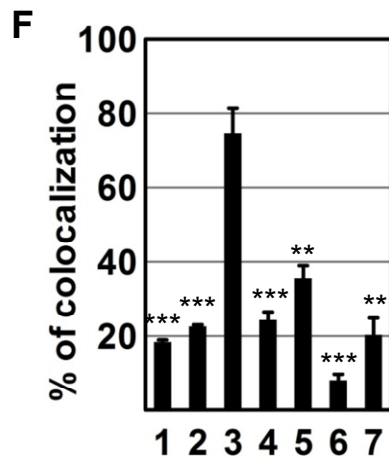
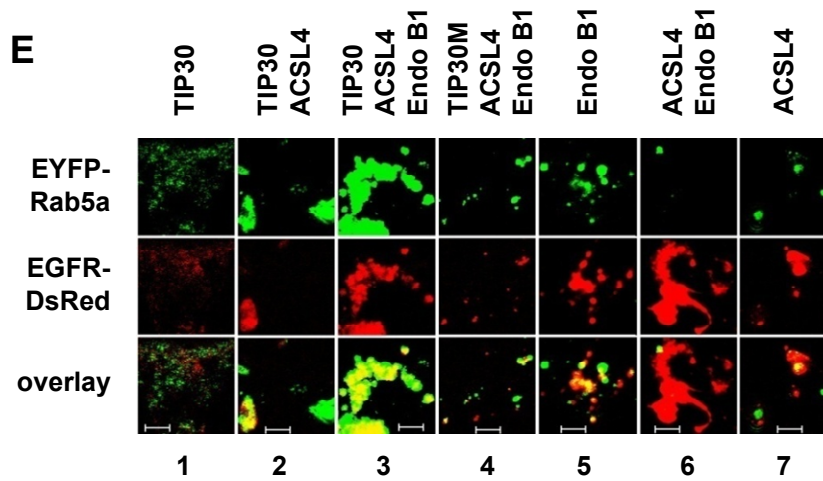
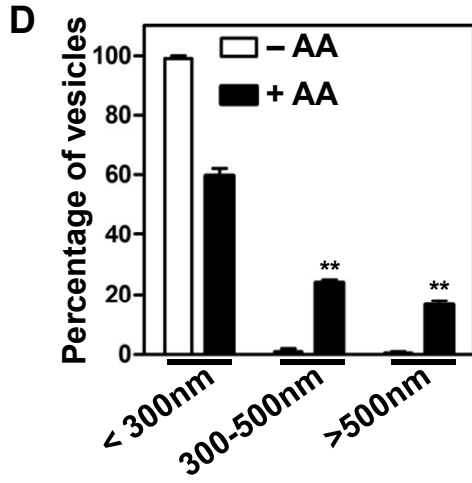


Figure 2.6 Cont'd



Similarly, no vesicle overlap was observed in the absence of arachidonic acid or in the presence of triacsin C (10  $\mu$ M), a potent inhibitor of long chain fatty acyl-CoA synthetase (Figure 2.6A and 2.6B). In contrast, in the presence of arachidonic acid and coenzyme A immunopurified TIP30 complex caused vesicle enlargement and significantly increased overlap between the two vesicles (TIP30 complex:  $50 \pm 6\%$ ; control eluates:  $20 \pm 3\%$ ; omitting coenzyme A:  $17 \pm 2\%$ ; omitting GTP:  $16 \pm 4\%$ ;  $n = 6$  representative confocal images of  $143 \times 143 \mu\text{m}$ ,  $p < 0.01$  versus TIP30 complex), thereby resulting in much intensified fluorescence. Rab5a vesicles attached to aggregated endocytic vesicles, but remained as small particles when the TIP30 complex, coenzyme A or GTP was omitted. We next screened for other fatty acids that might promote the putative fusion, including palmitic, palmitoleic, oleic, linoleic, linolenic, eicosapentaenoic, and docosahexaenoic acids. None of these fatty acids could promote vesicle enlargement and vesicle overlap (data not shown). Given that arachidonic acid is specifically needed for vesicle membrane fusion (Creutz, 1981; Mayorga et al., 1993), these data imply that fluorescent overlap between Rab5a and endocytic vesicles promoted by the TIP30 complex and arachidonic acid was possibly due to membrane fusion.

To validate that the observed vesicle overlap was due to membrane fusion, we examined the vesicles that resulted from fusion reactions by transmission electron microscopy (TEM). Without the addition of arachidonic acid, all vesicles appeared spherical and ranged in diameter from 50 to 300 nm. In contrast, the complete fusion reaction led to the production of vesicles enlarged to more than 1  $\mu\text{m}$  in diameter (Figure 2.6C); the larger vesicles were not found in reactions without arachidonic acid. The captured ongoing fusion further confirmed that fusion actually happened (Figure S2.12A). Quantitative analysis revealed a significant increase in the amount of enlarged vesicles (with arachidonic acid: 300-500 nm,  $24 \pm 2\%$ ;  $> 500$  nm,  $16.5 \pm 1.5\%$ ; without

arachidonic acid: 300-500 nm,  $1 \pm 0.2\%$ ;  $> 500$  nm, 0;  $n = 150$ ,  $p < 0.01$ ; Figure 2.6D). Together, these data indicate that the TIP30 complex promotes the fusion of Rab5a vesicles with endocytic vesicles and that the synthesis of arachidonyl-CoA by ACSL4 is essential for vesicle membrane fusion.

To exclude possible influences of other associated or contaminating proteins in immunopurified TIP30 complexes, we replaced the complexes with bacterially expressed recombinant TIP30, ACSL4, and Endo B1 in cell free assays. The three highly purified recombinant proteins (Figure S2.12B) can efficiently promote overlap ( $75 \pm 6\%$ ) between the two vesicles, whereas lack of any of these proteins led to significantly less overlap (TIP30:  $18 \pm 1\%$ ; TIP30 and ACSL4:  $23 \pm 1\%$ ; Endo B1:  $35 \pm 3\%$ ; ACSL4 and EndoB1:  $8 \pm 2\%$ ; ACSL4:  $20 \pm 5\%$ ;  $n = 6$  representative images of  $143 \times 143 \mu\text{m}$ ;  $p < 0.01$  versus TIP30, ACSL4 and Endo B1; Figure 2.6E and 2.6F). TIP30M, a TIP30 mutant with a mutated putative nucleotide binding motif (GXXGXXG) (Xiao et al., 2000), only promoted  $24 \pm 2\%$  overlap ( $n = 6$  representative images of  $143 \times 143 \mu\text{m}$ ;  $p < 0.01$  versus TIP30, ACSL4 and Endo B1; Figure 2.6D, panel 4). These data suggest that TIP30, ACSL4 and Endo B1 together are capable of promoting the heterotypic fusion between endocytic and Rab5a vesicles.

### **Vesicle tethering and stacking induced by acylation of phosphatidic acid**

To gain further insight into how TIP30 and its interacting proteins mediate membrane fusion, we first used  $^3\text{H}$ -arachidonic acid to label membrane lipids and found that at least one lipid species in purified early endosomes was specifically labeled by the TIP30 complex (Figure 2.7A). The production of the labeled lipid was significantly less in the reaction using control eluates or TIP30M immunoprecipitates, and was blocked by triacsin C. These data indicate that

lipids on early endosomes are the specific recipients of the arachidonyl group. Endophilins were suggested as lysophosphatidic acid (LPA) acyl transferases (Modregger et al., 2003; Schmidt et al., 1999). Consistent with a previous report (Gallop et al., 2005), we did not detect the acyl transferase activity of Endo B1 when using LPA as the substrate (Figure S2.13A). To identify the lipids that are modified, we performed protein-lipid overlay assays using membrane strips prespotted with 15 cellular membrane lipids (Figure S2.13B). TIP30 and Endo B1 specifically bind phosphatidic acid (PA) and cardiolipin, while Endo B1 also binds phosphatidylinositol 4-phosphate (PtdIns(4)P; Figure 2.7B). ACSL4 and Rab5a did not bind any lipids spotted on the membrane (data not shown). Cardiolipin is found predominantly in the inner mitochondrial membrane, whereas PA has been implicated in fusion of various intracellular membranes (Haucke and Di Paolo, 2007; Jenkins and Frohman, 2005). Therefore, we focused on PA and tested whether the TIP30 complex could convert PA to PA-derivatives. Lipids extracted from the acylation reactions with PA and arachidonic acid as substrates were subjected to MS/MS and LC-MS/MS spectrometry analyses (Figure S2.13C-S2.13E). The flow injection precursor scan in both modes revealed one predominant peak with an  $m/z$  (mass-to-charge ratio) value of 940.2, which is close to the exact mass (940.85) of triacylglycerols ( $C_{61}H_{112}O_6$ ). Thus, we speculate that triacylglycerol might be the PA derivative. To determine how PA derivatives would affect membrane fusion, we carried out acylation reactions by incubating PA or phosphoinositide (PI) with the TIP30 complex under the same condition as *in vitro* fusion assays. The resulting lipids were purified, resuspended by sonication, and incubated with vesicles. Interestingly, the PA derivatives promoted dramatic aggregation among endocytic and Rab5a vesicles on ice; however, vesicles remained to be visibly individual particles (Figure 2.7C).

Figure 2.7 Acylation of phosphatidic acid promotes vesicle tethering and stacking.

(A) Fatty acylation of endosomal lipids by the TIP30 complex. [<sup>3</sup>H]-arachidonic acid can be transferred to endosomal membrane lipids by TIP30 immunoprecipitates, but not by TIP30M immunoprecipitates or control immunoprecipitates (left panel). The reaction was blocked by 10 μM triacsin C. Image was acquired by scanning lipids resolved on TLC plate with a Molecular Dynamics Storm 860. \* indicates the radiolabeled lipid.

(B) TIP30 and Endo B1 strongly bind phosphatidic acid (PA). Protein-lipid overlay assays were carried out by incubating recombinant proteins with membranes containing 15 pre-spotted lipids. Bound proteins were detected by immunoblot.

(C) Triacylglycerol and modified PA promote vesicle tethering. Lipids were extracted after incubating 100 nmol PA and phosphatidylinositol (PI) with TIP30 complex or control eluates. Lipids were resuspended in homogenization buffer by sonication and were mixed with EGFR-DsRed and EYFP-Rab5a vesicles. Reaction mixtures were spotted on glass slides and images were taken using confocal microscope. Scale bars, 5 μm.

(D-H) Effects of lipid acylation were determined using electron microscope. Lipids were extracted after incubating PA with TIP30 immunoprecipitates (D), PA with recombinant TIP30, ACSL4, and Endo B1 (E), PA with control immunoprecipitates (G), or PI with TIP30 immunoprecipitates (H). Vesicles were incubated on ice with the extracted lipids or triacylglycerol (F) suspended in homogenization buffer and examined using electron microscope. Scale bars, 500 nm.

Figure 2.7 Cont'd

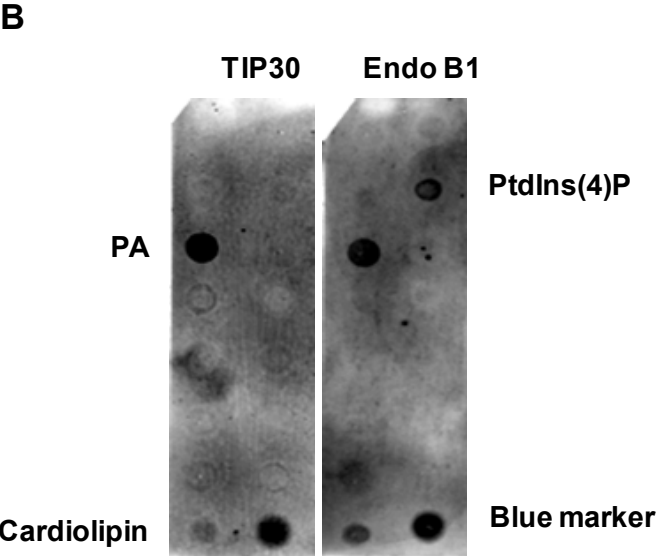
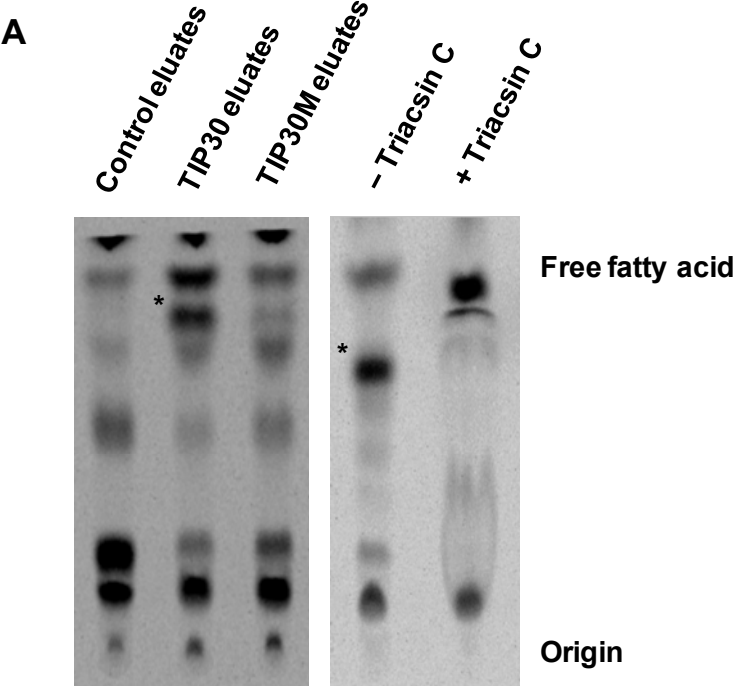
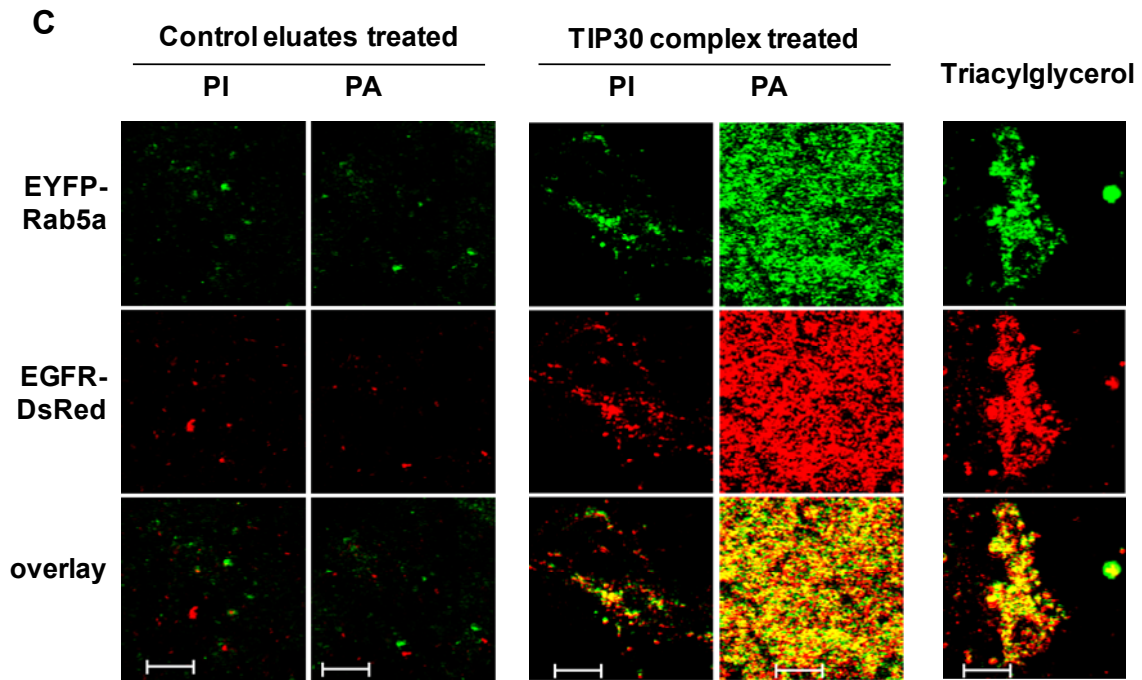


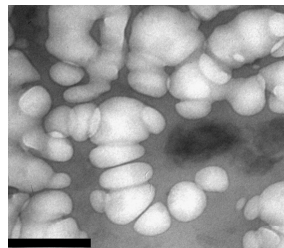
Figure 2.7 Cont'd



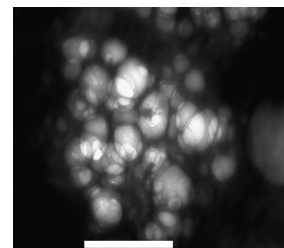
**D**  
PA+TIP30 complex



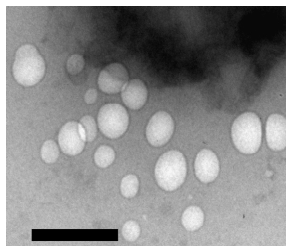
**E** PA+recombinant TIP30, ACSL4, Endo B1



**F** Triacylglycerol



**G** PA+control eluates



**H** PI+TIP30 complex



In contrast, unmodified PA incubated with control eluates did not promote significant membrane aggregation, nor did phosphoinositide (PI) that was prepared with the same procedure as the PA derivative. A triacylglycerol (1,2-Dilinoleoyl-3-palmitoyl-*rac*-glycerol) with a palmitoyl tail at the sn-3 position promoted significant aggregation (Figure 2.7C).

Finally, we used electron microscope to examine the vesicles after incubation with PA derivatives on ice. The vesicle aggregation caused by PA derivatives generated by immunopurified TIP30 complexes or recombinant proteins was apparently the result of both tethering and stacking (Figure 2.7D, 2.7E and S2.6F). In contrast the vesicle aggregation caused by the triacylglycerol seemed due only to tethering (Figure 2.7F), indicating that chain saturation and length (C20:4 vs C16:0) at the sn-3 position is important. Consistent with the confocal microscopy data, PA treated with control eluates (Figure 2.7G) or PI treated with immunopurified TIP30 complex (Figure 2.7H) had no apparent effect. These data indicate that the final product of the acyl transfer reaction, triacylglycerol, can promote aggregation among vesicles, although intermediates in the reaction are not ruled out to have a similar function.

Nonetheless, we did not observe complete fluorescence overlap and enlarged endosomes (> 1 $\mu$ m in diameter) as seen in Figure 2.6, suggesting that additional activities of the TIP30 complex or other proteins on the membranes, such as SNAREs, SNARE accessory factors, Rab5a and its effectors, are needed to accomplish the fusion steps following close membrane contact. Collectively, these data indicate that TIP30, ACSL4, and Endo B1 promote vesicle membrane fusion by fatty acylating PA.

## **Discussion**

### **Function of TIP30, ACSL4 and Endo B1 in endocytic trafficking**

Elucidating the molecular basis of intracellular trafficking and sorting of internalized receptors in early endosomes requires the identification of the critical components participating in these processes. The present study led to the identification of three new players that act together in controlling receptor-mediated endocytosis and revealed new insights into the mechanism of vesicle membrane fusion. Specifically, we showed that TIP30, Endo B1, and ACSL4 act as a functional unit to facilitate the Rab5a localization to early endosomes by promoting the fusion of Rab5a vesicles with endocytic vesicles. TIP30 and Endo B1 have been proposed to be tumor suppressors because their deficiency leads to spontaneous development of tumors in mice (Ito et al., 2003; Takahashi et al., 2007). Thus, our results indicate that TIP30 and Endo B1 suppress tumor growth, at least in part, through the regulation of the EGFR signaling pathway.

Endo B1 is particularly interesting, since it belongs to a family of proteins that have N-terminal BAR domains, which may sense and stabilize membrane curvature (Masuda et al., 2006b; McMahon and Gallop, 2005). Endo B1 and its homologue Endophilin 1 can directly bind and invaginate lipid bilayers into narrow tubules, suggesting a role of Endo B1 in membrane deformation (Farsad et al., 2001). It was proposed that Endophilins create membrane curvature by transferring arachidonic acid to lysophosphatidic acid (Schmidt et al., 1999). However, our data support the observation that Endophilins cannot transfer arachidonyl group to LPA (Gallop et al., 2005). The strong binding of PA to Endo B1 (Figure 2.7B) raised the question of whether Endo B1 takes PA as a potential substrate for its acyl transferase activity.

### **A role for Rab5a in transport of endosomal targeting proteins**

Rab5a is one of the Rab GTPases that are key regulators in vesicle formation, motility, tethering and docking, and membrane fusion (Grosshans et al., 2006; Pfeffer, 2001; Zerial and McBride, 2001). Rab5 on early endosomes has been shown to be able to promote endosome fusion *in vitro* (Gorvel et al., 1991). Our data showed that Rab5a vesicles can fuse with endocytic vesicles in a GTP dependant manner, suggesting that Rab5a also actively participates in the fusion of these two types of vesicles. Unlike homotypic endosome fusion, this type fusion requires the TIP30 complex, arachidonic acid and coenzyme A, but does not require additional NSF, SNARE proteins and Rab5 effectors. Given that high fusion efficiency of biological intact endosomes was not achieved *in vitro* in a recent study (Ohya et al., 2009), it would be interesting to further determine whether the TIP30 complex, arachidonic acid and coenzyme A could also promote homotypic endosome fusion.

The Rab family proteins anchor themselves at the cytoplasmic face of vesicles by their C-terminal modification with hydrophobic geranylgeranyl groups (Takai et al., 2001). This special way of membrane association makes them ideal candidates as identity tags that determine specificity during vesicle transport (Jahn et al., 2003). Interestingly, our data revealed that besides its function in early endosomes, Rab5a also appeared in vesicles carrying the integral membrane protein V-ATPase, a proton pump responsible for ligand-receptor dissociation. The localization of V-ATPase in early endosomes depends on Rab5a, suggesting that Rab5a is involved in delivering V-ATPases to the early endosome. Thus, Rab5a may share similar functions with many other Rab GTPases in determining specific destinations during vesicle transport.

### **Lipids and membrane fusion**

One of the unsolved issues in protein trafficking is to understand the mechanism underlying membrane fusion. It is widely believed that membrane fusion events are facilitated by the core protein machinery consisting of SNAREs, SNARE accessory factors, Rab5 and its effectors (Ohya et al., 2009; Stenmark, 2009). The SNAREs are thought to bring membranes together, whereas Rab5 recruits specific effectors to mediate vesicle tethering by controlling SNARE complexes. However, it is not known how these proteins establish the minimal fusion events, such as the local deformation of the membrane, the dehydration of lipid head groups, and overcoming the energy barrier caused by opposing charges in the membranes (Sorensen, 2009).

Cumulative evidence also supports the idea that certain fatty acids including arachidonic acid also play key roles in membrane fusion. For instance, arachidonic acid is required for endosome fusion *in vitro* (Mayorga et al., 1993), and is the most effective fusogen in chromaffin granule fusion (Creutz, 1981). In addition, membrane-bound arachidonic acid can drive annexin II-mediated membrane fusion of the lamellar body with the plasma membrane during the exocytosis (Chattopadhyay et al., 2003).

How does arachidonic acid promote membrane fusion? Arachidonic acid has been proposed to stimulate SNARE complex assembly (Connell et al., 2007; Latham et al., 2007; Rickman and Davletov, 2005). However, our data show that arachidonic acid is insufficient to support efficient membrane fusion without the TIP30 complex (Figures 2.6). We show that the arachidonyl group is transferred to endosomal PA to generate triacylglycerol that induces vesicle tethering and stacking (Figure 2.7). Thus, we suggest that arachidonic acid promotes membrane fusion by contributing to both PA acylation and SNARE complex assembly. Consistent with this, PA and its synthetase phospholipase D (PLD) are known to participate in membrane fusion during vesicle transport (Jenkins and Frohman, 2005; Jones et al., 1999). Moreover, as integral

components of many biological membranes, triacylglycerols have been demonstrated to possess great potency to promote spontaneous curvature in an acyl chain length dependent manner (Lee et al., 1996), which may alter membrane structure to support membrane fusion (Martens and McMahon, 2008; McMahon et al., 2010). We speculate that the addition of the hydrophobic acyl chain to endosomal PA may help to overcome the repulsive hydration force generated from water bound to the lipid headgroups. In addition, triacylglycerol can exhibit an extended conformation (Fahey and Small, 1986) with the 3-arachidonyl group in the opposite direction of the other two acyl chains, thereby allowing for attachment and fusion between two membranes (Kinnunen, 1992; Kinnunen and Holopainen, 2000). Our results suggest that as an initiation event, acylation of endosomal PA enables the close contact between donor and recipient membranes, thus allowing for fusion to be accomplished by SNAREs, SNARE accessory factors, Rab5 and its effectors. Clearly, more work is needed to determine how acylation of PA and other lipid derivatives are involved in the action of SNAREs, Rab5, and their effectors in membrane fusion. It is expected that a more precise mechanism underlying membrane fusion will emerge by integrating information from studies of both lipids and proteins.

## **Materials and methods**

Cell culture, DNA constructs, shRNA, antibodies, and immunoprecipitation were described in the Extended Experimental Procedures.

## **EGFR internalization and immunofluorescence**

PLC/PRF/5 cells were infected by lentiviruses producing shRNA against indicated genes. Cells were pooled after being selected for 4 days with 2 ug/ml puromycin. At least two confirmed knockdown pools for each targeted gene were used for the experiments in figures 2.2-

2.5. Control and knockdown cells were cultured on cover glass and serum starved for 24 hours in DMEM. Wild type and *Tip30*<sup>-/-</sup> primary hepatocytes were starved for three hours. Cells were incubated with 100 ng/ml Alexa<sup>488</sup> EGF (Invitrogen) and 20 µg/ml cycloheximide on ice for 1 hour and then washed 4 times with cold PBS and incubated in DMEM with 20 µg/ml cycloheximide at 37 °C for different time periods. Cells were fixed in 4% paraformaldehyde in PBS for 15 min, permeabilized with 0.1% Triton X-100 for 2 min and stained for the indicated proteins. Images were obtained with a Zeiss LSM 510 Meta confocal microscope (Carl Zeiss) using Plan-Apochromat 63×/1.40 Oil objective. Pinhole size was set to 1 airy unit for all channels. All images are representative single optical sections. To determine EGFR stability upon EGF treatment, cells were cultured in 6-cm dishes and treated as above except that unlabeled EGF was used, and the cells were collected for immunoblot at various time points.

### **Purification of endocytic and Rab5a vesicles**

HepG2 cells were transduced by the lentiviral vector pSin-EGFR-DsRed or pSin-EYFP-Rab5a and selected for 4 days with 2 µg/ml puromycin. To prepare endosomes carrying EGFR-DsRed, we treated cells with 10 ng/ml Alexa<sup>647</sup>-EGF at 37 °C for 10 minutes. Early endosomes were prepared on the flotation gradient essentially as described (Gorvel et al., 1995). Rab5 vesicles containing EYFP-Rab5a were prepared as described (Fuchs and Ellinger, 2002).

### ***In vitro* vesicle fusion assay**

The assay was performed as described previously with modifications (Bethani et al., 2009; Brandhorst et al., 2006) Briefly, EGFR-DsRED endocytic vesicles and EYFP-Rab5a vesicles (aliquotes of both contain 20 µg proteins) were gently mixed in a total volume of 20 µl fusion

buffer (10 mM Hepes, pH 7.4, 1.5 mM MgOAc, 1 mM DTT, 50 mM KOAc, 100 nmol arachidonic acid, 1 mM coenzyme A, 5 mM GTP, complemented with 4  $\mu$ l of an ATP-regenerating system containing 1:1:1 mixture of 100 mM ATP, 600 mM creatine phosphate, and 4 mg/ml creatine phosphokinase). After incubating with indicated purified proteins at 37 °C for 40 min, a portion of the reactions were spotted on slides and examined using Zeiss LSM 510 Meta confocal microscope. All images are representative single optical sections. Colocalization analysis was done using MBF\_ImageJ. For reactions in Figure 2.6D, vesicles were incubated in homogenization buffer (250 mM sucrose, 5 mM Hepes, pH 7.4) with indicated lipids. Electron microscopy (TEM JEOL 100CX) was performed as described previously (Ohya et al., 2009).

### **Lipid acylation**

Purified endocytic vesicles (aliquots containing 20  $\mu$ g proteins) were incubated with indicated proteins and [<sup>3</sup>H]-arachidonic acid (PerkinElmer) in the presence or absence of 10  $\mu$ M triacsin C at 37 °C for 1 hour in total volume of 200  $\mu$ l fusion buffer. For preparation of PA derivatives, 100 nM 1,2-dioleoyl-sn-glycero-3-phosphate (Avanti Polar Lipids) were incubated with immunopurified TIP30 complex or recombinant TIP30, ACSL4 and Endo B1 and arachidonic acid (Sigma) in the fusion buffer. Lipids were extracted using Bligh-Dyer Method (Bligh and Dyer, 1959).

### **Statistical analysis**

All statistical tests were two-tailed t-test. Data represent means  $\pm$  SEM. \* $P$  < 0.05, \*\* $P$  < 0.01, \*\*\* $P$  < 0.001.

### **Acknowledgments**

We are grateful to Stephen Prescott for generously sharing ACSL4 antibody and to Changdeng Hu for generously sharing BiFC plasmids. We thank Sandra Haslam, Christine Eischen and Karen Friderici for critical reading of the manuscript and Alicia Pastor for electron microscopic analysis. This work was supported by grants RO1 DK066110-01 and W81XWH-08-1-0377 (to H.X.) from the NIDDK and Department of Defense.

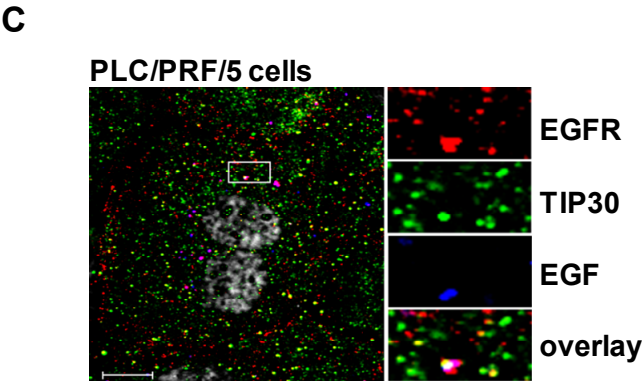
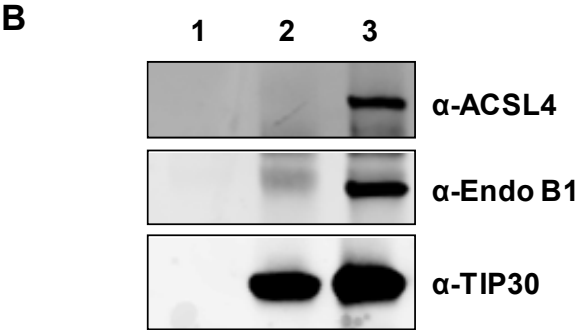
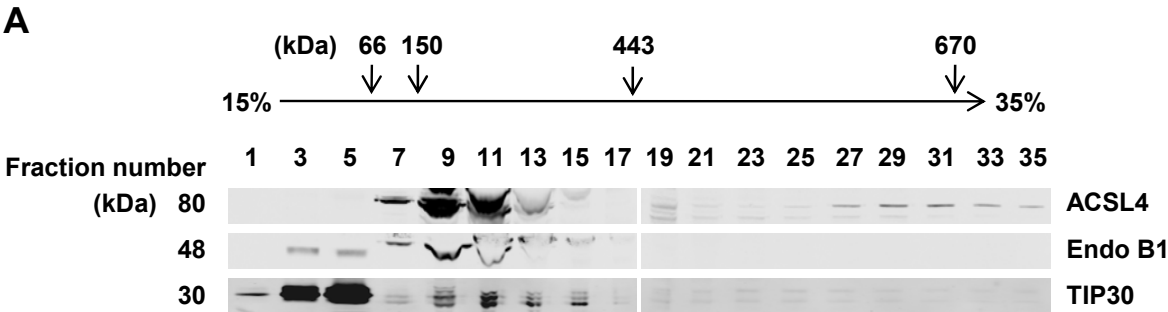
Supplemental Figure 2.8 Related to Figure 2.1, TIP30, ACSL4 and Endo B1 forms a protein complex that may function on the EGFR endocytic pathway.

**(A)** Endogenous TIP30, ACSL4 and Endo B1 are co-sedimented in a glycerol gradient. Whole cell extracts of PLC/PRF/5 cells and protein markers were loaded on the top of linear 10-35% (V/V) glycerol gradients (10 ml) formed from the bottom of 12-ml Beckman tubes. The buffer throughout the gradients was 20 mM Hepes-KOH (pH 7.0), 100 mM KCl, 1 mM dithiothreitol. The gradients were centrifuged at 200,000 g in a SW41 Ti rotor (Beckman) at 4°C for 20 h. After centrifugation, fractions were collected, concentrated and subjected to immunoblot analysis. Albumin (66 kDa), alcohol dehydrogenase (150 kDa) apoferritin (443 kDa), thyroglobulin (670 kDa), and blue dextran (2,000 kDa) were run in parallel as molecular weight indicators.

**(B)** Direct interaction of TIP30, ACSL4, and Endo B1. GST-ACSL4 and His-Endo B1 (Lane 1), Flag-TIP30 (Lane 2), or GST-ACSL4, His-Endo B1, and Flag-TIP30 (Lane 3) were subjected to anti-Flag M2 immunoprecipitation. Aliquots of precipitates were resolved on SDS-PAGE and analyzed by immunoblot with the indicated antibodies. Purified Flag-TIP30 was described previously (Xiao et al., 2000). Bacterially-expressed GST-ACSL4 was purchased from Abnova. His-Endo B1 was expressed in BL21 and purified as described in Figure S2.13A.

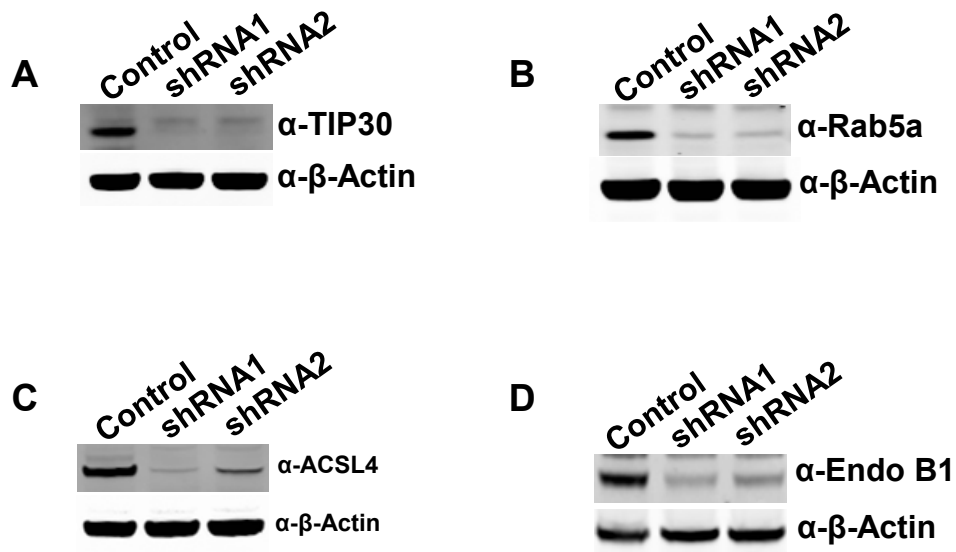
**(C)** TIP30 is localized to EGFR positive endosomes. PLC/PRF/5 cells were immunostained with antibodies for EGFR (red) and TIP30 (green) after 30 min Alexa<sup>488</sup> conjugated EGF (blue) internalization. Boxed areas are magnified. Bars, 10  $\mu$ m.

Supplemental Figure 2.8 Cont'd



Supplemental Figure 2.9 Related to Figure 2.2, Knockdown of TIP30, Rab5a, ACSL4, and Endo B1 in PLC/PRF/5 cells.

(A-D) Immunoblot analyses show knockdown of TIP30, Rab5a, ACSL4 or Endo B1 in PLC/PRF/5 cell. Whole cell lysates were made from cells expressing a scramble shRNA or shRNA against TIP30 (A), Rab5a (B), ACSL4 (C), or Endo B1 (D). Two shRNAs against each gene were used and equal amounts of protein were loaded per lane.

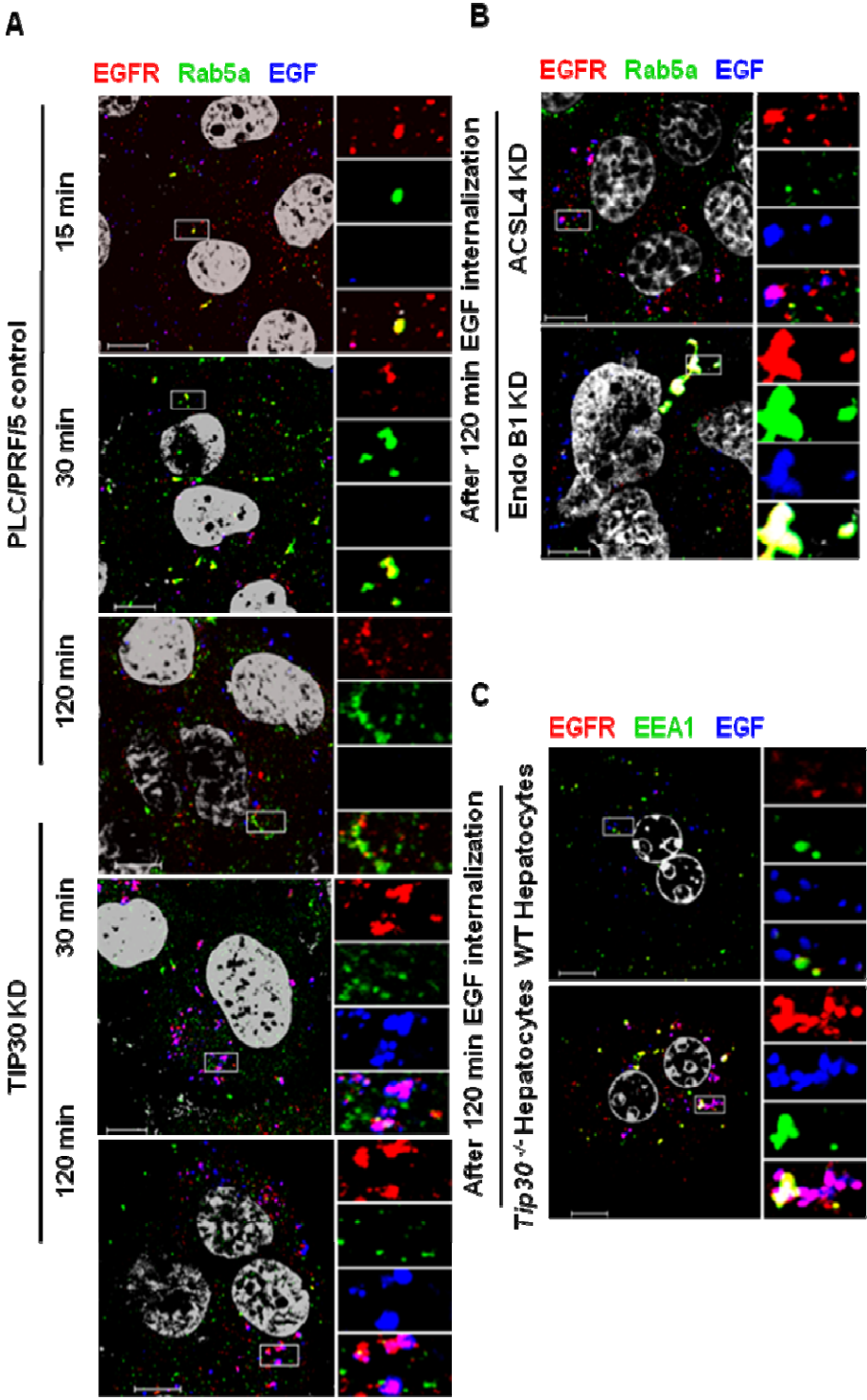


Supplemental Figure 2.10 Related to Figure 2.3 and 2.4, Deletion of TIP30, ACSL4, or Endo B1 Delays EGF-EGFR dissociation and inhibits the recruitment of Rab5a to endocytic vesicles.

**(A-B)** TIP30, ACSL4, or Endo B1 knockdown delays EGF-EGFR dissociation and inhibits the recruitment of Rab5a to endocytic vesicles. Localization of EGFR (red) and Rab5a (green) in control, TIP30 KD, ACSL4 KD and Endo B1 KD cells were monitored 120 min after Alexa<sup>488</sup>-EGF (blue) internalization. Nucleus is stained by DAPI (gray). Typical images of cells in each group are shown. Boxed areas are magnified. Magenta represents red and blue overlap. Bars, 10  $\mu$ m.

**(C)** TIP30 deletion in primary hepatocytes leads to delayed EGF-EGFR dissociation and inhibits the recruitment of Rab5a to endocytic vesicles. Wild type and *Tip30*<sup>-/-</sup> primary hepatocytes were subjected to EGFR internalization analysis and were immunostained for EGFR (red) and Rab5a (green) 120 min after Alexa<sup>488</sup>-EGF (blue) internalization. Bars, 10  $\mu$ m.

Supplemental Figure 2.10 Cont'd

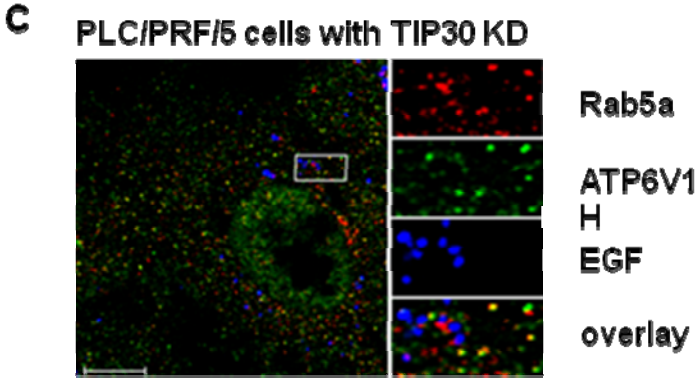
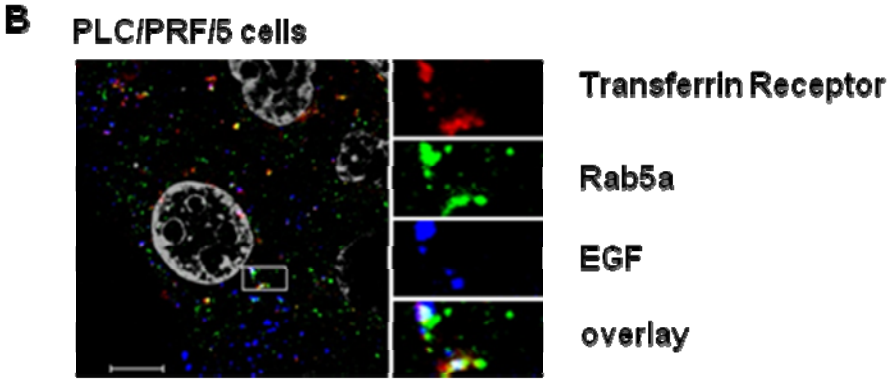
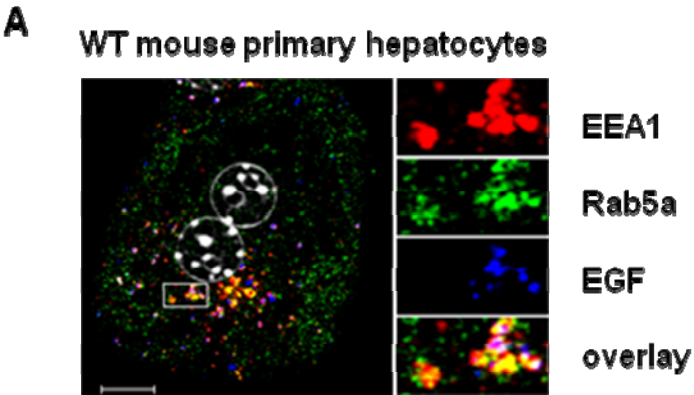


Supplemental Figure 2.11 Related to Figure 2.5, Rab5a vesicles carry V-ATPases.

**(A)** EGFR negative Rab5a vesicles are not early endosomes. Wild type mouse primary hepatocytes were immunostained for EEA1 (red) and Rab5a (green) after 30 min EGF (blue) internalization. Scale bars, 10  $\mu\text{m}$ .

**(B)** Transferrin receptor partially colocalizes with Rab5a. PLC/PRF/5 cells were immunostained for transferrin receptor (red) and Rab5a (green) after 10 min EGF (blue) internalization. Scale bars, 10  $\mu\text{m}$ .

**(C)** V-ATPase colocalizes with Rab5a in transporting vesicles. TIP30 knockdown cells were immunostained for V-ATPase (red) and Rab5a (green) after 30 min EGF (blue) internalization. Scale bars, 10  $\mu\text{m}$ .



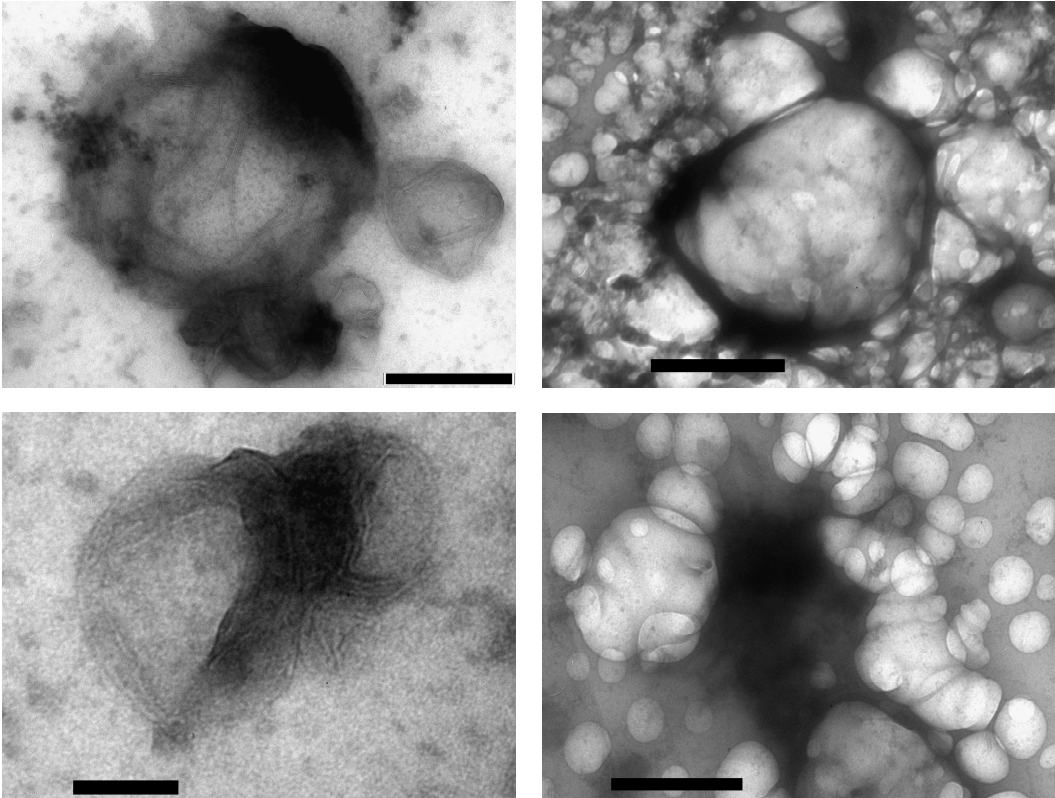
Supplemental Figure 2.12 Related to Figure 2.6, Examination of vesicle fusion using TEM and the purification of recombinant proteins.

**(A)** Vesicles were stained and visualized with electron microscope after being incubated with immunopurified TIP30 complex and arachidonic acid. Representative images are shown. Bars, 500 nm.

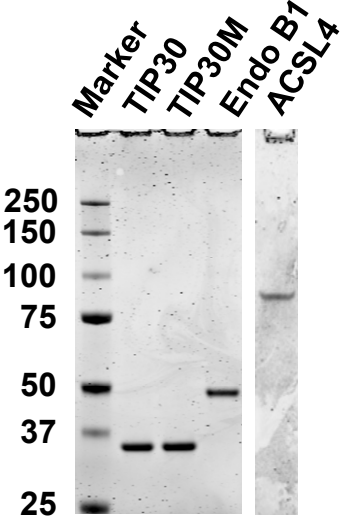
**(B)** Recombinant proteins were expressed in BL21 cells and purified using cobalt affinity resins. Eluted proteins were dialyzed against BC300 and subjected to SDS-PAGE analysis followed by coomassie blue staining. Images were acquired using Li-Cor scanner.

Supplemental Figure 2.12 Cont'd

**A**



**B**



Supplemental Figure 2.13 Related to Figure 2.6, Spectrometric analysis of PA derivatives.

(A) Endo B1 cannot transfer arachidonic acid to LPA. LPA and [3H]-arachidonic acid were incubated at 37 °C with or without bacterially expressed Endo B1 in fusion buffer. Image was acquired by scanning lipids resolved on TLC plate with a Molecular Dynamics Storm 860.

(B) The schematic diagram shows the lipid species prespotted on membranes that are used in lipid-protein overlay assays.

(C) The flow injection negative scan in the range of 400-1400 u. A predominant peak of 699.5 was detected. Atomic mass: arachidonic acid, 304.5 u; 18:1 PA, 699.5 u. The lipids in the smaller peaks have molecular weights that do not match any of the expected PA derivatives.

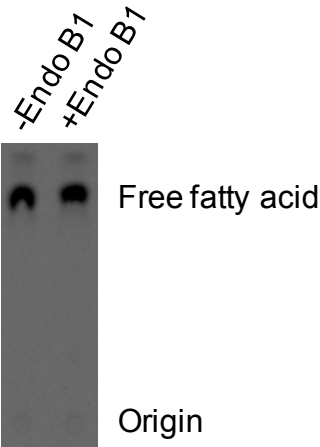
(D) The flow injection negative precursor scan for 303.2 u over a mass range of 400-1400 u.

(E) The LC-C18 negative precursor scan for 303.2 u over a mass range of 400-1400 u. The lipids after the acylation reaction was extracted and chromatographed on a C-18 column to reduce possible adduction mechanisms of compounds detected in the flow injection negative precursor scan of 303.2 u.

(F) Acylated PA causes tethering and stacking of endocytic and Rab5a vesicles. A representative electron microscopy picture is shown. Bars, 1  $\mu$ m.

Supplemental Figure 2.13 Cont'd

**A**

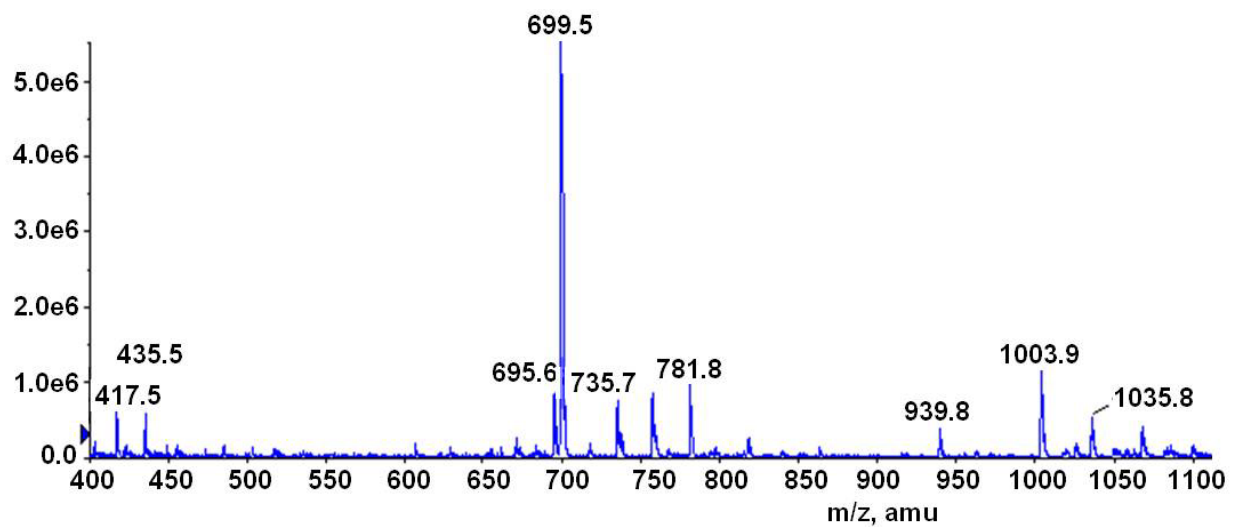


**B**

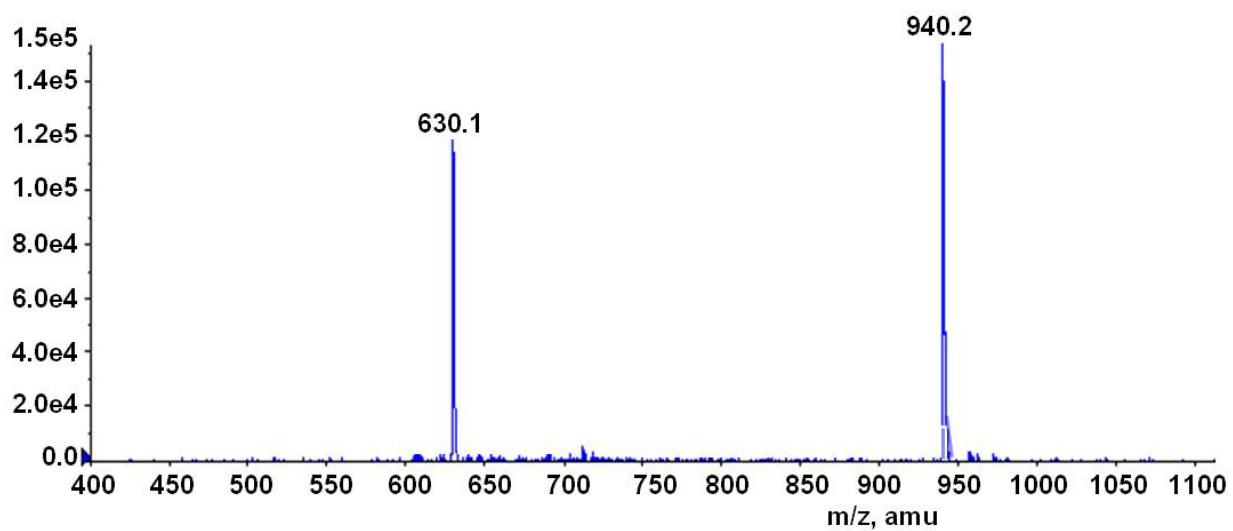
Triglyceride	<input type="radio"/>	<input type="radio"/>	Phosphatidylinositol (PI)
Diacylglycerol (DAG)	<input type="radio"/>	<input type="radio"/>	PtdIns(4)P
Phosphatidic Acid (PA)	<input type="radio"/>	<input type="radio"/>	PtdIns(4,5)P2
Phosphatidylserine (PS)	<input type="radio"/>	<input type="radio"/>	PtdIns(3,4,5)P3
Phosphatidylethanolamine (PE)	<input type="radio"/>	<input type="radio"/>	Cholesterol
Phosphatidylcholine (PC)	<input type="radio"/>	<input type="radio"/>	Sphingomyelin
Phosphatidylglycerol (PG)	<input type="radio"/>	<input type="radio"/>	3-sulfogalactosylceramide
Cardiolipin	<input type="radio"/>	<input checked="" type="radio"/>	Blue Blank

Supplemental Figure 2.13 Cont'd

C Flow injection MS scan

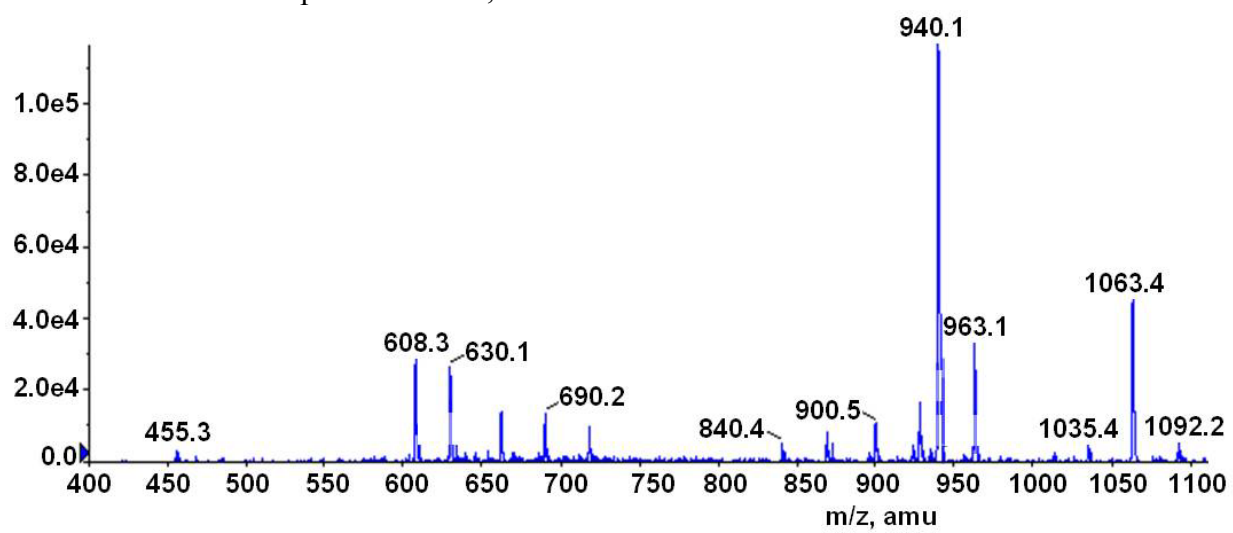


D Flow injection MS precursor scan, 303.2u

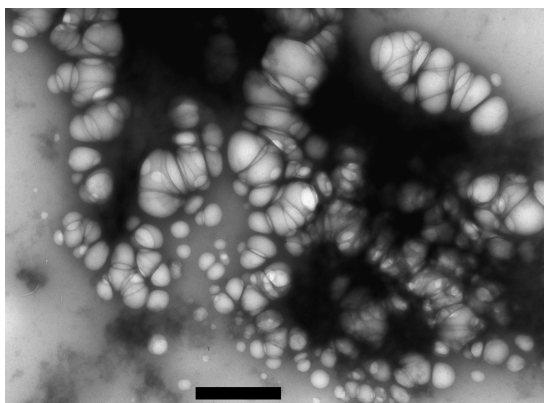


Supplemental Figure 2.13 Cont'd

E LC-C18/MS/MS precursor scan, 303.2u



F



## **Supplemental materials and methods**

### **Cell culture, DNA constructs and shRNAs**

The pSin-EF2 vector (Yu et al., 2007) was converted to destination vectors by cloning the Gateway cassette rfa (Reading frame A, Invitrogen) with either N-terminal or C-terminal HA tag, CFP, EYFP, or DsRed fluorescent proteins into blunted SpeI and EcoRI sites. For BiFC assays, VC155 and VN173 (Hu et al., 2005) were cloned into pCDNA3.1 and pSin-EF2, respectively, and both were also converted to destination vectors. Lentiviral plasmids producing shRNAs against TIP30, Rab5a, and ACSL4 were from Sigma-Aldrich. Lentiviral plasmids for shRNAs against Endo B1 were from Open Biosystems. See the supplemental experimental procedures for antibodies, cell lines and other reagents.

PLC/PRF/5 and HepG2 cell lines were purchased from ATCC. cDNA clones of human Rab5a, ACSL4 and EndoB1 were amplified using RT-PCR of mRNA isolated from PLC/PRF/5 cells. TIP30 was subcloned from pFlag7-TIP30 and pFlag7-TIP30M (Xiao et al., 2000).

Antibodies against HA (HA-7),  $\beta$ -Actin (AC-15) and Endo B1 were from Sigma. Antibodies for AKT, AKT-pS473, EEA1 and Rab5a were from Cell Signaling. Anti-EGFR-pY845, anti-transferrin receptor, Alexa Fluor 546 goat anti-mouse, Alexa Fluor 594 goat anti-rabbit antibodies were from Invitrogen. Anti-EGFR antibodies were from Millipore. Anti-ATP6V1H antibody was from Santa Cruz. Anti-LAMP1 was from The Developmental Studies Hybridoma Bank at University of Iowa. Triacylglycerol (1,2-Dilinoleoyl-3-palmitoyl-rac-glycerol) and phosphoinositide (PI) were purchased from Sigma.

### **Immunoprecipitation**

PLC/PRF/5 cells were transfected with indicated constructs. Whole cell extracts were prepared from pooled stable clones as described previously with modifications (Stringer et al., 1990). Briefly, cells were homogenized by 20 strokes in two packed cell pellet volumes (*p.c.v.*) of buffer A (10 mM Hepes, pH7.9, 10 mM KCl, 0.5 mM DTT, protease inhibitor cocktail) using Kontes homogenizer (B pestle). Another 20 strokes were applied after adding 1.5 *p.c.v.* of buffer B (50 mM Hepes, pH7.9, 0.6 mM EDTA, 1.5 mM DTT, 1.26 M NaCl, 75% Glycerol) followed by centrifugation at 100,000g for 1 hour. The supernatant was dialyzed against BC300 (20 mM Hepes, pH 7.9, 20% glycerol, 0.2 mM EDTA, 0.5 mM DTT, 0.3 M KCl) (Chiang and Roeder, 1995) and centrifuged at 15000 rpm for 20 min followed by rotating with anti-HA agarose beads (Roche Diagnostics) overnight at 4 °C. The beads were centrifuged and extensively washed using BC300 buffer. Immunoprecipitates were eluted with HA peptides (Roche Diagnostics), denatured, resolved on SDS-PAGE, and subjected to silver stain, immunoblot, or LC-MS/MS spectral analyses (The MSU Proteomics Facility, Michigan State University).

### **Purification of recombinant proteins**

Bacterially expressed TIP30, mutant TIP30, Endo B1 and ACSL4 proteins were His tagged and purified as described (Xiao et al., 2000). TIP30, TIP30M, Endo B1, and ACSL4 were subcloned into pRSETb vector. Purified proteins were dialyzed against BC300 and stored at -80 °C.

### **Mouse hepatocyte isolation**

Primary hepatocytes were isolated from 8 week-old wild type and *Tip30*<sup>-/-</sup> mice as described (Seglen, 1972) with modifications. Briefly, the inferior vena cava was cannulated and the liver was first perfused in situ with an oxygenated Krebs Ringer buffer (115 mM NaCl, 5.9 mM KCl,

25 mM NaHCO<sub>3</sub>, 10 mM glucose, 20 mM Hepes, pH 7.4) with 0.1 mM EGTA at 37 °C, followed by perfusion with oxygenated Krebs Ringer buffer containing 0.25 mM CaCl<sub>2</sub> and 20 µg/ml Liberase Blendzyme 3 (Roche Applied Science). Liver was removed and then gently minced in ice cold Krebs Ringer buffer. Liver cell suspension was then filtered with Falcon cell strainers (Becton Dickinson) and washed three times by centrifugation at 50 g for 2 min at 4 °C. Cell viability was determined by trypan blue exclusion. Cells were cultured in DMEM (with 10% FBS and 1× Pen/Strep) at 37 °C with 5% CO<sub>2</sub>.

### **MS/MS spectrometry analysis**

MS/MS spectrometry analysis of PA derivatives were performed in Avanti Polar Lipids Inc. Briefly, PA derivatives were extracted according to Bligh-Dyer method and redissolved in methanol/chloroform (85/18) with 10 mM NH<sub>4</sub>OAC and 1 µg/ml NH<sub>4</sub>OH. First, standards of 17:0-20:4 PA and 17:0-20:4 PI were prepared in the above solution and infused in the API 4000 QTrap triple quadrupole with linear ion trap instrument for optimization of collisional energy to provide mass fragments of arachidonic acid (20:4) at 303.2 u. Then samples were flow injected into the MS/MS in negative scan mode to discover products from the described reaction. The m/z value was used to search the most likely molecular species at <http://www.lipidmaps.org>.

## REFERENCES

## REFERENCES

- Authier F, Chauvet G (1999) In vitro endosome-lysosome transfer of dephosphorylated EGF receptor and Shc in rat liver. *FEBS Letters* **461**: 25-31
- Backer JM, Kahn CR, White MF (1990) The dissociation and degradation of internalized insulin occur in the endosomes of rat hepatoma cells. *Journal of Biological Chemistry* **265**: 14828-14835
- Bethani I, Werner A, Kadian C, Geumann U, Jahn R, Rizzoli SO (2009) Endosomal fusion upon SNARE knockdown is maintained by residual SNARE activity and enhanced docking. *Traffic* **10**: 1543-1559
- Bligh EG, Dyer WJ (1959) A rapid method of total lipid extraction and purification. *Can J Biochem Physiol* **37**: 911-917
- Brandhorst D, Zwilling D, Rizzoli SO, Lippert U, Lang T, Jahn R (2006) Homotypic fusion of early endosomes: SNAREs do not determine fusion specificity. *Proc Natl Acad Sci U S A* **103**: 2701-2706
- Burke P, Schooler K, Wiley HS (2001) Regulation of Epidermal Growth Factor Receptor Signaling by Endocytosis and Intracellular Trafficking. *Mol Biol Cell* **12**: 1897-1910
- Cao Y, Traer E, Zimmerman GA, McIntyre TM, Prescott SM (1998) Cloning, Expression, and Chromosomal Localization of Human Long-Chain Fatty Acid-CoA Ligase 4 (FACL4). *Genomics* **49**: 327-330
- Chattopadhyay S, Sun P, Wang P, Abonyo B, Cross NL, Liu L (2003) Fusion of Lamellar Body with Plasma Membrane Is Driven by the Dual Action of Annexin II Tetramer and Arachidonic Acid. *Journal of Biological Chemistry* **278**: 39675-39683
- Chen P-I, Kong C, Su X, Stahl PD (2009) Rab5 Isoforms Differentially Regulate the Trafficking and Degradation of Epidermal Growth Factor Receptors. *Journal of Biological Chemistry* **284**: 30328-30338
- Clague MJ, Urbe S, Aniento F, Gruenberg J (1994) Vacuolar ATPase activity is required for endosomal carrier vesicle formation. *J Biol Chem* **269**: 21-24
- Connell E, Darios F, Broersen K, Gatsby N, Peak-Chew SY, Rickman C, Davletov B (2007) Mechanism of arachidonic acid action on syntaxin-Munc18. *EMBO Rep* **8**: 414-419
- Creutz CE (1981) cis-Unsaturated Fatty Acids Induce the Fusion of Chromaffin Granules Aggregated by Synexin. *The Journal of Cell Biology* **91**: 247-256

- Fahey DA, Small DM (1986) Surface properties of 1,2-dipalmitoyl-3-acyl-sn-glycerols. *Biochemistry* **25**: 4468-4472
- Farsad K, Ringstad N, Takei K, Floyd SR, Rose K, De Camilli P (2001) Generation of high curvature membranes mediated by direct endophilin bilayer interactions. *The Journal of Cell Biology* **155**: 193-200
- Fuchs R, Ellinger I (2002) Free-flow electrophoretic analysis of endosome subpopulations of rat hepatocytes. *Curr Protoc Cell Biol* **Chapter 3**: Unit 3 11
- Gallop JL, Butler PJG, McMahon HT (2005) Endophilin and CtBP/BARS are not acyl transferases in endocytosis or Golgi fission. *Nature* **438**: 675-678
- Gorvel JP, Chavrier P, Zerial M, Gruenberg J (1991) rab5 controls early endosome fusion in vitro. *Cell* **64**: 915-925
- Gorvel JP, Escola JM, Stang E, Bakke O (1995) Invariant chain induces a delayed transport from early to late endosomes. *J Biol Chem* **270**: 2741-2746
- Grosshans BL, Ortiz D, Novick P (2006) Rabs and their effectors: Achieving specificity in membrane traffic. *Proceedings of the National Academy of Sciences* **103**: 11821-11827
- Haucke V, Di Paolo G (2007) Lipids and lipid modifications in the regulation of membrane traffic. *Curr Opin Cell Biol* **19**: 426-435
- Hu CD, Grinberg AV, Kerppola TK (2005) Visualization of protein interactions in living cells using bimolecular fluorescence complementation (BiFC) analysis. *Curr Protoc Protein Sci* **Chapter 19**: Unit 19 10
- Ito M, Jiang C, Krumm K, Zhang X, Pecha J, Zhao J, Guo Y, Roeder RG, Xiao H (2003) TIP30 deficiency increases susceptibility to tumorigenesis. *Cancer Res* **63**: 8763-8767
- Jahn R, Lang T, Südhof TC (2003) Membrane Fusion. *Cell* **112**: 519-533
- Jenkins G, Frohman M (2005) Phospholipase D: a lipid centric review. *Cellular and Molecular Life Sciences* **62**: 2305-2316
- Jiang C, Ito M, Piening V, Bruck K, Roeder RG, Xiao H (2004) TIP30 Interacts with an Estrogen Receptor  $\alpha$ -interacting Coactivator CIA and Regulates c-myc Transcription. *Journal of Biological Chemistry* **279**: 27781-27789
- Jiang C, Pecha J, Hoshino I, Ankrapp D, Xiao H (2007) TIP30 mutant derived from hepatocellular carcinoma specimens promotes growth of HepG2 cells through up-regulation of N-cadherin. *Cancer Res* **67**: 3574-3582

- Jones D, Morgan C, Cockcroft S (1999) Phospholipase D and membrane traffic: Potential roles in regulated exocytosis, membrane delivery and vesicle budding. *Biochimica et Biophysica Acta (BBA) - Molecular and Cell Biology of Lipids* **1439**: 229-244
- Jun Y, Fratti RA, Wickner W (2004) Diacylglycerol and Its Formation by Phospholipase C Regulate Rab- and SNARE-dependent Yeast Vacuole Fusion. *Journal of Biological Chemistry* **279**: 53186-53195
- Kinnunen PK (1992) Fusion of lipid bilayers: a model involving mechanistic connection to HII phase forming lipids. *Chem Phys Lipids* **63**: 251-258
- Kinnunen PK, Holopainen JM (2000) Mechanisms of initiation of membrane fusion: role of lipids. *Biosci Rep* **20**: 465-482
- Lakadamyali M, Rust MJ, Zhuang X (2006) Ligands for clathrin-mediated endocytosis are differentially sorted into distinct populations of early endosomes. *Cell* **124**: 997-1009
- Latham CF, Osborne SL, Cryle MJ, Meunier FA (2007) Arachidonic acid potentiates exocytosis and allows neuronal SNARE complex to interact with Munc18a. *J Neurochem* **100**: 1543-1554
- Lee LW, Zhang DH, Lee KT, Koay ES, Hewitt RE (2004) CC3/TIP30 expression was strongly associated with HER-2/NEU status in breast cancer. *Ann Acad Med Singapore* **33**: S30-32
- Lee YC, Zheng YO, Taraschi TF, Janes N (1996) Hydrophobic alkyl headgroups strongly promote membrane curvature and violate the headgroup volume correlation due to "headgroup" insertion. *Biochemistry* **35**: 3677-3684
- Leonard D, Hayakawa A, Lawe D, Lambright D, Bellve KD, Standley C, Lifshitz LM, Fogarty KE, Corvera S (2008) Sorting of EGF and transferrin at the plasma membrane and by cargo-specific signaling to EEA1-enriched endosomes. *J Cell Sci* **121**: 3445-3458
- Martens S, McMahon HT (2008) Mechanisms of membrane fusion: disparate players and common principles. *Nat Rev Mol Cell Biol* **9**: 543-556
- Masuda M, Takeda S, Sone M, Ohki T, Mori H, Kamioka Y, Mochizuki N (2006) Endophilin BAR domain drives membrane curvature by two newly identified structure-based mechanisms. *EMBO J* **25**: 2889-2897
- Maxfield FR, McGraw TE (2004) Endocytic recycling. *Nat Rev Mol Cell Biol* **5**: 121-132
- Mayorga LS, Colombo MI, Lennartz M, Brown EJ, Rahman KH, Weiss R, Lennon PJ, Stahl PD (1993) Inhibition of endosome fusion by phospholipase A2 (PLA2) inhibitors points to a role for PLA2 in endocytosis. *Proc Natl Acad Sci U S A* **90**: 10255-10259
- McMahon HT, Gallop JL (2005) Membrane curvature and mechanisms of dynamic cell membrane remodelling. *Nature* **438**: 590-596

McMahon HT, Kozlov MM, Martens S (2010) Membrane Curvature in Synaptic Vesicle Fusion and Beyond. *Cell* **140**: 601-605

Mellman I (1996) ENDOCYTOSIS AND MOLECULAR SORTING. *Annual Review of Cell and Developmental Biology* **12**: 575-625

Miaczynska M, Pelkmans L, Zerial M (2004) Not just a sink: endosomes in control of signal transduction. *Current Opinion in Cell Biology* **16**: 400-406

Mima J, Hickey CM, Xu H, Jun Y, Wickner W (2008) Reconstituted membrane fusion requires regulatory lipids, SNAREs and synergistic SNARE chaperones. *EMBO J* **27**: 2031-2042

Modregger J, Schmidt AA, Ritter B, Huttner WB, Plomann M (2003) Characterization of Endophilin B1b, a brain-specific membrane-associated lysophosphatidic acid acyl transferase with properties distinct from endophilin A1. *J Biol Chem* **278**: 4160-4167

Murphy JE, Padilla BE, Hasdemir B, Cottrell GS, Bunnett NW (2009) Endosomes: A legitimate platform for the signaling train. *Proceedings of the National Academy of Sciences* **106**: 17615-17622

Nielsen E, Severin F, Backer JM, Hyman AA, Zerial M (1999) Rab5 regulates motility of early endosomes on microtubules. *Nat Cell Biol* **1**: 376-382

Nishi T, Forgac M (2002) The vacuolar (H<sup>+</sup>)-ATPases — nature's most versatile proton pumps. *Nat Rev Mol Cell Biol* **3**: 94-103

Ohya T, Miaczynska M, Coskun U, Lommer B, Runge A, Drechsel D, Kalaidzidis Y, Zerial M (2009) Reconstitution of Rab- and SNARE-dependent membrane fusion by synthetic endosomes. *Nature* **459**: 1091-1097

Pfanner N, Glick BS, Arden SR, Rothman JE (1990) Fatty acylation promotes fusion of transport vesicles with Golgi cisternae. *J Cell Biol* **110**: 955-961

Pfanner N, Orci L, Glick BS, Amherdt M, Arden SR, Malhotra V, Rothman JE (1989) Fatty acyl-coenzyme a is required for budding of transport vesicles from Golgi cisternae. *Cell* **59**: 95-102

Pfeffer SR (2001) Rab GTPases: specifying and deciphering organelle identity and function. *Trends in Cell Biology* **11**: 487-491

Polo S, Di Fiore PP (2006) Endocytosis Conducts the Cell Signaling Orchestra. *Cell* **124**: 897-900

Rickman C, Davletov B (2005) Arachidonic acid allows SNARE complex formation in the presence of Munc18. *Chem Biol* **12**: 545-553

- Rink J, Ghigo E, Kalaidzidis Y, Zerial M (2005) Rab conversion as a mechanism of progression from early to late endosomes. *Cell* **122**: 735-749
- Rosenfeld JL, Moore RH, Zimmer K-P, Alpizar-Foster E, Dai W, Zarka MN, Knoll BJ (2001) Lysosome proteins are redistributed during expression of a GTP-hydrolysis-defective rab5a. *J Cell Sci* **114**: 4499-4508
- Schmidt A, Wolde M, Thiele C, Fest W, Kratzin H, Podtelejnikov AV, Witke W, Huttner WB, Soling H-D (1999) Endophilin I mediates synaptic vesicle formation by transfer of arachidonate to lysophosphatidic acid. *Nature* **401**: 133-141
- Shtivelman E (1997) A link between metastasis and resistance to apoptosis of variant small cell lung carcinoma. *Oncogene* **14**: 2167-2173
- Sorkin A, von Zastrow M (2009) Endocytosis and signalling: intertwining molecular networks. *Nat Rev Mol Cell Biol* **10**: 609-622
- Stenmark H (2009) Rab GTPases as coordinators of vesicle traffic. *Nat Rev Mol Cell Biol* **10**: 513-525
- Takahashi Y, Coppola D, Matsushita N, Cualing HD, Sun M, Sato Y, Liang C, Jung JU, Cheng JQ, Mule JJ, Pledger WJ, Wang HG (2007) Bif-1 interacts with Beclin 1 through UVRAG and regulates autophagy and tumorigenesis. *Nat Cell Biol* **9**: 1142-1151
- Takai Y, Sasaki T, Matozaki T (2001) Small GTP-Binding Proteins. *Physiol Rev* **81**: 153-208
- Tong X, Li K, Luo Z, Lu B, Liu X, Wang T, Pang M, Liang B, Tan M, Wu M, Zhao J, Guo Y (2009) Decreased TIP30 expression promotes tumor metastasis in lung cancer. *Am J Pathol* **174**: 1931-1939
- Umebayashi K, Stenmark H, Yoshimori T (2008) Ubc4/5 and c-Cbl Continue to Ubiquitinate EGF Receptor after Internalization to Facilitate Polyubiquitination and Degradation. *Mol Biol Cell* **19**: 3454-3462
- Wickner W, Schekman R (2008) Membrane fusion. *Nat Struct Mol Biol* **15**: 658-664
- Xiao H, Palhan V, Yang Y, Roeder RG (2000) TIP30 has an intrinsic kinase activity required for up-regulation of a subset of apoptotic genes. *Embo J* **19**: 956-963
- Xiao H, Tao Y, Greenblatt J, Roeder RG (1998) A cofactor, TIP30, specifically enhances HIV-1 Tat-activated transcription. *Proc Natl Acad Sci U S A* **95**: 2146-2151
- Yamashiro DJ, Tycko B, Fluss SR, Maxfield FR (1984) Segregation of transferrin to a mildly acidic (pH 6.5) para-golgi compartment in the recycling pathway. *Cell* **37**: 789-800

Zerial M, McBride H (2001) Rab proteins as membrane organizers. *Nat Rev Mol Cell Biol* **2**: 107-117

Zhao J, Lu B, Xu H, Tong X, Wu G, Zhang X, Liang A, Cong W, Dai J, Wang H, Wu M, Guo Y (2008) Thirty-kilodalton Tat-interacting protein suppresses tumor metastasis by inhibition of osteopontin transcription in human hepatocellular carcinoma. *Hepatology* **48**: 265-275

Zhao J, Ni H, Ma Y, Dong L, Dai J, Zhao F, Yan X, Lu B, Xu H, Guo Y (2007) TIP30/CC3 expression in breast carcinoma: relation to metastasis, clinicopathologic parameters, and P53 expression. *Hum Pathol* **38**: 293-298

**Chapter 3 *Tip30* Deletion in MMTV-Neu Mice Leads to the Development of Estrogen Receptor-Positive and Progesterone Receptor-Negative Mammary Tumors via Enhancing EGFR Signaling**

\*Chengliang Zhang, \*Mikito Mori, Shenglan Gao, Aimin Li, Isamu Hoshino, Mark D.

Aupperlee, Sandra Z. Haslam and Hua Xiao

*Cancer Research*, in press

\* CL. Zhang and M. Mori contribute equally to this work

## Abstract

Estrogen receptor-positive and progesterone receptor-negative (ER+/PR-) breast cancers account for 15-25% of all human breast cancers and display more aggressive malignant characteristics compared to ER+/PR+ cancers. However, the molecular mechanism underlying development of ER+/PR- breast cancers still remains elusive. We show here that *Tip30* deletion dramatically accelerated the onset of mammary tumors in the MMTV-Neu mouse model of breast cancer. The mammary tumors arising in *Tip30*<sup>-/-</sup>/MMTV-Neu mice were exclusively ER+/PR- and exhibit estrogen and progesterone-dependent growth. Tip30 is predominantly expressed in ER+ mammary epithelial cells (MECs) and its deletion leads to an increase in the number of phospho-ER $\alpha$  positive cells in mammary glands and accelerated activation of Akt in MMTV-Neu mice. Moreover, we found that Tip30 regulates the PI3K/Akt pathway through controlling endocytic downregulation of EGFR protein level and signaling. Together, these findings suggest a novel mechanism in which loss of Tip30 cooperates with Neu activation to enhance the activation of Akt signaling, leading to the development of ER+/PR- mammary tumors.

## Introduction

Despite considerable success in the treatment of ER+/PR+ breast cancers with therapies directed at targeting estrogen and ER $\alpha$ , a substantial fraction of patients with ER+/PR- tumors do not benefit significantly from these therapies (Osborne et al., 2005; Ponzzone et al., 2006). It is estimated that 15-25% of all human breast cancers are ER+/PR- with more aggressive malignant characteristics and poorer response to SERMs compared to ER+/PR+ breast cancers (Arpino et al., 2005; Creighton et al., 2009; Ponzzone et al., 2006). Moreover, 25% of ER+/PR- tumors are found to have HER2/Neu overexpression; patients with this subtype of ER+/PR- breast cancer have an extremely poor response to endocrine treatment. While several lines of evidence suggest that ER+/PR- tumors can be derived from ER+/PR+ tumors by the loss of PR expression due to anti-hormone therapy, other studies indicate that ER+/PR- tumors could arise by de novo etiological factors (Kim et al., 2006). To date, the mechanisms underlying de novo and acquired ER+/PR- breast cancer remain poorly defined. Thus, elucidation of the molecular basis of ER+/PR- breast tumor development has the potential to reveal new therapeutic targets for the treatment, and even prevention of the resistance to anti-estrogen therapy in breast cancer patients.

There are several hypotheses to explain the generation of ER+/PR- breast cancers. These include inhibition of PR transcription by aberrant ER cofactors or by nonfunctional ER, lower circulating levels of estrogen leading to reduced ER activity, hypermethylation of PR promoter, or by growth factor signaling pathways (Cui et al., 2005). Of particular interest are growth factor signaling pathways, in which aberrations are common in many human cancers (Dowsett et al., 2005; Konecny et al., 2003). Among the growth factor receptors, HER2/Neu is the most frequently altered receptor in breast cancers. Most of HER2 positive breast cancers are ER-/PR-

only a small fraction are ER+/PR+ or ER+/PR-, suggesting that HER2 may inhibit ER expression as well as PR expression (Cui et al., 2005). This hypothesis is supported by the observation that mouse models of breast cancer harboring a HER2/Neu transgene almost exclusively develop ER-/PR- mammary tumors. Additionally, when transfected with HER2 expressing vectors, ER+/PR+ breast cancer cells exhibited a significant decrease in PR expression (Konecny et al., 2003). Nevertheless, the mechanism by which activation of HER2/Neu leads to development of ER-/PR-, but not ER+ breast cancer remains poorly understood.

TIP30, also known as CC3, is a 30-kDa human cellular protein that was purified as a HIV-1 Tat interacting protein (Xiao et al., 1998) and its expression is altered in human liver, lung and breast cancers (Ito et al., 2003; Lee et al., 2004; Tong et al., 2009; Zhao et al., 2007). Our previous studies demonstrated that Tip30-deficient mice spontaneously develop tumors in several tissues and mammary preneoplastic lesions, suggesting that TIP30 acts as a tumor suppressor (Ito et al., 2003; Pecha et al., 2007). Its tumor suppressor activity is probably due to multiple mechanisms. TIP30 functions as a transcription cofactor to repress expression of genes that are involved in proliferation and apoptosis (Jiang et al., 2004a; Zhao et al., 2008b) and it can induce apoptosis as an inhibitor of nuclear import (King and Shtivelman, 2004). In particular, TIP30 can act as a repressor of ER $\alpha$ -mediated c-Myc transcription in mammary glands and breast cancer cells (Jiang et al., 2004a). Additionally, recent evidence has highlighted that TIP30 controls endocytic downregulation of the EGFR signaling pathway in primary hepatocytes and hepatocellular carcinoma cells<sup>7</sup>.

The multiple functions of TIP30 have prompted the speculation that TIP30 loss may contribute to mammary tumorigenesis induced by activation of oncogenes. Therefore, we aimed

to determine whether *Tip30* deletion enhances mammary tumorigenesis in MMTV-*Neu* mice. We report here that *Tip30* deletion cooperates with HER2/*Neu* activation to promote development of ER+/PR- mammary tumors, in part, through up-regulation of EGFR/Akt signaling. The *Neu*+/*Tip30*<sup>-/-</sup> mouse model may help decipher the mechanisms leading to ER+/PR- mammary tumors and identify therapeutic targets for this subgroup of tumors.

## Results

### ***Tip30* deletion significantly accelerates mammary tumorigenesis in MMTV-*Neu* mice.**

To investigate whether *Tip30* deletion cooperates with HER2/*Neu* to promote mammary tumorigenesis, we generated *Tip30* knockout mice with overexpression of *Neu* by crossing MMTV-*Neu* transgene from MMTV-*Neu* mice (FVB/N-Tg; (Guy et al., 1992) into *Tip30*<sup>-/-</sup> FVB mice. *Neu*+/*Tip30*<sup>-/-</sup> mice appeared similar to *Neu*+/*Tip30*<sup>+/+</sup> mice in size and reached weaning age at the expected Mendelian frequency. A cohort of *Neu*+/*Tip30*<sup>-/-</sup>, *Neu*+/*Tip30*<sup>+/-</sup> and *Neu*+/*Tip30*<sup>+/+</sup> female mice were monitored for 75 weeks. Mammary tumors were noted to appear earlier in *Neu*+/*Tip30*<sup>-/-</sup> mice compared to *Neu*+/*Tip30*<sup>+/+</sup> mice. Kaplan-Meier survival curves (Fig. 3.1A) were generated based on the timing of mammary tumors becoming  $\geq 0.5\text{cm}^3$  in volume ( $\geq 1$  cm in diameter). We observed that 50% of *Neu*+/*Tip30*<sup>+/+</sup> mice developed mammary tumors with a relatively long median latency of 60 weeks. The relatively longer median latency and lower frequency of tumors arising in *Neu*+/*Tip30*<sup>+/+</sup> mice in comparison with that in MMTV-*Neu* mice (Guy et al., 1992) are possibly due to only one MMTV-*Neu* wild-type transgene allele in *Neu*+/*Tip30*<sup>+/+</sup> mice. By contrast, all *Neu*+/*Tip30*<sup>-/-</sup> mice developed tumors at a median age of 39 weeks and 87% of *Neu*+/*Tip30*<sup>+/-</sup> mice developed tumors at a median age of 47 weeks.

Figure 3.1 *Tip30* deletion significantly accelerates the onset of mammary tumors in MMTV-Neu mice.

*Neu+/Tip30<sup>+/+</sup>* (n = 10), *Neu+/Tip30<sup>+/-</sup>* (n = 15) and *Neu+/Tip30<sup>-/-</sup>* (n = 10) female mice were monitored weekly for a period of 75 weeks and sacrificed at the endpoint or when a tumor became palpable  $\geq 0.5 \text{ cm}^3$ . *A*, Kaplan-Meier curves show the timing of mammary tumors became palpable  $\geq 0.5 \text{ cm}^3$  in mice. The data were plotted as percentage of tumor-free animals against the time in weeks.  $P \leq 0.0001$  (log-rank test). *B*, Representative hematoxylin and eosin (H&E) stained mammary tumors arising in *Neu+/Tip30<sup>-/-</sup>* mice. A poorly differentiated adenocarcinoma with solid growth pattern (B1); A moderately differentiated adenocarcinoma with glandular growth pattern (B2); A pulmonary metastasis (B3). Scale bar, 50  $\mu\text{m}$ . *C*, Representative immunohistochemical staining of mammary tumors for K8 (brown staining indicates presence of K8) and  $\alpha\text{SMA}$  (lack of brown staining indicates lack of  $\alpha\text{SMA}$ ). Scale bar, 10  $\mu\text{m}$ .

Figure 3.1 Cont'd

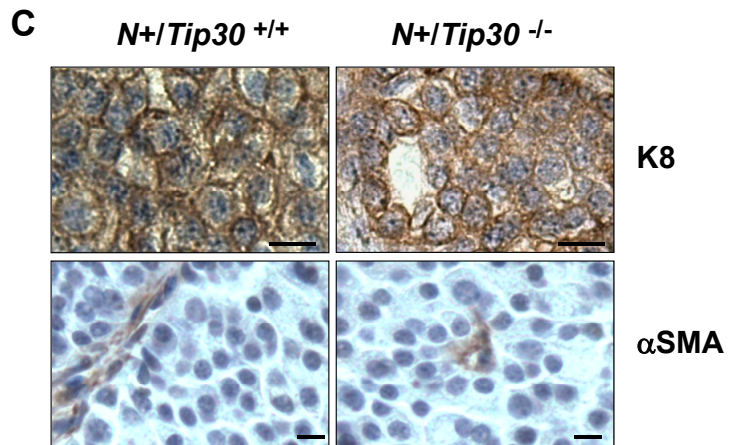
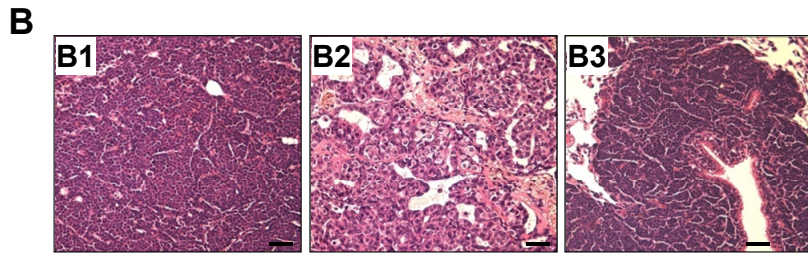
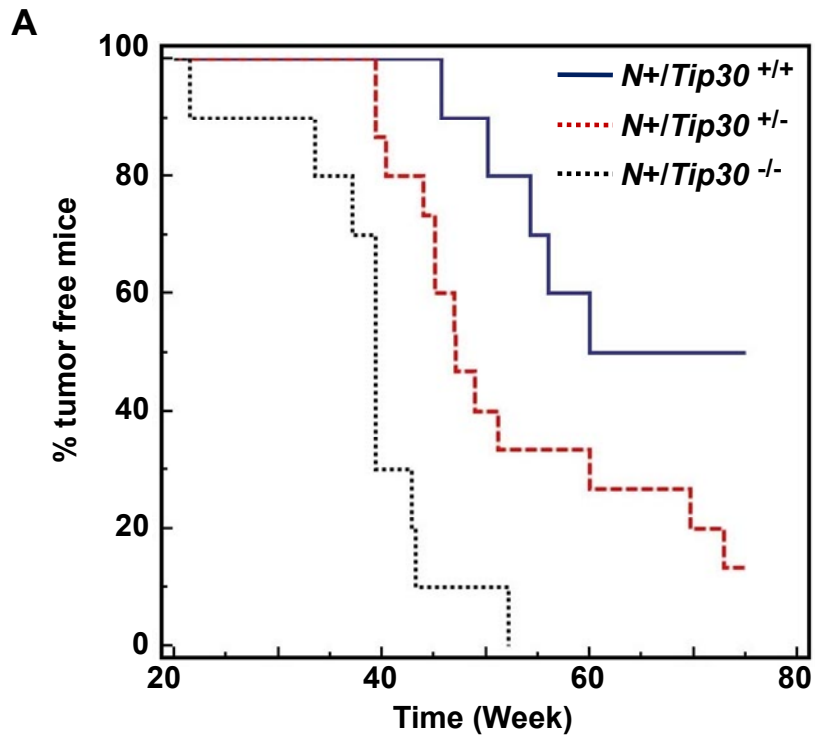


Table 3.1 ER $\alpha$  and PR staining in mammary tumors

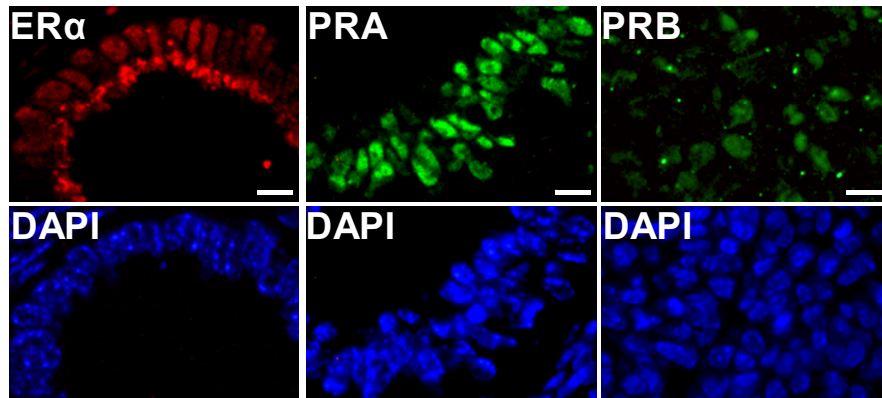
Tumors	ER+/PR-	ER-/PR-
<i>Neu+/Tip30<sup>-/-</sup></i>	100% (8/8)	0% (0/8)
<i>Neu+/Tip30<sup>+/-</sup></i>	50% (3/6)	50% (3/6)
<i>Neu+/Tip30<sup>+/+</sup></i>	11% (1/9)	89% (8/9)

Figure 3.2 Mammary tumors arising in *Neu+/Tip30<sup>-/-</sup>* mice are exclusively ER+/PR-.

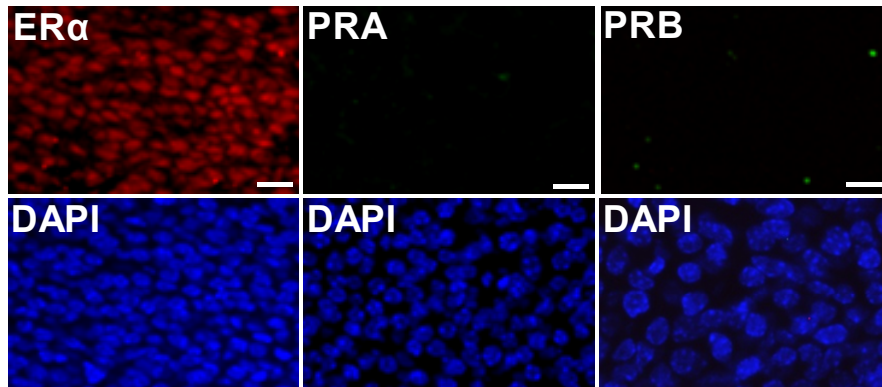
*A-C*, Representative immunofluorescent staining of ER $\alpha$  (red), PR-A (green) and PR-B (green) in the positive control uterus (*A*) and mammary tumors arising in *Neu+/Tip30<sup>-/-</sup>* mice (*B*) or *Neu+/Tip30<sup>+/+</sup>* mice (*C*). Tumor sections were stained with anti-ER $\alpha$ , anti-PR-A (hPRa7) or anti-PR-B (hPRa6) specific antibodies, followed by counterstaining with DAPI. Scale bar, 10  $\mu$ m.

Figure 3.2 Cont'd

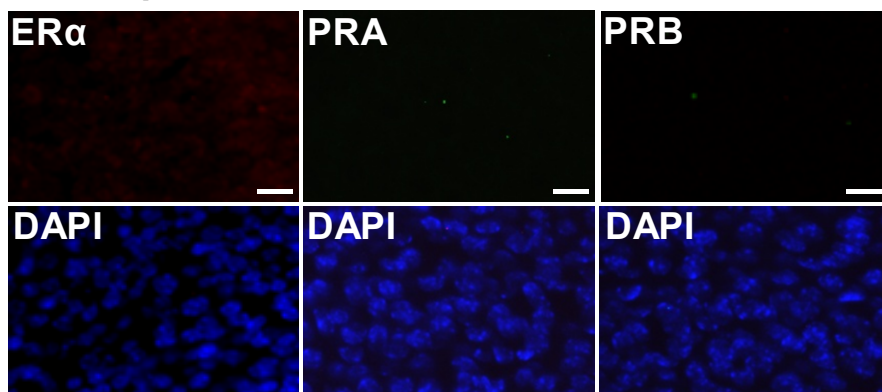
**A Uterus**



**B *Neu+ / Tip30<sup>-/-</sup>* tumors**



**C *Neu+ / Tip30<sup>+/+</sup>* tumors**



Histological analysis showed that tumors arising in *Neu+ / Tip30<sup>-/-</sup>* mice were poorly or moderately differentiated mammary tumors with solid growth or glandular growth patterns, morphologically similar to the mammary tumors arising in MMTV-Neu mice (Fig. 3.1, B1 and B2). Immunohistochemical staining revealed that mammary tumors arising in *Neu+ / Tip30<sup>-/-</sup>* or *Neu+ / Tip30<sup>+ / +</sup>* mice consisted of mostly cytokeratin (K8)-positive and  $\alpha$ -smooth muscle actin ( $\alpha$ SMA)-negative tumor cells (Fig. 3.1C), indicating that *Neu+ / Tip30<sup>-/-</sup>* tumors like MMTV-Neu tumors (Huang et al., 2005b) are of the luminal cell type. The presence of metastasis in the lung was observed in 4 out of 10 *Neu+ / Tip30<sup>-/-</sup>* mice, whereas metastasis was detected in 1 out of 10 *Neu+ / Tip30<sup>+ / +</sup>* mice. These results suggest that Tip30 loss accelerates the onset of mammary luminal tumors in MMTV-Neu mice and possibly increases metastasis.

#### **Deletion of *Tip30* results in a shift from development of ER-/PR- tumors to ER+/PR- tumors in the MMTV-Neu mouse model.**

It is well known that MMTV-Neu transgenic mice develop mammary tumors composed almost exclusively of ER-/PR- luminal epithelial cells. Surprisingly, we found that all *Neu+ / Tip30<sup>-/-</sup>* tumors (n = 8) and 50% of *Neu+ / Tip30<sup>+ / -</sup>* tumors (n = 6) examined showed an ER+/PR- staining pattern (Fig. 3.2B), whereas 89% *Neu+ / Tip30<sup>+ / +</sup>* tumors (n = 9) were ER-/PR- (Fig. 3.2C), indicating that *Neu+ / Tip30<sup>-/-</sup>* mice were more likely to develop ER+/PR- mammary tumors compared to *Neu+ / Tip30<sup>+ / +</sup>* mice (Table 3.1, 100% versus 11%;  $P = 0.004$ ). These results suggest that Tip30 loss combined with activation of Neu promotes development of ER+/PR- mammary tumors.

Figure 3.3 Growth of ER+/PR- tumors arising in *Neu+/Tip30<sup>-/-</sup>* mice depends upon estrogen and progesterone.

*A*, Two ER+/PR- mammary tumors from *Neu+/Tip30<sup>-/-</sup>* mice were minced and inoculated subcutaneously (s.c.) in the front flanks of ovary-intact (n = 16) or ovariectomized (n = 9) mice. The graph represents the measurements of tumors by the end of three months after transplantations or when the tumor volume reaches 1 cm<sup>3</sup>. *B* and *C*, Two ER+/PR- mammary tumors from *Neu+/Tip30<sup>-/-</sup>* mice were minced and inoculated s.c. in the front flanks of ovariectomized mice supplemented with Placebo (n = 10), estrogen (E2, n = 6), progesterone (P4, n = 6) or E2 plus P4 (n = 7) pellets. *P* = 0.012. The graphs show the measurements of tumor volumes by the end of three months after transplantations or when the tumor volume becoming 1 cm<sup>3</sup> (*B*) and the timing of tumors becoming 1 cm<sup>3</sup> in volume or by the end of three months of tumors becoming  $\geq 0.25$  cm<sup>3</sup> (*C*). \* *P* = 0.009 (Placebo vs E2 + P4). Note that growth of tumors in two mice of the placebo group were independent of ovarian hormones. *D*, Growth of ER+/PR- tumors after being treated with saline/ethanol vehicle or RU486. Two ER+/PR- tumors arising in *Neu+/Tip30<sup>-/-</sup>* female mice were minced and inoculated s.c. to nude mice. After transplanted tumors reached approximately 0.5 cm in diameter, mice were divided into two groups. The groups received either RU486 (6.5 mg/kg body weight) or saline/ethanol vehicle solution s.c. daily for 7 days. Tumor size was measured by caliper (length and width) for another 7 days. Tumor increase rate was calculated by comparing tumor volume ( $1/2 \times \text{length} \times \text{width}^2$ ) before and after treatment. *P* = 0.025. *E*, Primary tumor cells derived from two ER+/PR- tumors (T1 and T2) were isolated and cultured in the presence or absence of MG132. Cell lysates were subjected to immunoblotting with hPRa7 antibodies that detect both PR-A and PR-B by immunoblot.

Figure 3.3 Cont'd

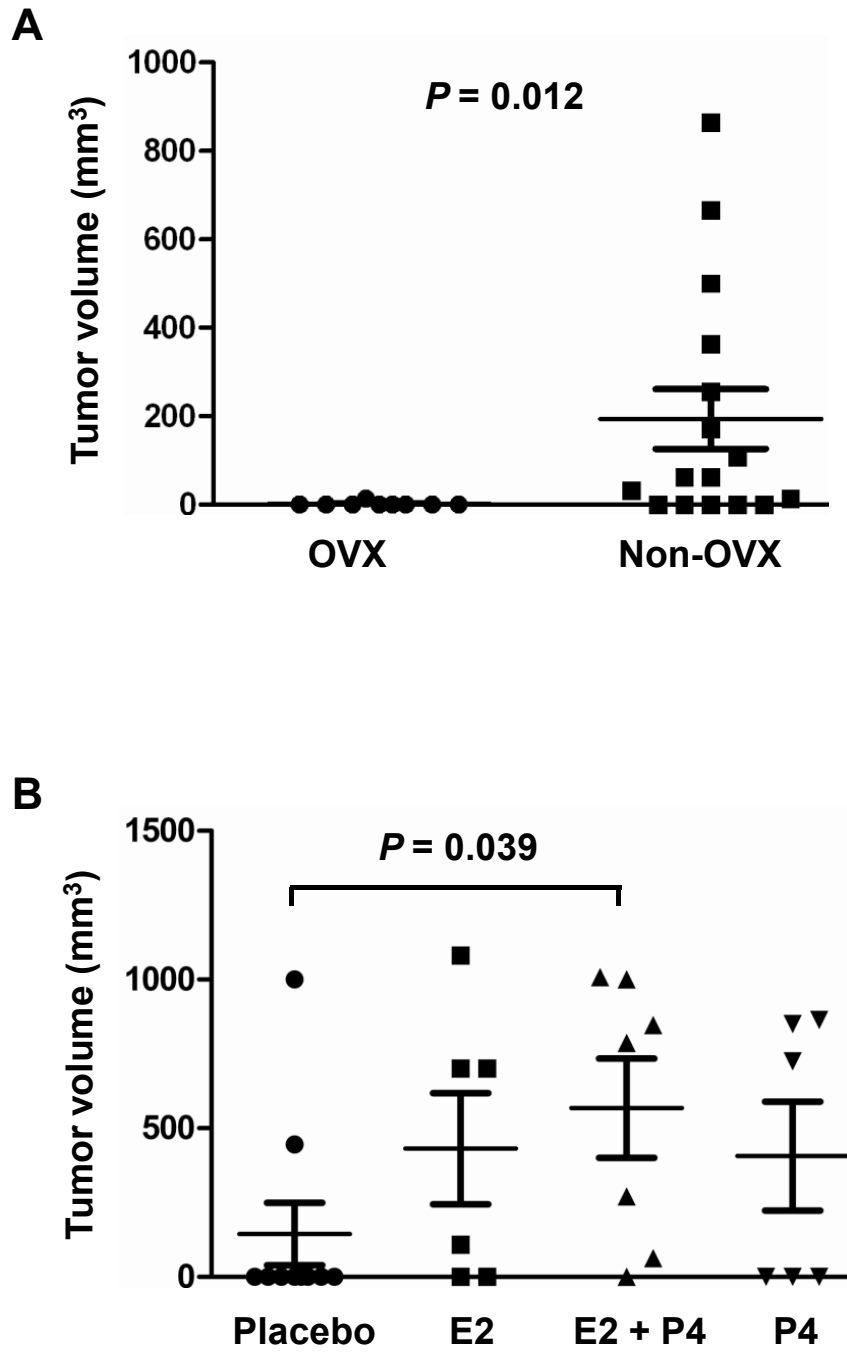
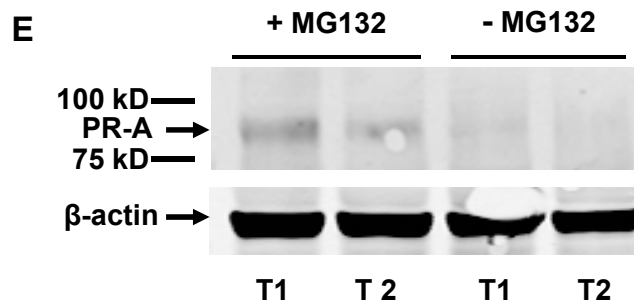
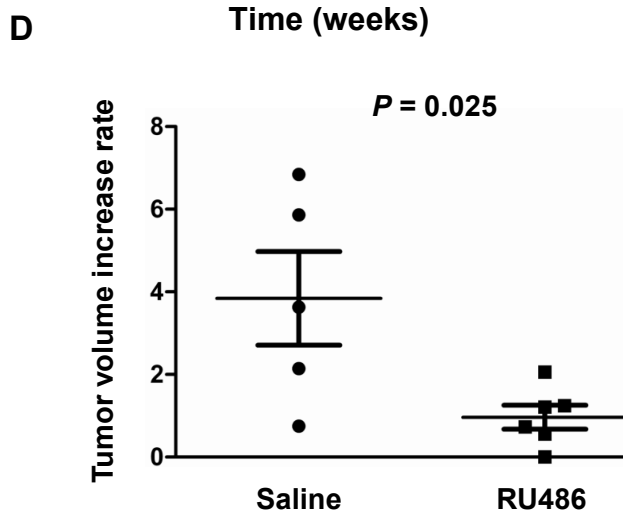
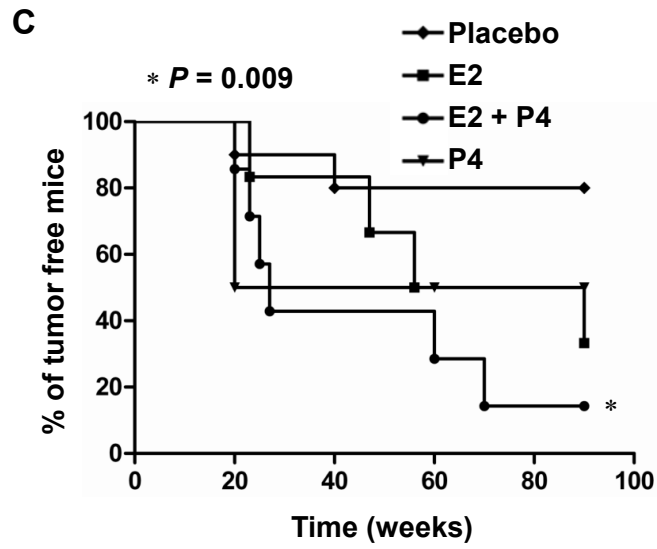


Figure 3.3 Cont'd



### **Estrogen and progesterone promote growth of *Neu+/*Tip30*<sup>-/-</sup>* mammary tumors.**

To determine whether ER+/PR- mammary tumors arising in *Neu+/*Tip30*<sup>-/-</sup>* were ovarian hormone-dependent, we first transplanted small pieces of freshly dissected tumors into ovary-intact (Non-OVX) and ovariectomized (OVX) nude mice and then monitored the growth of transplanted tumor tissues. Remarkably, removal of both ovaries from recipient mice drastically reduced growth and progress of transplanted tumors, suggesting that ER+/PR- mammary tumors that developed in *Neu+/*Tip30*<sup>-/-</sup>* mice are ovary-dependent (Fig. 3.3A). Next, we transplanted small pieces of freshly dissected tumors into OVX mice supplemented with placebo, estrogen, progesterone or estrogen plus progesterone pellets (Fig. 3.3B and 3.3C). Surprisingly, estrogen plus progesterone strongly promoted tumor growth compared to placebo ( $P = 0.04$ ), while estrogen or progesterone alone only slightly increased tumor growth compared to placebo ( $P > 0.05$ ). Moreover, the progesterone antagonist RU486 was able to significantly delay the growth of *Neu+/*Tip30*<sup>-/-</sup>* tumors (Fig. 3.3D). These results suggest that both estrogen and progesterone are required for promoting growth of ER+/PR- tumors arising in *Neu+/*Tip30*<sup>-/-</sup>* mice.

The effect of progesterone on the growth of ER+/PR- tumors from *Neu+/*Tip30*<sup>-/-</sup>* mice raises the question of whether these tumor cells express any PR proteins. Because previous studies have suggested that active PRs are rapidly degraded in breast cells (Lange et al., 2000), we speculated that PR was expressed and then degraded rapidly in ER+/PR- tumors. To test this hypothesis, we examined PR-A and PR-B expression in cultured tumor cells derived from ER+/PR- tumors. Indeed, PR-A, but not PR-B, was clearly detected by Western Blot analysis after treatment of cells with the proteasome inhibitor, MG132 (Fig. 3.3E), implying that PR-A is expressed but rapidly turned over in these tumors. Together, these results suggest that estrogen

and progesterone play stimulating roles in the development of ER+/PR- mammary tumors in *Neu+/Tip30<sup>-/-</sup>* mice.

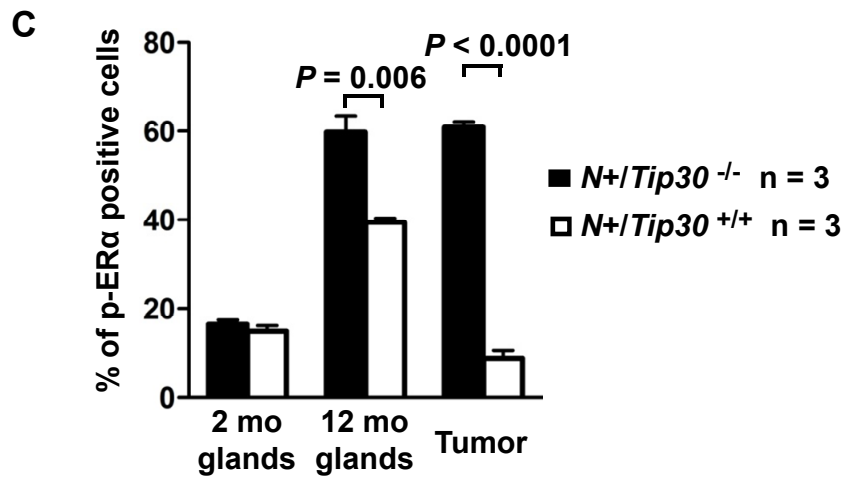
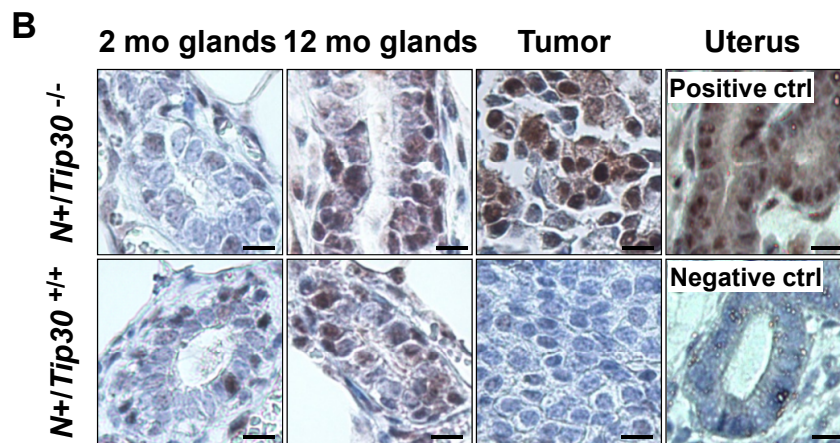
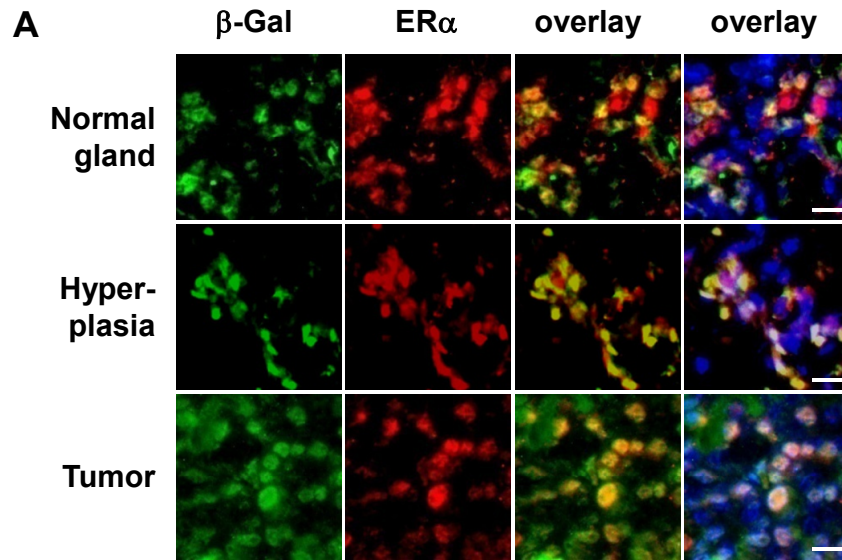
**Deletion of *Tip30* leads to a progressively increased numbers of p-ER $\alpha$  and p-Akt positive cells in the mammary gland from MMTV-*Neu* mice.**

The preceding data imply that *Tip30* may play a key role in suppressing tumorigenesis in ER $\alpha$ -positive (ER+) epithelial cells. To test whether the *Tip30* gene promoter is active in ER+ epithelial cells and ER+/PR- tumors, we performed immunofluorescent double staining for ER $\alpha$  and  $\beta$ -galactosidase in the mammary glands and tumors derived from *Neu+/Tip30<sup>+/-</sup>* mice harboring a knock-in  $\beta$ -galactosidase ( $\beta$ -Gal) gene at the *Tip30* gene locus under the control of *Tip30* promoter. The  $\beta$ -Gal protein was predominantly detected in ER+ mammary epithelial cells and tumor cells (Fig. 3.4A), indicating that the *Tip30* promoter is activated mainly in ER+ MECs and tumor cells. Given that ER $\alpha$  is activated through ligand binding and phosphorylation in response to estrogen and growth factor induced signaling and that *Tip30<sup>-/-</sup>* mice do not exhibit a significant increase in the number of ER $\alpha$  positive cells in the mammary gland at the age of 4 months (Pecha et al., 2007), we therefore asked whether the proportion of p-ER $\alpha$  positive cells is altered in *Neu+/Tip30<sup>-/-</sup>* mammary glands. Immunohistochemistry analysis was used to examine phospho-ER (p-ER $\alpha$ ) at Ser-171 (equivalent to Ser167 in human) in mammary glands and tumors from *Neu+/Tip30<sup>-/-</sup>* and *Neu+/Tip30<sup>+/+</sup>* mice (Fig. 3.4B). No significant difference in the numbers of p-ER $\alpha$  positive cells was detected in 2-month-old mammary glands from *Neu+/Tip30<sup>-/-</sup>* and *Neu+/Tip30<sup>+/+</sup>* mice (Fig. 3.4C). Strikingly, 12-month-old *Neu+/Tip30<sup>-/-</sup>* mammary glands and tumors displayed an increase in the number of p-ER $\alpha$  positive cells compared to *Neu+/Tip30<sup>+/+</sup>* mammary glands and tumors ( $P < 0.05$ ).

Figure 3.4 Representative immunohistochemical staining of p-ER $\alpha$  in mammary glands and mammary tumors from *Neu+ / Tip30<sup>-/-</sup>* and *Neu+ / Tip30<sup>+/+</sup>* mice.

*A*, Representative immunofluorescent double staining of mammary gland and tumor sections from a *Neu+ / Tip30<sup>-/-</sup>* mouse for ER $\alpha$  (red) and  $\beta$ -Gal (green), following by counterstaining with DAPI (blue). Scale bar, 10  $\mu$ m. *B*. Representative immunohistochemical staining of p-ER $\alpha$  in 2-month-old and 12-month-old mammary glands and mammary tumors from *Neu+ / Tip30<sup>-/-</sup>* and *Neu+ / Tip30<sup>+/+</sup>* mice. As a negative control, a uterus section was stained without using the primary antibody (anti-pER $\alpha$ ). Scale bar, 10  $\mu$ m. *C*, Data represent means  $\pm$  SEM of the percentage of p-ER $\alpha$  positive cells in the mammary glands and tumors derived from *Neu+ / Tip30<sup>-/-</sup>* and *Neu+ / Tip30<sup>+/+</sup>* mice. p-ER $\alpha$  positive cells were counted in the sections of mammary glands and tumors derived from three mice of each genotype (randomly selected fields per section). 50 cells were counted per field and 10 fields were counted per mouse.

Figure 3.4 Cont'd



These results suggest that *Tip30* deletion preferentially increases the number of p-ER $\alpha$  positive luminal cells in the mammary gland of MMTV-Neu mice.

Akt is one of the most important downstream factors in HER2/Neu and EGFR signaling pathways that can phosphorylate ER $\alpha$  and regulate MEC and apoptosis (Campbell et al., 2001; Lannigan, 2003). Previous studies have demonstrated that activation of Akt-1 signaling accelerates HER2/Neu-mediated mammary tumor formation (Hutchinson et al., 2004), whereas disruption of Akt-1 delays HER2/Neu-mediated mammary tumorigenesis (Ju et al., 2007; Maroulakou et al., 2007; Nardulli and Katzenellenbogen, 1988). To examine whether the deletion of *Tip30* affects the activation of Akt (p-Akt) in preneoplastic mammary glands from MMTV-Neu mice, we performed the immunohistochemical analysis for p-Akt in preneoplastic mammary glands from *Neu+/Tip30<sup>-/-</sup>* and *Neu+/Tip30<sup>+/+</sup>* mice at the age of 2 and 12 months. MECs at the different ages exhibit negative, weak, intermediate or strong staining for p-Akt (Fig. 3.5; A1, A2, A3 or A4, respectively).

Figure 3.5 Representative immunohistochemical staining for p-Akt in mammary tumors and mammary glands from *Neu+/Tip30<sup>-/-</sup>* and *Neu+/Tip30<sup>+/+</sup>* mice.

A, Representative immunohistochemical staining of p-Akt in mammary glands. p-Akt staining in 2-month-old mammary glands ranges from negative to weak (A1 and A2) and is more intense in 12-month-old mammary glands (A3 and A4, intermediate and strong, respectively). Scale bar, 10  $\mu$ m. B-D, Data represent means  $\pm$  SEM of the percentage of cells that were stained positive or negative for p-Akt in 2-month-old (B) and 12-month-old (C) mammary glands and tumors (D) derived from *Neu+/Tip30<sup>-/-</sup>* and *Neu+/Tip30<sup>+/+</sup>* mice. Fifty cells were counted per field and 10 fields were counted per mouse. Data were analyzed by two-tailed *t* test.

Figure 3.5 Cont'd

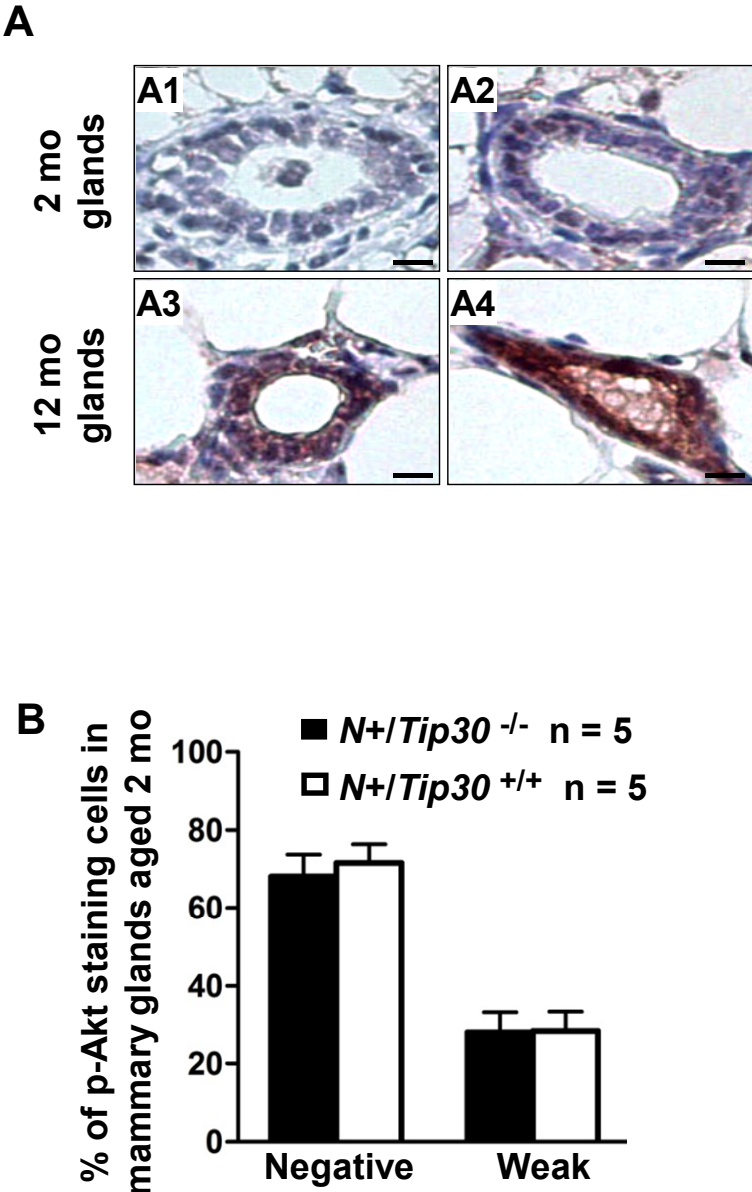


Figure 3.5 Cont'd

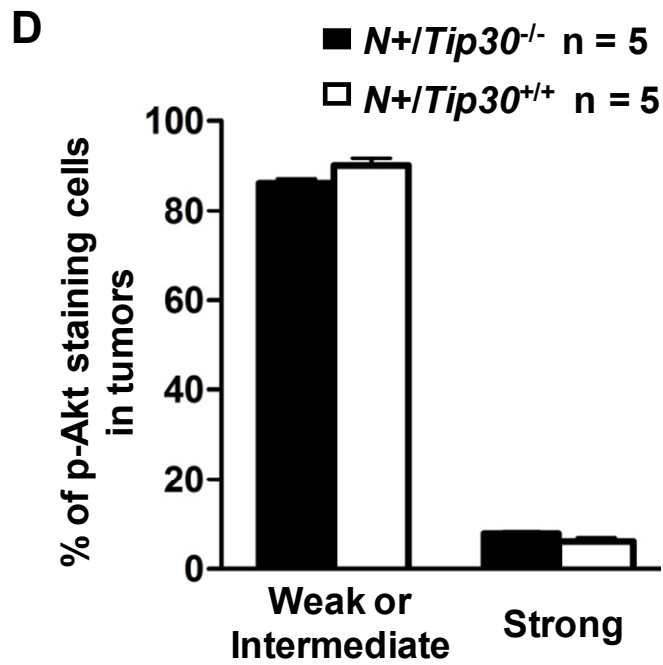
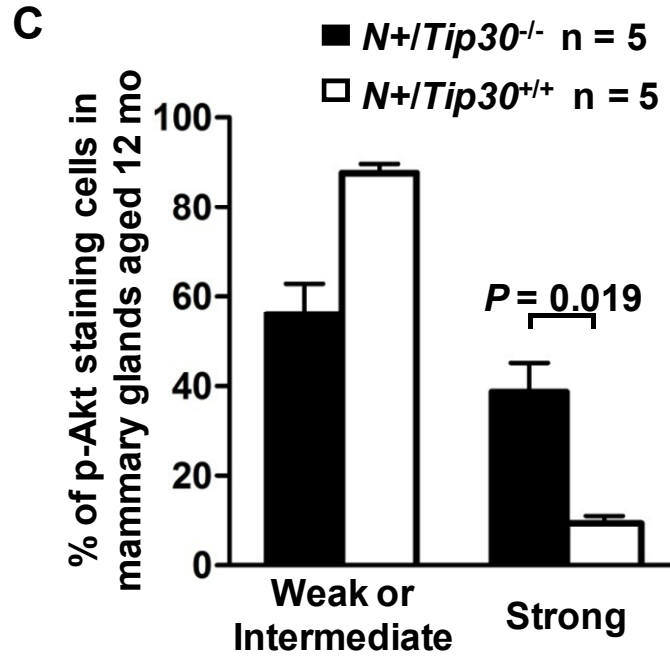


Figure 3.6 Deletion of *Tip30* in MECs leads to delayed EGFR degradation.

*A*, mammary tumor cells isolated from *Neu+ / Tip30<sup>-/-</sup>* and *Neu+ / Tip30<sup>+/+</sup>* mice were incubated with 100 ng/ml of EGF for 1 hour on ice followed by washing with cold PBS and then incubated in serum-free medium containing 20 µg/ml of cycloheximide for the indicated times. Whole cell lysates were blotted with the indicated antibodies. *B*, Quantification of EGFR protein levels in (*A*) using Odyssey 2.1 software. *C*, primary *Tip30<sup>+/+</sup>* and *Tip30<sup>-/-</sup>* MECs were subjected to EGFR internalization analysis. Representative confocal microscope images show the localization of EGFR (red) in endosomes after two hours of Alexa<sup>488</sup>-EGF (green) internalization. Results are typical and representative of three experiments on primary cells from two mice of each genotype. Boxed areas are magnified. Representative cells are outlined in white. The colocalization of EGF and EGFR (yellow) in *Tip30<sup>-/-</sup>* cells is indicative of delayed endocytic degradation of EGFR; the nucleus was stained with DAPI (Grey). Scale bar, 10 µm. *D*, Quantitative analysis of EGF and EGFR colocalization. Twenty cells in each group were analyzed using MBF\_imageJ. Pearson's colocalization coefficients were calculated and converted to percentages.  $P = 0.035$ ; *t* test.

Figure 3.6 Cont'd

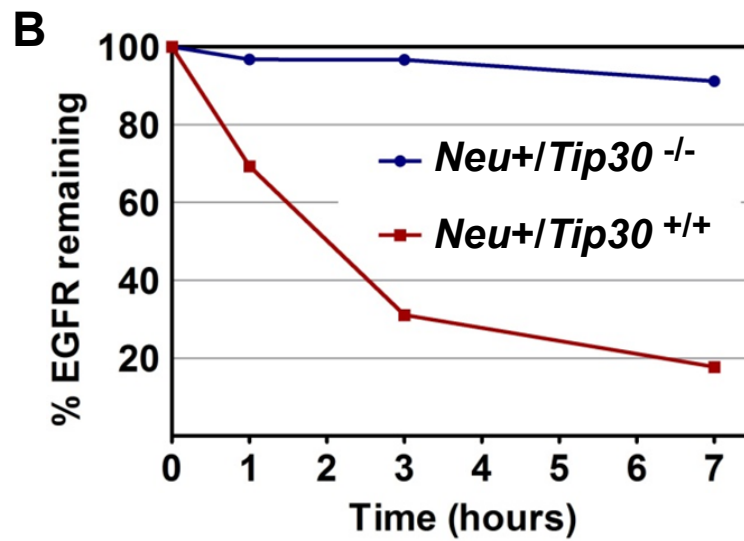
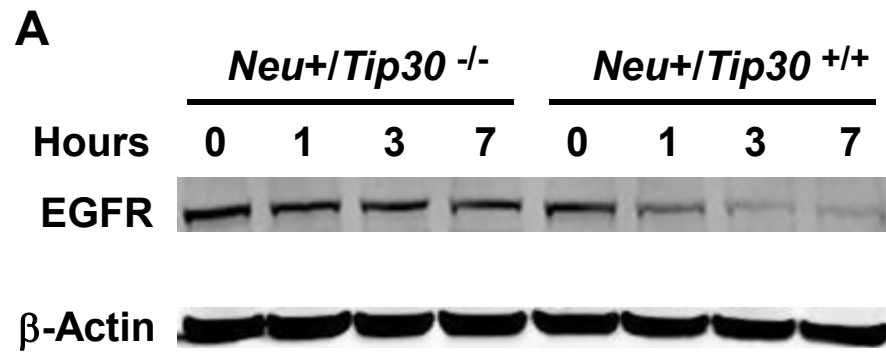
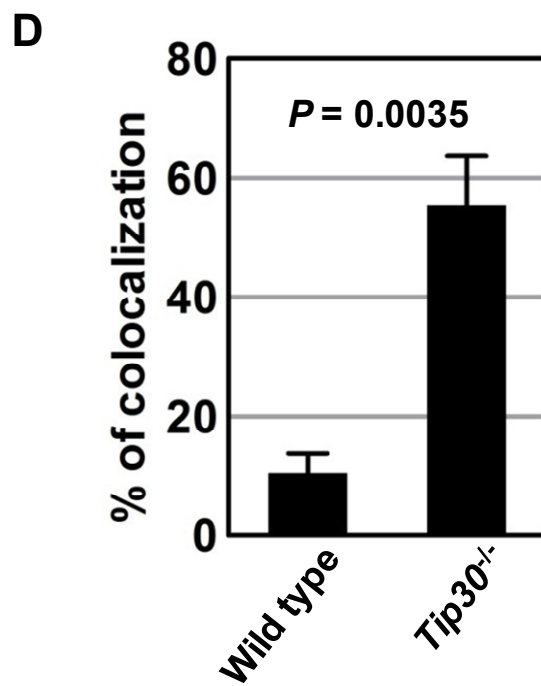
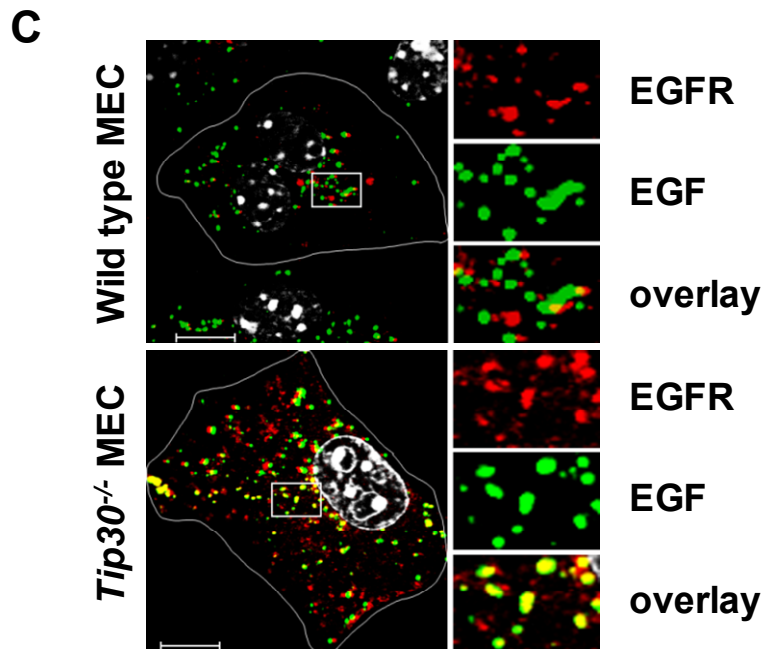


Figure 3.6 Cont'd



No significant difference in p-Akt expression levels and numbers of p-Akt-positive cells ( $P = 0.678$  or  $0.972$ , respectively) was detected between *Neu+ / Tip30<sup>-/-</sup>* and *Neu+ / Tip30<sup>+/+</sup>* mammary glands at 2 months of age (Fig. 3.5B). However, at 12 months, the number of MECs having strongly positive p-Akt staining in *Neu+ / Tip30<sup>-/-</sup>* mammary glands was significantly increased compared to that in *Neu+ / Tip30<sup>+/+</sup>* mammary glands (Strong staining in *Neu+ / Tip30<sup>-/-</sup>* mammary gland: 41.4%; Strong staining in *Neu+ / Tip30<sup>+/+</sup>* mammary gland: 9.9%;  $P = 0.02$ ; Fig. 3.5C). However, there was no significant difference in the levels of p-Akt between mammary tumors from *Neu+ / Tip30<sup>-/-</sup>* and *Neu+ / Tip30<sup>+/+</sup>* mice (Fig. 3.5D). These data indicate that the relatively earlier onset of enhanced activation p-Akt in the mammary glands due to *Tip30* loss may contribute to accelerated mammary tumorigenesis in *Neu+ / Tip30<sup>-/-</sup>* mice.

#### **Tip30 deletion leads to delayed EGFR degradation and sustained EGFR signaling.**

Upon binding EGF, EGFR proteins are rapidly internalized and localized in early endosomes, where they are either sent back to the plasma membrane or sorted into late endosomes and lysosomes for destruction (Mellman, 1996b; Sorkin and Goh, 2009). Early endosomes serve as a platform for signaling receptors to activate specific downstream signaling until ligand-receptor dissociation occurs due to early endosomal acidification mediated by vacuolar ( $H^+$ )-ATPases (Forgac, 2007; Murphy et al., 2009a). Recently, we have demonstrated that TIP30 regulates EGFR signaling by controlling endocytic downregulation of EGFR in primary hepatocytes and liver cancer cells. *Tip30* deletion impairs the fusion of Rab5 vesicles carrying vacuolar ( $H^+$ )-ATPases with early endosomes that contain internalized EGF and EGFR, leading to delayed EGFR degradation and sustained EGFR signaling<sup>7</sup>. Therefore, we questioned whether the increased phosphorylation of Akt and ER $\alpha$  in *Neu+ / Tip30<sup>-/-</sup>* mammary gland are also caused by a similar mechanism. First, we measured the protein levels of EGFR in mammary tumors cells

isolated from *Neu+ / Tip30<sup>-/-</sup>* and *Neu+ / Tip30<sup>+/+</sup>* mammary tumors in response to EGF treatment at various times after EGF internalization. We used an experimental approach that eliminates the interference from continuous ligand internalization and nascent protein synthesis to measure endocytic degradation of EGFR. The comparison revealed that endocytic degradation of EGFR was significantly delayed in *Neu+ / Tip30<sup>-/-</sup>* mammary tumors cells compared to *Neu+ / Tip30<sup>+/+</sup>* mammary tumors cells, indicating that *Tip30* deletion impairs endocytic degradation of EGFR (Fig. 3.6A and B).

To determine whether *Tip30* deletion can block EGFR trafficking from early endosomes to lysosomes for degradation, we tracked Alexa-488 conjugated EGF (Alexa<sup>488</sup>-EGF) and EGFR in normal primary MECs isolated from *Tip30<sup>-/-</sup>* and *Tip30<sup>+/+</sup>* mice. The majority of internalized EGF dissociated from EGFR in wild type MECs two hours after EGF internalization. In contrast, they remained associated with EGFR in *Tip30<sup>-/-</sup>* MECs (EGF-EGFR colocalization in wild type primary MECs: 11%; EGF-EGFR colocalization in *Tip30<sup>-/-</sup>* primary MECs: 55%; n = 20, *P* = 0.004; Fig. 3.6C and D), indicating that *Tip30* deletion causes the trapping of EGF-EGFR complex in endosomes and sustained endosomal EGFR signaling. To rule out the possibility that *Tip30* deletion increased Neu transgene expression at the level of transcription, we used quantitative RT-PCR to examine the mRNA expression of Neu transgene in 5- to 9-week-old *Neu+ / Tip30<sup>+/+</sup>* and *Neu+ / Tip30<sup>-/-</sup>* mice and found no significant difference (data not shown). Together, these results suggest that *Tip30* loss may prolong EGFR signaling, which cooperates with Neu activation to accelerate Akt activation and to promote the formation of ER+/PR- tumors.

## **Discussion**

This study was designed to investigate the relationship between HER2/Neu overexpression and *Tip30* deletion in mammary tumorigenesis by using genetically engineered mice containing both *Tip30* deletion and an MMTV-Neu transgene. Strikingly, the data demonstrate that *Tip30* deletion cooperates with Neu overexpression to promote exclusive development of ER+/PR- mammary tumors in mice. In addition, we show that Tip30 loss impairs endocytic trafficking of EGF-EGFR, delays EGFR degradation in primary MECs and tumor cells and enhances Akt and ER $\alpha$  phosphorylation in the mammary gland. These findings, combined with our recent observation that TIP30 formed a protein complex with ACSL4 and EndoB1 to control EGF-EGFR endocytic trafficking in hepatocytes<sup>7</sup>, strongly suggest a novel mechanism by which loss of Tip30 contributes to the development of ER+/PR- tumors, at least in part, through enhancing EGFR/Akt signaling in ER+ MECs.

It is not immediately obvious why *Tip30* deletion combined with Neu overexpression cause the exclusive development of ER+/PR- mammary tumors. The observation that the promoter of *Tip30* was predominantly active in ER+ MECs suggest that *Tip30* deletion may mainly affect the proliferation of ER+ cells by inducing enhanced ER $\alpha$  activities, thereby selecting ER+ cells to initiate tumorigenesis. Indeed, ER+/PR+ mammary tumors developed spontaneously in 22% of aged *Tip30* knockout female mice in the BALB/c genetic background<sup>8</sup>; and TIP30 was able to inhibit ER $\alpha$ -mediated transcription (Jiang et al., 2004a). The correlation between progressively increased p-Akt and p-ER $\alpha$  positive cells in *Neu+ /Tip30<sup>-/-</sup>* mammary glands observed in this study implies that *Tip30* deletion may promote the development of ER+ mammary tumors by enhancing Akt activation and increasing active ER $\alpha$  positive cells. Consistent with this scenario, a previous study showed that Akt overexpression can increase the intensity of ER $\alpha$  staining, the number of ER $\alpha$  positive cells and the frequency of ER+ tumors in DMBA-treated mice (Blanco-

Aparicio et al., 2007), although it did not show whether these tumors were PR positive. Moreover, expression and phosphorylation of ER $\alpha$  in ER+ human breast cells is enhanced by the activation of Akt (Blanco-Aparicio et al., 2007; Campbell et al., 2001). It should be noted that enhanced Akt activation alone is insufficient for driving the tumorigenic process in mouse MECs *in vivo* (Hutchinson et al., 2001); therefore, other mechanisms such as increased expression of c-Myc and IGF-1 induced by *Tip30* deletion may also contribute to the formation of ER+/PR- mammary tumors in MMTV-Neu mouse models.

Although tumors arising in *Neu+/Tip30<sup>-/-</sup>* mice are stained negatively for PRs, these ER+/PR- tumors were sensitive to progesterone stimulation and RU486 inhibition, and PR proteins were detectable in cultured tumor cells from ER+/PR- tumors when proteasomes were inhibited. One explanation for these observations is that PR-A is expressed in ER+/PR- tumors but rapidly turned over due to enhanced activation of EGFR and HER2/Neu *in vivo*. This explanation is supported by previous reports that PRs were targeted for degradation by the 26S proteasome and regulated by MAPK-induced phosphorylation of PRs in cultured breast cancer cells (Lange et al., 2000). Thus, it is possible that both activated EGFR and HER2 signaling pathways induce PR hyperphosphorylation and rapid degradation, consequently resulting in a negative staining for PRs in tumors.

Our data seem to support the hypothesis that ER+ breast cancers arise from ER+ or otherwise estrogen-responsive progenitor cells (Allred et al., 2004). However, our data do not exclude the possibility that *Tip30* deletion may cause ER-/PR- cells to re-express ER $\alpha$  or promote transformed ER-/PR- luminal progenitor cells to differentiate to ER+/PR- epithelial cells. Studies on the origin of tumor cells in MMTV-Neu mice have suggested that tumor cells from this model

originate from transformed luminal progenitor cells committing to ER-PR- cells (Vaillant et al., 2008). Therefore, the cell origin of ER+/PR- tumors arising in *Neu+/Tip30<sup>-/-</sup>* mice remains to be determined.

Currently there remains a profound need for more effective therapies for treating HER2+/ER+/PR- breast cancers because of their poor response and development of resistance to existing therapies. Nonetheless, the majority of pre-clinical studies of ER positive breast cancer have relied on cultured cell lines or on xenograft tumor models, in which breast tumor development and progression does not accurately represent clinical human breast cancer. Alternatively, the use of genetically engineered mouse models of breast cancer has major advantages for the investigation of the mechanisms fundamental to mammary tumorigenesis, as well as the development of anticancer agents. To date, there have been many mouse models of mammary cancer based on the overexpression or deletion of specific genes that are associated with human breast cancer. Unfortunately, most mammary tumors arising in those animal models are ER-/PR- and do not morphologically resemble the major subtype of human breast cancer (ER+ ductal carcinoma); ER+ mammary tumors are observed in only a few genetically-engineered mouse models (Liu et al., 2009; Medina et al., 2002; Rose-Hellekant et al., 2007; Zhang et al., 2005). To our knowledge, there has been no animal model of HER2+/ER+/PR- mammary tumors reported. Therefore, our mouse model of HER2+/ER+/PR- breast cancer provides a valuable tool for deciphering the mechanisms of HER2+/ER+/PR- breast cancer development and for testing single or combination therapies.

## **Materials and Methods**

### **Mice, primary MECs and tumor cells**

*Tip30*<sup>+/-</sup> mice in FBV genetic background were generated by backcrossing *Tip30*<sup>+/-</sup> C57BL/6 mice (Pecha et al., 2007) with FBV mice seven times. *Tip30*<sup>+/-</sup> mice in FBV background were bred with MMTV-Neu mice (FVB/N-Tg, Jackson Laboratory) to generate *Neu*<sup>+</sup>/*Tip30*<sup>+/-</sup>, *Neu*<sup>+</sup>/*Tip30*<sup>+/-</sup> and *Neu*<sup>+</sup>/*Tip30*<sup>+/+</sup> mice. Primary MECs and tumor cells were isolated and cultured as described previously (Medina, 2000). For tumor transplantation assays, all recipient mice were 8-week-old Nu/Nu female nude mice (Charles River). For ovariectomized mice both ovaries of mice were removed under anesthesia. Placebo (25 mg, 90 days release), 17-estradiol (0.1mg E2, 90-days release), Progesterone (35 mg P4, 21 days release) or E2 + P4 pellets (0.1 mg E2 + 32.5 mg P4, 90 days release) were purchased from Innovative Research of America and implanted subcutaneously in the front flanks of each mouse, respectively. RU486 was purchased from Calbiochem. Mice were sacrificed in the end of three months or when the tumor volume reached 1 cm<sup>3</sup>. All mice were housed and cared for in the Animal Facility at Michigan State University according to institutional guidelines.

### **Immunofluorescence and immunohistochemistry**

Immunofluorescent staining of mouse mammary tissues was performed as follow. After deparaffinization and rehydration, tissue sections were autoclaved and then incubated with primary antibody specific for ER $\alpha$  (MC-20, 1:50; Santa Cruz Biotechnology), p-ER $\alpha$  (Santa Cruz Biotechnology), PR-A (hPRa7, 1:50; Labvision), PR-B (hPRa6, 1:50; Labvision), or  $\beta$ -Gal (Promega) at 4 °C overnight. After PBS rinse, tissue sections were sequentially incubated for 30 min at room temperature with diluted goat anti-rabbit or mouse Alex-488 or -594-conjugated secondary antibody (1:200; Molecular Probes). Nuclei were counterstained with DAPI. Immunohistochemical staining of mouse mammary tissues was described previously (Jiang et

al., 2007). Immunohistochemical analysis of p-Akt at Ser-473 (1:50; Cell Signaling Technologies) and p-ER $\alpha$  (Santa Cruz Biotechnology) were performed as described previously (Jiang et al., 2007).

### **EGFR internalization assay**

*Tip30*<sup>+/+</sup> and *Tip30*<sup>-/-</sup> primary mammary epithelial cells were isolated from 2-month-old *Tip30*<sup>+/+</sup> and *Tip30*<sup>-/-</sup> female mice and cultured as previously described (Pecha et al., 2007) and then serum-starved for three hours. Cells were incubated on ice with 100 ng/ml Alexa<sup>488</sup>-EGF (Invitrogen) and 20  $\mu$ g/ml cycloheximide on ice for 1 hour and then washed 4 times with cold PBS before being moved to 37 °C and incubated in DMEM with 20  $\mu$ g/ml cycloheximide for two hours. Cells were fixed in 4% paraformaldehyde in PBS for 15 min, permeabilized with 0.1% Triton X-100 for 2 min and stained for EGFR. Images were obtained with a Zeiss LSM 510 Meta confocal microscope (Carl Zeiss) using Plan-Apochromat 63 $\times$ /1.40 Oil objective. Pinhole size was set to 1 airy unit for all channels. All images are representative single optical sections.

### **Statistical Analysis**

Comparisons among groups were analyzed by two-sided *t*-test or Fisher's exact test. A difference of  $P < 0.05$  was considered to be statistically significant. All analyses were done with SPSS software, Version 11.5. Data are expressed as mean  $\pm$  SEM.

### **Disclosure of Potential Conflicts of Interest**

No potential conflicts of interest were disclosed.

### **Acknowledgments**

We are grateful to Jill Pecha for backcrossing *Tip30* deletion allele into FBV mice and Ryan Brooks, Adam C. Edmunds, George Chen for the excellent technical assistance. We thank Ying Qin for histopathological expertise and Eran Andrechek for critical reading of the manuscript. This work was supported by grants RO1 DK066110-01 and W81XWH-08-1-0377 (to H.X.) from the NIDDK and Department of Defense and grant U01 ES/CA 012800 (to S.Z.H.) from the National Institute of Environment Health Science (NIEHS) and the National Cancer Institute (NCI), National Institutes of Health, Department of Health and Human Services. Its contents are solely the responsibility of the authors and do not necessarily represent the official views of the NIDDK, NIEHS or NCI, NIH.

## REFERENCES

## REFERENCES

1. Osborne CK, Schiff R, Arpino G, Lee AS, Hilsenbeck VG. Endocrine responsiveness: understanding how progesterone receptor can be used to select endocrine therapy. *Breast*. 2005;14:458-65.
2. Ponzzone R, Montemurro F, Maggiorotto F, Robba C, Gregori D, Jacomuzzi ME, et al. Clinical outcome of adjuvant endocrine treatment according to PR and HER-2 status in early breast cancer. *Ann Oncol*. 2006;17:1631-6.
3. Arpino G, Weiss H, Lee AV, Schiff R, De Placido S, Osborne CK, et al. Estrogen receptor-positive, progesterone receptor-negative breast cancer: association with growth factor receptor expression and tamoxifen resistance. *J Natl Cancer Inst*. 2005;97:1254-61.
4. Creighton CJ, Kent Osborne C, van de Vijver MJ, Foekens JA, Klijn JG, Horlings HM, et al. Molecular profiles of progesterone receptor loss in human breast tumors. *Breast Cancer Res Treat*. 2009;114:287-99.
5. Kim HJ, Cui X, Hilsenbeck SG, Lee AV. Progesterone receptor loss correlates with human epidermal growth factor receptor 2 overexpression in estrogen receptor-positive breast cancer. *Clin Cancer Res*. 2006;12:1013s-8s.
6. Cui X, Schiff R, Arpino G, Osborne CK, Lee AV. Biology of progesterone receptor loss in breast cancer and its implications for endocrine therapy. *J Clin Oncol*. 2005;23:7721-35.
7. Dowsett M, Johnston S, Martin LA, Salter J, Hills M, Detre S, et al. Growth factor signalling and response to endocrine therapy: the Royal Marsden Experience. *Endocr Relat Cancer*. 2005;12 Suppl 1:S113-7.
8. Konecny G, Pauletti G, Pegram M, Untch M, Dandekar S, Aguilar Z, et al. Quantitative association between HER-2/neu and steroid hormone receptors in hormone receptor-positive primary breast cancer. *J Natl Cancer Inst*. 2003;95:142-53.
9. Xiao H, Tao Y, Greenblatt J, Roeder RG. A cofactor, TIP30, specifically enhances HIV-1 Tat-activated transcription. *Proc Natl Acad Sci U S A*. 1998;95:2146-51.
10. Ito M, Jiang C, Krumm K, Zhang X, Pecha J, Zhao J, et al. TIP30 deficiency increases susceptibility to tumorigenesis. *Cancer Res*. 2003;63:8763-7.
11. Lee LW, Zhang DH, Lee KT, Koay ES, Hewitt RE. CC3/TIP30 expression was strongly associated with HER-2/NEU status in breast cancer. *Ann Acad Med Singapore*. 2004;33:S30-2.

12. Tong X, Li K, Luo Z, Lu B, Liu X, Wang T, et al. Decreased TIP30 expression promotes tumor metastasis in lung cancer. *Am J Pathol.* 2009;174:1931-9.
13. Zhao J, Ni H, Ma Y, Dong L, Dai J, Zhao F, et al. TIP30/CC3 expression in breast carcinoma: relation to metastasis, clinicopathologic parameters, and P53 expression. *Hum Pathol.* 2007;38:293-8.
14. Pecha J, Ankrapp D, Jiang C, Tang W, Hoshino I, Bruck K, et al. Deletion of Tip30 leads to rapid immortalization of murine mammary epithelial cells and ductal hyperplasia in the mammary gland. *Oncogene.* 2007;26:7423-31.
15. Jiang C, Ito M, Piening V, Bruck K, Roeder RG, Xiao H. TIP30 interacts with an estrogen receptor alpha-interacting coactivator CIA and regulates c-myc transcription. *J Biol Chem.* 2004;279:27781-9.
16. Zhao J, Lu B, Xu H, Tong X, Wu G, Zhang X, et al. Thirty-kilodalton Tat-interacting protein suppresses tumor metastasis by inhibition of osteopontin transcription in human hepatocellular carcinoma. *Hepatology.* 2008;48:265-75.
17. King FW, Shtivelman E. Inhibition of nuclear import by the proapoptotic protein CC3. *Mol Cell Biol.* 2004;24:7091-101.
18. Guy CT, Webster MA, Schaller M, Parsons TJ, Cardiff RD, Muller WJ. Expression of the neu protooncogene in the mammary epithelium of transgenic mice induces metastatic disease. *Proc Natl Acad Sci U S A.* 1992;89:10578-82.
19. Huang S, Li Y, Chen Y, Podsypanina K, Chamorro M, Olshen AB, et al. Changes in gene expression during the development of mammary tumors in MMTV-Wnt-1 transgenic mice. *Genome Biol.* 2005;6:R84.
20. Lange CA, Shen T, Horwitz KB. Phosphorylation of human progesterone receptors at serine-294 by mitogen-activated protein kinase signals their degradation by the 26S proteasome. *Proc Natl Acad Sci U S A.* 2000;97:1032-7.
21. Campbell RA, Bhat-Nakshatri P, Patel NM, Constantinidou D, Ali S, Nakshatri H. Phosphatidylinositol 3-kinase/AKT-mediated activation of estrogen receptor alpha: a new model for anti-estrogen resistance. *J Biol Chem.* 2001;276:9817-24.
22. Lannigan DA. Estrogen receptor phosphorylation. *Steroids.* 2003;68:1-9.
23. Hutchinson JN, Jin J, Cardiff RD, Woodgett JR, Muller WJ. Activation of Akt-1 (PKB-alpha) can accelerate ErbB-2-mediated mammary tumorigenesis but suppresses tumor invasion. *Cancer Res.* 2004;64:3171-8.

24. Ju X, Katiyar S, Wang C, Liu M, Jiao X, Li S, et al. Akt1 governs breast cancer progression in vivo. *Proc Natl Acad Sci U S A*. 2007;104:7438-43.
25. Maroulakou IG, Oemler W, Naber SP, Tschlis PN. Akt1 ablation inhibits, whereas Akt2 ablation accelerates, the development of mammary adenocarcinomas in mouse mammary tumor virus (MMTV)-ErbB2/neu and MMTV-polyoma middle T transgenic mice. *Cancer Res*. 2007;67:167-77.
26. Nardulli AM, Katzenellenbogen BS. Progesterone receptor regulation in T47D human breast cancer cells: analysis by density labeling of progesterone receptor synthesis and degradation and their modulation by progestin. *Endocrinology*. 1988;122:1532-40.
27. Mellman I. Membranes and sorting. *Curr Opin Cell Biol*. 1996;8:497-8.
28. Sorkin A, Goh LK. Endocytosis and intracellular trafficking of ErbBs. *Exp Cell Res*. 2009;315:683-96.
29. Forgac M. Vacuolar ATPases: rotary proton pumps in physiology and pathophysiology. *Nat Rev Mol Cell Biol*. 2007;8:917-29.
30. Murphy JE, Padilla BE, Hasdemir B, Cottrell GS, Bunnett NW. Endosomes: a legitimate platform for the signaling train. *Proc Natl Acad Sci U S A*. 2009;106:17615-22.
31. Blanco-Aparicio C, Perez-Gallego L, Pequeno B, Leal JF, Renner O, Carnero A. Mice expressing myrAKT1 in the mammary gland develop carcinogen-induced ER-positive mammary tumors that mimic human breast cancer. *Carcinogenesis*. 2007;28:584-94.
32. Hutchinson J, Jin J, Cardiff RD, Woodgett JR, Muller WJ. Activation of Akt (protein kinase B) in mammary epithelium provides a critical cell survival signal required for tumor progression. *Mol Cell Biol*. 2001;21:2203-12.
33. Shen T, Horwitz KB, Lange CA. Transcriptional hyperactivity of human progesterone receptors is coupled to their ligand-dependent down-regulation by mitogen-activated protein kinase-dependent phosphorylation of serine 294. *Mol Cell Biol*. 2001;21:6122-31.
34. Qiu M, Lange CA. MAP kinases couple multiple functions of human progesterone receptors: degradation, transcriptional synergy, and nuclear association. *J Steroid Biochem Mol Biol*. 2003;85:147-57.
35. Daniel AR, Faivre EJ, Lange CA. Phosphorylation-dependent antagonism of sumoylation derepresses progesterone receptor action in breast cancer cells. *Mol Endocrinol*. 2007;21:2890-906.

36. Aupperlee MD, Smith KT, Kariagina A, Haslam SZ. Progesterone receptor isoforms A and B: temporal and spatial differences in expression during murine mammary gland development. *Endocrinology*. 2005;146:3577-88.
37. Allred DC, Brown P, Medina D. The origins of estrogen receptor alpha-positive and estrogen receptor alpha-negative human breast cancer. *Breast Cancer Res*. 2004;6:240-5.
38. Vaillant F, Asselin-Labat ML, Shackleton M, Forrest NC, Lindeman GJ, Visvader JE. The mammary progenitor marker CD61/beta3 integrin identifies cancer stem cells in mouse models of mammary tumorigenesis. *Cancer Res*. 2008;68:7711-7.
39. Liu S, Umez-Goto M, Murph M, Lu Y, Liu W, Zhang F, et al. Expression of autotaxin and lysophosphatidic acid receptors increases mammary tumorigenesis, invasion, and metastases. *Cancer Cell*. 2009;15:539-50.
40. Medina D, Kittrell FS, Shepard A, Stephens LC, Jiang C, Lu J, et al. Biological and genetic properties of the p53 null preneoplastic mammary epithelium. *Faseb J*. 2002;16:881-3.
41. Rose-Hellekant TA, Schroeder MD, Brockman JL, Zhdankin O, Bolstad R, Chen KS, et al. Estrogen receptor-positive mammary tumorigenesis in TGFalpha transgenic mice progresses with progesterone receptor loss. *Oncogene*. 2007;26:5238-46.
42. Zhang X, Podsypanina K, Huang S, Mohsin SK, Chamness GC, Hatsell S, et al. Estrogen receptor positivity in mammary tumors of Wnt-1 transgenic mice is influenced by collaborating oncogenic mutations. *Oncogene*. 2005;24:4220-31.
43. Medina D, Kittrell, F. Establishment of mouse mammary cell lines. New York: Kluwer Academic/Plenum Publishers; 2000.
44. Jiang C, Pecha J, Hoshino I, Ankrapp D, Xiao H. TIP30 mutant derived from hepatocellular carcinoma specimens promotes growth of HepG2 cells through up-regulation of N-cadherin. *Cancer Res*. 2007;67:3574-82.
45. Ku NO, Omary MB. Keratins turn over by ubiquitination in a phosphorylation-modulated fashion. *J Cell Biol*. 2000;149:547-52.

## **Chapter 4 Conclusions, Discussions and Future Directions**

#### **4.1 EGF dissociates from EGFR and exits the early endosomes in membrane-bound vesicles**

It has become a general theme that receptors release their ligands in the early endosomes before being recycled back to the plasma membrane or being destroyed in lysosomes. In 1979, based on a study that individually tracked EGF and EGFR, Carpenter et al suggested that EGF-EGFR complexes travel together to lysosomes for degradation (Carpenter and Cohen, 1976, 1979). Our data generated in this study by simultaneously tracking multiple molecules showed that EGF, like many other ligands, is shed by EGFR earlier in the endocytic pathway. More strikingly, we demonstrated that EGF is enclosed in membrane-bound vesicles after leaving endosomes. The EGF vesicles are devoid of the currently known early endosome makers Rab5a and EEA1 and the late endosome/lysosome marker LAMP1, suggesting that they are previously undescribed vesicles (Figure 4.1). Significantly, the discovery and characterization of this new group of vesicles will revise the method that has been adopted to study EGFR trafficking by tracking the behavior of EGF vesicles.

The physiological significance of secluding EFG in vesicles remains to be determined. It would be interesting to know if under certain circumstances the enclosed EGF has an opportunity of being transported back outside of the cell and being reused. Another important question that needs to be answered is whether other ligands, such as insulin, IGF, TGF and LDL, are also enclosed in vesicles after being released from the early endosome.

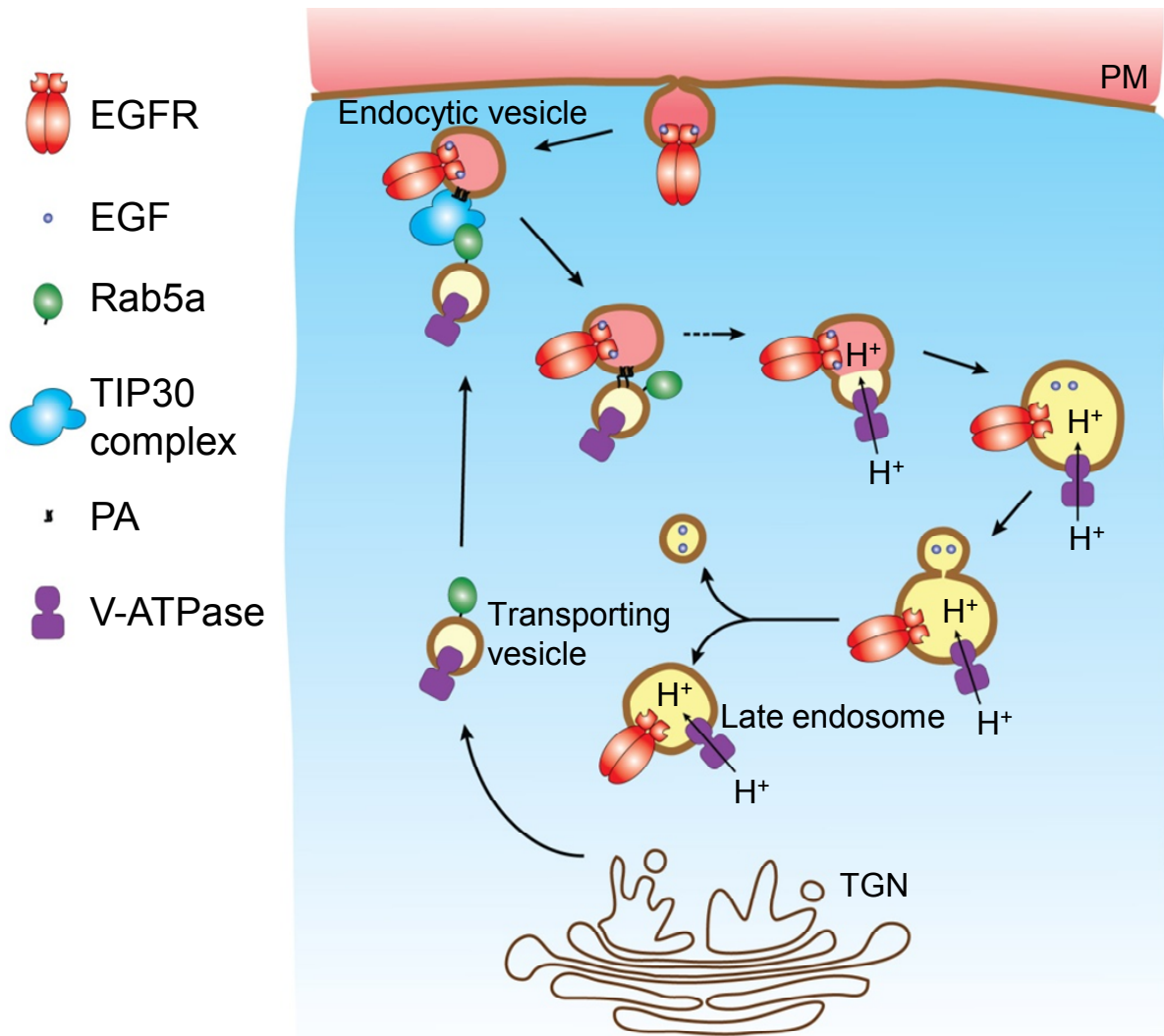


Figure 4.1 Function of the TIP30 complex

The TIP30 protein complex transfers arachidonic acid to PA to initiate membrane fusion between Rab5a vesicles and endocytic vesicles. Drawing not to scale.

## **4.2 Rab5a vesicles deliver endosomal targeting proteins via membrane fusion**

Rab5a is a well established early endosome marker. However, how Rab5a is recruited on early endosomes remains unclear. It was proposed that Rab5a either comes from the plasma membrane where it internalizes together with the incoming vesicles or is recruited from the cytoplasm (Bucci et al., 1992; Pfeffer and Aivazian, 2004). Nonetheless, our Triton X-114 partition experiments (Bordier, 1981) with mouse liver samples showed that Rab5a proteins exclusively appear in membrane fractions (Figure 4.2). Other members in the Rab protein family were also revealed in insoluble membrane fractions (Guo et al., 1999; Khosravi-Far et al., 1991). Moreover, Rab5a was localized in numerous smaller vesicles, which are redistributed from the perinuclear region to the cell periphery region where they are recruited to early endosomes in response to EGF (Bucci et al., 1992; Lakadamyali et al., 2006; Leonard et al., 2008; Nielsen et al., 1999). Our data clearly showed that Rab5a indeed is recruited on early endosomes in vesicles. Two populations of Rab5a-positive vesicles were characterized. One population is EEA1-positive endocytic vesicles; another one is EEA1 negative transporting vesicles. More significantly, we provided a direct mechanistic explanation of how Rab5a regulates endocytic trafficking by showing that Rab5a vesicles are responsible for the delivery of V-ATPase, a proton pump that is crucial for ligand-receptor dissociation. Failure to release ligands resulted in the trapping of ligand-receptor complexes in endosomes.

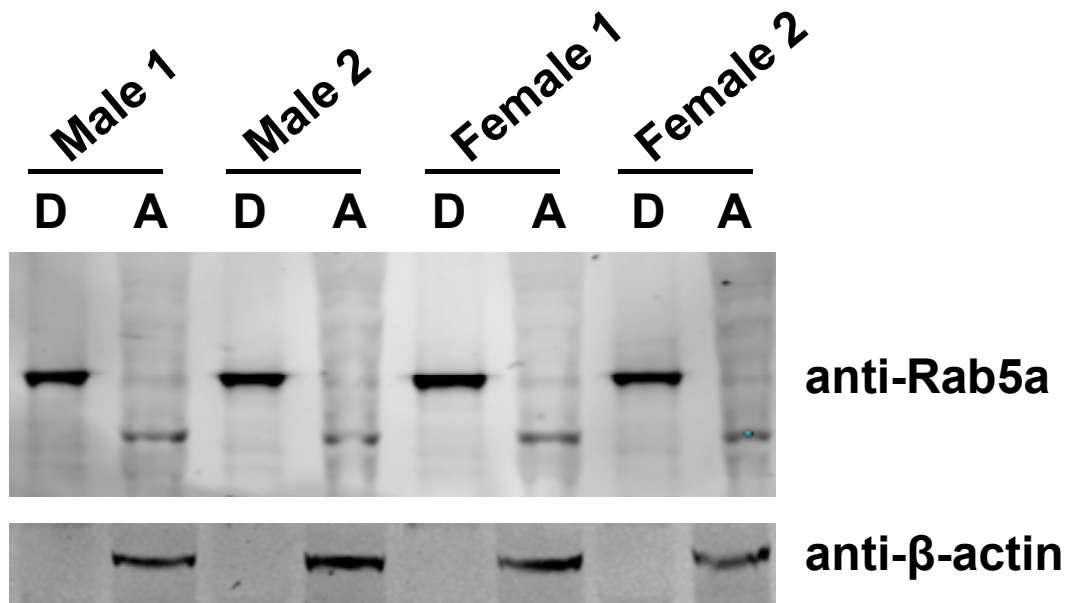


Figure 4.2 Phase separation of Rab5a in Triton X-114

Phase separation of integral membrane proteins in Triton X-114 was performed as described (Bordier, 1981). Protein samples were prepared from two male mice and two female mice. Detergent phase (D) and aqueous phases (A) were subjected to SDS-PAGE and immunoblot using indicated antibodies.

During endocytosis, a number of proteins are recruited to endosomes and lysosomes to facilitate the movement and maturation of these vesicles and to digest the contents of lysosomes. It would be interesting to know what other proteins may be carried by the Rab5a vesicles. In addition to endosome maturation, Rab5a was also required for the maturation of autophagosomes (Kitano et al., 2008). This observation raised the possibility that Rab5a might also deliver V-ATPase to phagosomes to create the low pH environment that is needed for content digestion by acidic proteolytic enzymes.

### **4.3 TIP30, ACSL4 and Endo B1 form a protein complex that interacts with Rab5a and mediates the fusion of Rab5a vesicles with endocytic vesicles**

In this study, we identified a novel TIP30 protein complex containing TIP30, ACSL4, Endo B1 and Rab5a. Rab5a has been reported as regulator of the endocytic pathway (Bucci et al., 1992; Chen et al., 2009b; Lanzetti et al., 2004; Miaczynska et al., 2004a; Nielsen et al., 1999; Sonnichsen et al., 2000). Identification of these two proteins in the protein complex led us to study the regulation of receptor-mediated endocytosis by these proteins. We first found that these proteins are required for the endocytic downregulation of EGFR protein levels and signaling levels. It was later discovered that without these proteins Rab5a vesicles cannot deliver V-ATPase to endocytic vesicles, leading to the trapping of EGF-EGFR complexes in early endosomes. *In vitro* membrane fusion assays indicated that the TIP30 complex acts coordinately to promote membrane fusion between Rab5a vesicles and endocytic vesicles likely by fatty acylating phosphatidic acid (PA).

Although proteins in the TIP30 complex have been shown to be important for vesicular membrane fusion, the precise roles of these proteins in this process are not known. How do these proteins help the Rab5a vesicles find the specific target membrane to fuse? EEA1 was purified as a Rab5a effector, which can promote endosome-endosome fusion *in vitro*. It was shown that the recruitment of EEA1 to the early endosome membrane depends on its interaction with Rab5a and its binding to phosphatidylinositol-3-phosphate (Simonsen et al., 1998; Stenmark et al., 1996). However, a recent study showed that depletion of Rab5a in cells does not affect the distribution of EEA1 on early endosomes (Chen et al., 2009b). Our data support this observation by demonstrating that EEA1 appears on early endosomes that are devoid of Rab5a. Therefore, it is possible that EEA1 is recruited to early endosomes through binding to phosphatidylinositol-3-

phosphate with its FYVE finger. Then specificity is achieved by the recognition and binding of Rab5a to EEA1. In the meantime, Rab5a recruits the other proteins in the TIP30 complex to the fusion sites for the initiation of lipid modification.

Another important question is how these proteins facilitate membrane fusion. The ability of the TIP30 complex to initiate membrane fusion seems to rely on the transfer of an arachidonyl group to endosomal PA. Of the four proteins that have been tested for membrane lipid binding, TIP30 and Endo B1 strongly bind to PA, raising the possibility that they may be involved in the transferring arachidonyl group to PA. This hypothesis is supported by the finding that PA incubated with the TIP30 complex and arachidonic acid is capable of inducing dramatic membrane tethering and stacking.

#### **4.4 Arachidonic acid and the synthesis of arachidonyl-coA by ACSL4 is essential for membrane fusion**

The essential role of arachidonic acid in vesicle membrane fusion was first described by Carl Creutz 30 years ago (Creutz, 1981). He also found that arachidonic acid loses its fusogenic function if its head group is methylated, suggesting that the carboxyl group needs to be available for other reactions during membrane fusion. In the following years, the essential role of arachidonic acid in a variety of membrane fusion events has been reported (Chattopadhyay et al., 2003; Freeman et al., 1990; Latham et al., 2007; Nishio et al., 1996; Paiement et al., 1994; Williams et al., 1989). However, the underlying mechanism for its pivotal function remained a mystery. Recently, *in vitro* protein binding studies indicated that arachidonic acid directly binds to syntaxin 1 and stimulates its association with SNAP25 to form SNARE complexes (Connell et al., 2007). A non-hydrolysable analogue of arachidonic acid was shown to have a similar effect

(Latham et al., 2007), raising the question of whether arachidonic acid needs to be activated for its fusogenic function. Consistent with the Creutz report, our data showed that arachidonic acid is essential for membrane fusion and that it must be activated by ACSL4 to produce arachidonyl-coA.

*In vitro* membrane fusion experiments utilizing artificial membranes have demonstrated that a set of proteins are capable of promoting fusion at a physiologically meaningful speed (Ohya et al., 2009). Significantly, our data showed that at least three more proteins are required for efficient fusion of biological intact membranes. The next important issue that needs to be addressed is whether lipid modification by the TIP30 protein complex is universal to all vesicular membrane fusion events.

#### **4.5 Tip30 deletion in MMTV-Neu transgenic mice leads to the development of ER+/PR- tumors**

Approximately 5% of breast cancer patients are found with HER2+/ER+/PR- mammary tumors, which have more aggressive malignant characteristics and an extremely poor response to endocrine treatment. Mechanistic study of the development of tumors with this phenotype has been hampered by the lack of mouse models. Significantly, we discovered that Tip30 deletion resulted in not only earlier onset of tumors in MMTV-Neu transgenic mice, but also the development of ER+/PR- mammary tumors. Similar to liver cells, deletion of Tip30 in mouse mammary cells also delayed EGFR destruction and sustained EGFR signaling in response to EGF treatment, suggesting that the regulation of endocytic trafficking by Tip30 can expand to other cell types.

Enhanced EGFR/Akt signaling has been correlated with hyperphosphorylation of ER and accelerated protein turnover of PR (Campbell et al., 2001; Kim et al., 2006). Consistently, our data showed that the levels of pAkt<sup>S473</sup> and pER<sup>S167</sup> were significantly elevated in *Tip30*<sup>-/-</sup>/MMTV-Neu. PR was undetectable by western blot analysis in mammary cells that were isolated from these mice unless protease inhibitor was added. Together, these data suggest a mechanism of the development of HER2/ER+/PR- mammary tumors.

The clinical significance of this study points to the possibility of adding four genes, TIP30, Rab5a, Endo B1, and ACSL4, as prognosis markers for HER2/ER+/PR- mammary tumors. The activation sites for Akt have been restricted to early endosomes containing signaling receptors (Murphy et al., 2009b; Vieira et al., 1996; Wang et al., 2002). Therefore, drugs that target molecules downstream of the signaling receptor have to be taken into consideration for the treatment of HER2/ER+/PR- breast cancer patients.

## REFERENCES

## REFERENCES

- Bordier, C. (1981). Phase separation of integral membrane proteins in Triton X-114 solution. *J Biol Chem* 256, 1604-1607.
- Bucci, C., Parton, R.G., Mather, I.H., Stunnenberg, H., Simons, K., Hoflack, B., and Zerial, M. (1992). The small GTPase rab5 functions as a regulatory factor in the early endocytic pathway. *Cell* 70, 715-728.
- Campbell, R.A., Bhat-Nakshatri, P., Patel, N.M., Constantinidou, D., Ali, S., and Nakshatri, H. (2001). Phosphatidylinositol 3-kinase/AKT-mediated activation of estrogen receptor alpha: a new model for anti-estrogen resistance. *J Biol Chem* 276, 9817-9824.
- Carpenter, G., and Cohen, S. (1976). 125I-labeled human epidermal growth factor. Binding, internalization, and degradation in human fibroblasts. *J Cell Biol* 71, 159-171.
- Carpenter, G., and Cohen, S. (1979). Epidermal growth factor. *Annu Rev Biochem* 48, 193-216.
- Chattopadhyay, S., Sun, P., Wang, P., Abonyo, B., Cross, N.L., and Liu, L. (2003). Fusion of Lamellar Body with Plasma Membrane Is Driven by the Dual Action of Annexin II Tetramer and Arachidonic Acid. *Journal of Biological Chemistry* 278, 39675-39683.
- Chen, P.I., Kong, C., Su, X., and Stahl, P.D. (2009). Rab5 isoforms differentially regulate the trafficking and degradation of epidermal growth factor receptors. *J Biol Chem* 284, 30328-30338.
- Connell, E., Darios, F., Broersen, K., Gatsby, N., Peak-Chew, S.Y., Rickman, C., and Davletov, B. (2007). Mechanism of arachidonic acid action on syntaxin-Munc18. *EMBO Rep* 8, 414-419.
- Creutz, C.E. (1981). cis-Unsaturated Fatty Acids Induce the Fusion of Chromaffin Granules Aggregated by Synexin. *The Journal of Cell Biology* 91, 247-256.
- Freeman, E.J., Terrian, D.M., and Dorman, R.V. (1990). Presynaptic facilitation of glutamate release from isolated hippocampal mossy fiber nerve endings by arachidonic acid. *Neurochem Res* 15, 743-750.
- Guo, W., Roth, D., Walch-Solimena, C., and Novick, P. (1999). The exocyst is an effector for Sec4p, targeting secretory vesicles to sites of exocytosis. *EMBO J* 18, 1071-1080.
- Khosravi-Far, R., Lutz, R.J., Cox, A.D., Conroy, L., Bourne, J.R., Sinensky, M., Balch, W.E., Buss, J.E., and Der, C.J. (1991). Isoprenoid modification of rab proteins terminating in CC or CXC motifs. *Proc Natl Acad Sci U S A* 88, 6264-6268.

- Kim, H.J., Cui, X., Hilsenbeck, S.G., and Lee, A.V. (2006). Progesterone receptor loss correlates with human epidermal growth factor receptor 2 overexpression in estrogen receptor-positive breast cancer. *Clin Cancer Res* *12*, 1013s-1018s.
- Kitano, M., Nakaya, M., Nakamura, T., Nagata, S., and Matsuda, M. (2008). Imaging of Rab5 activity identifies essential regulators for phagosome maturation. *Nature* *453*, 241-245.
- Lakadamyali, M., Rust, M.J., and Zhuang, X. (2006). Ligands for clathrin-mediated endocytosis are differentially sorted into distinct populations of early endosomes. *Cell* *124*, 997-1009.
- Lanzetti, L., Palamidessi, A., Areces, L., Scita, G., and Di Fiore, P.P. (2004). Rab5 is a signalling GTPase involved in actin remodelling by receptor tyrosine kinases. *Nature* *429*, 309-314.
- Latham, C.F., Osborne, S.L., Cryle, M.J., and Meunier, F.A. (2007). Arachidonic acid potentiates exocytosis and allows neuronal SNARE complex to interact with Munc18a. *J Neurochem* *100*, 1543-1554.
- Leonard, D., Hayakawa, A., Lawe, D., Lambright, D., Bellve, K.D., Standley, C., Lifshitz, L.M., Fogarty, K.E., and Corvera, S. (2008). Sorting of EGF and transferrin at the plasma membrane and by cargo-specific signaling to EEA1-enriched endosomes. *J Cell Sci* *121*, 3445-3458.
- Miaczynska, M., Christoforidis, S., Giner, A., Shevchenko, A., Uttenweiler-Joseph, S., Habermann, B., Wilm, M., Parton, R.G., and Zerial, M. (2004). APPL proteins link Rab5 to nuclear signal transduction via an endosomal compartment. *Cell* *116*, 445-456.
- Murphy, J.E., Padilla, B.E., Hasdemir, B., Cottrell, G.S., and Bunnett, N.W. (2009). Endosomes: A legitimate platform for the signaling train. *Proceedings of the National Academy of Sciences* *106*, 17615-17622.
- Nielsen, E., Severin, F., Backer, J.M., Hyman, A.A., and Zerial, M. (1999). Rab5 regulates motility of early endosomes on microtubules. *Nat Cell Biol* *1*, 376-382.
- Nishio, H., Takeuchi, T., Hata, F., and Yagasaki, O. (1996). Ca<sup>2+</sup>-independent fusion of synaptic vesicles with phospholipase A2-treated presynaptic membranes *in vitro*. *Biochem J* *318*, 981-987.
- Ohya, T., Miaczynska, M., Coskun, U., Lommer, B., Runge, A., Drechsel, D., Kalaidzidis, Y., and Zerial, M. (2009). Reconstitution of Rab- and SNARE-dependent membrane fusion by synthetic endosomes. *Nature* *459*, 1091-1097.
- Paiement, J., Lavoie, C., Gavino, G.R., and Gavino, V.C. (1994). Modulation of GTP-dependent fusion by linoleic and arachidonic acid in derivatives of rough endoplasmic reticulum from rat liver. *Biochimica et Biophysica Acta (BBA) - Biomembranes* *1190*, 199-212.

Pfeffer, S., and Aivazian, D. (2004). Targeting Rab GTPases to distinct membrane compartments. *Nat Rev Mol Cell Biol* 5, 886-896.

Simonsen, A., Lippe, R., Christoforidis, S., Gaullier, J.M., Brech, A., Callaghan, J., Toh, B.H., Murphy, C., Zerial, M., and Stenmark, H. (1998). EEA1 links PI(3)K function to Rab5 regulation of endosome fusion. *Nature* 394, 494-498.

Sonnichsen, B., De Renzis, S., Nielsen, E., Rietdorf, J., and Zerial, M. (2000). Distinct membrane domains on endosomes in the recycling pathway visualized by multicolor imaging of Rab4, Rab5, and Rab11. *J Cell Biol* 149, 901-914.

Stenmark, H., Aasland, R., Toh, B.H., and D'Arrigo, A. (1996). Endosomal localization of the autoantigen EEA1 is mediated by a zinc-binding FYVE finger. *J Biol Chem* 271, 24048-24054.

Vieira, A.V., Lamaze, C., and Schmid, S.L. (1996). Control of EGF Receptor Signaling by Clathrin-Mediated Endocytosis. *Science* 274, 2086-2089.

Wang, Y., Pennock, S., Chen, X., and Wang, Z. (2002). Endosomal Signaling of Epidermal Growth Factor Receptor Stimulates Signal Transduction Pathways Leading to Cell Survival. *Mol Cell Biol* 22, 7279-7290.

Williams, J.H., Errington, M.L., Lynch, M.A., and Bliss, T.V. (1989). Arachidonic acid induces a long-term activity-dependent enhancement of synaptic transmission in the hippocampus. *Nature* 341, 739-742.